Carbon Dots as Heterogeneous Catalysts for the Sustainable Production of Biodiesel

Alexia Macina

A Thesis in the

Department of Chemistry and Biochemistry

Presented in Partial Fulfillment of the Requirements

For the Degree of Master of Science (Chemistry) at

Concordia University

Montreal, Quebec, Canada

August 2020

CONCORDIA UNIVERSITY

School of Graduate Studies

This is to certify that the thesis prepared

By: Alexia Macina

Entitled: Carbon Dots as Heterogeneous Catalysts for the Sustainable Production of Biodiesel

And submitted in partial fulfillment of the requirements for the degree of

Master of Science (Chemistry)

complies with the regulations of the University and meets the accepted standards with respect to

originality and quality.

Signed by the final examining committee:

_____ Chair

Dr. Xavier Ottenwaelder

_____ Examiner

Dr. Ashlee Howarth

_____ Examiner

Dr. Louis Cuccia

_____ Supervisor

Dr. Rafik Naccache

Approved by   _____ Graduate Program Director

Dr. Yves Gélinas

_____ Dean of Faculty

Dr. Pascale Sicotte

Date   _____

Abstract

Carbon Dots as Heterogeneous Catalysts for the Sustainable Production of Biodiesel

Alexia Macina

With rising global energy demands, fossil fuels are being consumed at their quickest rate yet. Overconsumption, unsustainable practices and environmental concerns have accelerated the search for alternative, renewable and environmentally friendly energy sources. One such promising source is biodiesel, which is formed through the transesterification of refined vegetable oils in the presence of methanol and a homogeneous catalyst such as sodium/potassium hydroxide. While the reaction is efficient, limitations associated with tedious purification coupled with the inability to reuse the catalyst have limited its global production and adoption.

A variety of heterogeneous catalysts have been investigated as catalytically efficient alternatives yet their preparation often entails tedious synthetic procedures or the use of heavy metals, which can lead to metal leaching and increased purification costs. It is in this regard that carbon dots, a new member of the carbon nanomaterial family, has been be explored as a potential metal-free alternative. Carbon dots offer several advantages namely cost effective and facile preparation from accessible and sustainable precursors coupled with a tunable surface chemistry.

In this work, carbon dots derived from glycine were synthesized using microwave and hydrothermal techniques. Their physico-chemical properties were characterized and their catalytic efficiency towards the transesterification reaction of canola oil was investigated resulting in biodiesel conversions > 95%. We investigated the mechanism of catalysis and we exploited our findings to design a carbon dot catalyst from precursors such as lignin and glycerol, the principle waste product of the biodiesel reaction. By rendering the production process cost effective and energetically favorable, while maintaining sustainable practices, biodiesel global adoption can increase and global energy demands may be met in an energy efficient, sustainable and financially feasible manner.

Acknowledgements

This MSc thesis, although bearing my name on the front page, could not and would not be written without the help, guidance, love and support from some dear people.

To Dr. Rafik Naccache, who is not only the greatest supervisor one can have but also the greatest mentor an aspiring scientist can hope for. My journey in the Naccache lab began with a CHEM 419 project and soon after starting I knew it would hopefully translate into an MSc degree. The guidance, encouragement and devotion that Dr. Naccache gives to his students is truly the mark of a great supervisor, one that wants to see his students excel and reach beyond what they think they can achieve. Thank you Dr. Naccache for all the exciting discussions and conversations, science related and not, and for always taking time out of your schedule to simply listen to me complain or cry. Lastly, thank you for always reminding me which way the lab is.

To my committee members, Dr. Louis Cuccia and Dr. Ashlee Howarth, thank you for all your guidance and critical constructive criticism towards my work. I am very grateful for your insightful comments and questions which have helped me become more critical about my own work and to never stop asking questions.

To the amazing administrative staff and lab technicians in the department of chemistry and biochemistry, thank you for making my master's experience that much brighter. I think I speak for all grad students when I say how appreciative I am of your kindness, support and patience towards us all.

To all my lab colleagues, past and present, thank you for all the laughs, cries, fun times and dark times we've had together. The lab environment would not be the same without each and every one of you. But most importantly, thank you for always being available for pizza, sushi, McDonald's, Chinese food and brunch.

To my mentor, Tayline de Medeiros, thank you for always having endless patience with me and providing me with endless motivation. I could not have asked for a better mentor and teacher. Thank you for always reassuring me when I lost confidence and constantly reminding me that it's ok if science doesn't always work.

To my forever friends, Tayline de Medeiros and Florence Victoria, this thesis could not have been written without the both of you. I thank you for being my biggest support system. Our friendship speaks volumes and I could not have been luckier than to have you two come into my life during this time. Our relationship goes above and beyond science. Thank you for all the endless laughter and the amazing memories, with many more to come.

To my amazingly supportive boyfriend, Sultan, thank you for always being my rock and believing in me. I will be forever grateful for your never-ending encouragement and patience in the last two years and I could not have done it without you by my side. Thank you for being who you are.

To my mom and dad who have always been by my side throughout my whole educational journey. You both have always given me the opportunity to excel in what I love and given me the strength and confidence to reach my full potential. I am forever grateful.

Contribution of Authors

The work in chapter 3 was primarily carried out by myself. Specifically, I carried out the synthesis and characterization of GlyCDs, LCDs and GCDs in chapter 3.1, the biodiesel characterization ^{1}H NMR protocol in chapter 3.3, as well as the transesterification experiments in chapter 3.4. Analysis and interpretation of results in chapter 3 were carried out with extensive help from Ms. Tayline de Medeiros at Concordia University. The work resulted in a cover article publication in the Journal of Materials Chemistry A as an invited feature in the Emerging Investigator Issue, including Ms. Tayline de Medeiros as a co-author (**Macina, A**.; de Medeiros, T.V.; Naccache, R. A carbon dot-catalyzed transesterification reaction for the production of biodiesel. *J. Mater. Chem. A.* **2019).** The work in chapter 3 also resulted in a patent filing (**Macina, A**.; de Medeiros. T.V.; and Naccache, R.; Carbon Dots, methods of manufacture thereof, and uses thereof in the production of biofuel. Patent Number 62/868.677. 2019).

The preliminary work and results in chapters 3.1.2, 3.1.3, 3.4.2 and 3.4.3 have resulted in two manuscripts currently in progress, slated for journal submission in 4Q 2020 to the Green Chemistry journal and ACS Sustainable Chemistry and Engineering. The work will be co-authored with Tayline de Medeiros as she continuously provides her help and knowledge on the data acquisition, characterization, and interpretation of results.

The work in this thesis has inspired a new avenue of research and collaborative efforts in the Naccache lab focusing on sustainable biodiesel production using heterogeneous catalysis.

Table of Contents

List of Figures

x

List of Tables

List of Abbreviations

BET	Brunauer, Emmett and Teller
CDs	Carbon dots
DT3	Diethylenetriamine
FAEE	Fatty acid ethyl esters
FAME	Fatty acid methyl esters
FFAs	Free fatty acids
FT-IR	Fourier-transform infrared spectroscopy
GC	Gas-chromatography
GCDs	Glycerol-derived CDs
GCDs-0.3	Glycerol-derived CDs using 0.3 g of sodium citrate
GCDs-0.6	Glycerol-derived CDs using 0.6 g of sodium citrate
GCDs-1.2	Glycerol-derived CDs using 1.2 g of sodium citrate
GlyCDs	Glycine-derived CDs
LCDs	Lignin-derived CDs
LCDs-b	Base-treated LCDs
NMR	Nuclear magnetic resonance
TEM	Transmission electron microscopy
TGA	Thermogravimetric analysis
XPS	X-ray photoelectron spectroscopy
HR-XPS	High Resolution X-ray photoelectron spectroscopy
XRD	X-ray diffraction

Chapter 1 – Introduction

1.1 – Fossil Fuels and Their Impending Demise

According to the world energy outlook 2019 report by the International Energy Agency, global energy demands will grow by 1.3% per year until 2040.[1] Currently, approximately 80% of the world's energy market is dominated by fossil fuel-derived energy and trends suggest that it will continue to do so for the next 20 years.[2] Fossil fuels, made up of coal, oil and natural gas, are obtained from the decomposition of plants and organisms over millions of years that resulted in carbon rich deposits underneath the earth's crust **(figure 1a)**. While highly energy efficient, the excessive burning of fossil fuels over the last hundred years has resulted in severe damage to the earth's atmosphere and ozone layer and is the primary contributor to global warming. Fossil fuels are made up of hydrocarbons along with some sulfur, nitrogen and oxygen, and upon combustion, these compounds oxidize to form the primary pollutants in greenhouse gases, namely, carbon monoxide, carbon dioxide and sulfur dioxide. The industrial revolution began in the year 1760 and sprung foreword the use and consumption of coal, oil and gas, consequently causing a drastic increase in CO_2 emissions **(figure 1b)**.[3] Along with their detrimental environmental impact, there is no doubt that fossil fuels are a finite resource, and multiple reports have hypothesized their depletion could occur as soon as the next 50-100 years.[4,5] The non-renewable nature of fossil fuels poses a significant threat to future generations and it must be replaced with an equally energy efficient, renewable and sustainable source. Promising renewables currently consist of solar energy, wind power, hydro power and biofuels with the latter touted to replace conventional fossil fuel-derived diesel. Biofuels consist of bioethanol or biodiesel, both which have seen a significant increase in production over the last 30 years **(figure 1c)**[6].
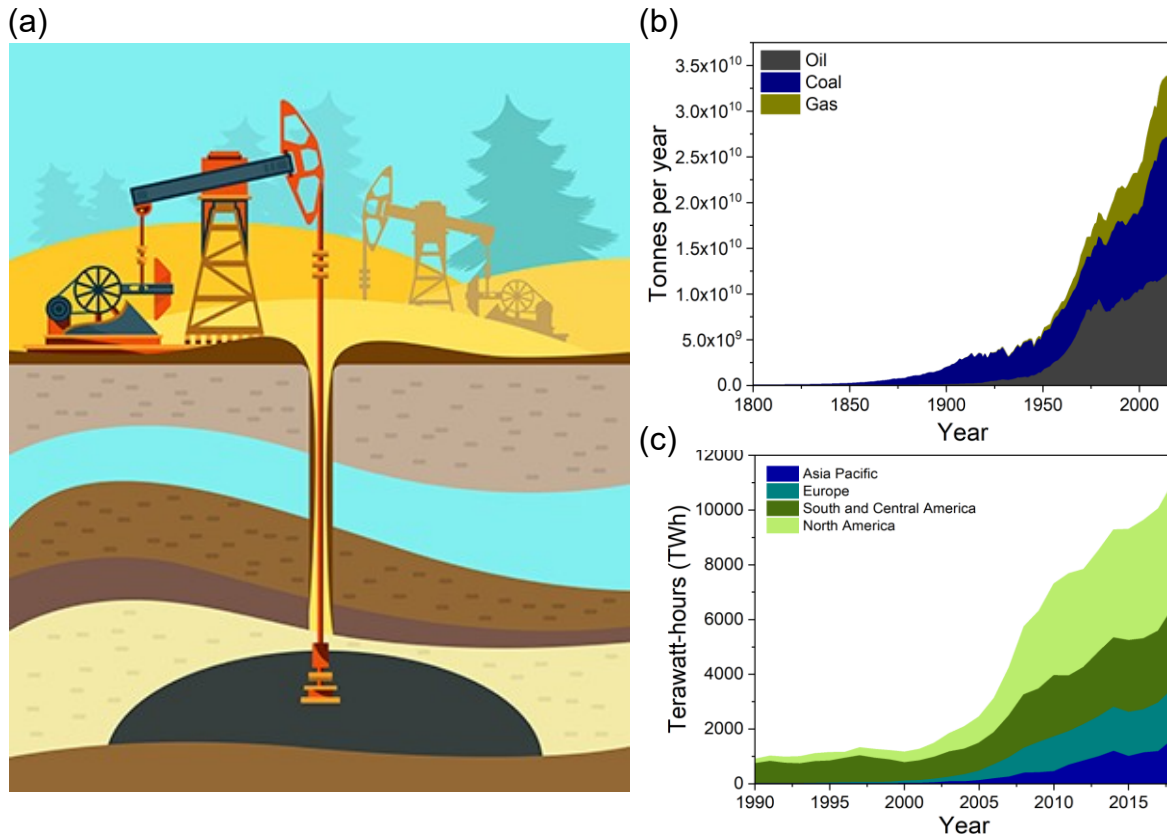
Figure 1. (a) Oil extraction process where fossil fuels, oil and natural gas, are present within the multiple layers of the earth's crust and/or under the ocean floor. (b) The drastic increase in CO_2 emissions as a result of fossil fuel consumption (figure adapted from ourworldindata).[3] (c) Increase in biofuel production, including bioethanol and biodiesel, since 1990 (figure adapted from ourworldindata).[6]

1.2 – What is Biodiesel?

The term *biodiesel* was first coined in the year 1984, however, its existence predates by about 50 years.[7] Since the invention of the diesel engine in the 1890's it was known that it could run on many different fuel types, including pure vegetable oil. However, due to engine limitations and the availability of very cheap petroleum, vegetable oil was quickly overlooked. It wasn't until 1937, when a patent for an ethyl ester derivative of palm oil was granted to fuel a passenger bus in Brussels, that *biodiesel,* as we know it today, was first used.[7,8]

Chemically speaking, biodiesel is formed through the transesterification reaction of triglycerides with a primary alcohol to form long chain fatty acid methyl- or ethyl- esters (FAME or FAEE), along with glycerol as a by-product. Both methanol and ethanol can be used as the primary alcohol, however the former is more commonly used in the commercial production of biodiesel due to cost considerations and reaction efficiency. Although the use of methanol is significantly cheaper as it is derived from fossil fuels, it is not considered to be the "greenest" alternative for biodiesel production, despite its adoption as the main industrial practice. Alternatively, the use of bioethanol for the production of FAEE would significantly increase the sustainability and viability of biodiesel however, presents its own set of limitations. The transesterification reaction between triglycerides and ethanol requires higher energy inputs and a higher ethanol content compared to methanol due to increased steric hindrance during both ethoxide formation and nucleophilic attack on the carbonyl of the triglyceride (*vide infra*), resulting in high reaction temperatures and longer reaction times.[9] Since the transesterification reaction is reversible, a catalyst must be used to drive the reaction forward and an excess amount of methanol must be used. Stoichiometrically, 1:3 oil to methanol molar ratio is required however, a minimum of 1:6 is typically used to drive the reaction towards the formation of biodiesel.[10,11] The reaction can undergo a base- or acid-catalyzed process, with both having their own benefits and drawbacks. A general scheme of the transesterification reaction is presented in **figure 2**.
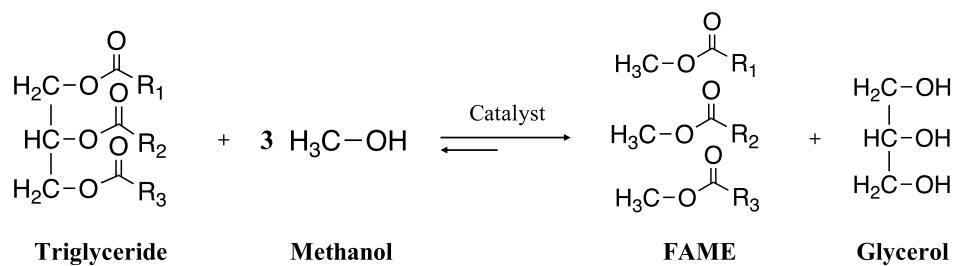
Figure 2. General reaction scheme for the transesterification reaction of vegetable oil to biodiesel.

1.2.1 – Homogeneous Catalysts for Biodiesel Production

Catalysts are often used in a number of chemical reactions to increase the rate of reaction by lowering the energy barrier and thus decreasing their stoichiometric dependencies to drive the reaction in the forward direction **(figure 3a).** The current commercial standard for biodiesel production requires the use of a homogeneous catalyst, either a strong acid, most commonly H_2SO_4, or a strong base, such as KOH or NaOH. In general, homogeneous catalysts are those which are present in the same physical phase as the reactants, meaning they will dissociate into ions once dissolved in the solvent, and usually cannot be recuperated from the final reaction mixture, ultimately requiring additional purification steps. Commercially, biodiesel is typically produced using a strong base. NaOH and/or KOH homogeneous catalysts offer fast reaction times, often ~1 hour, along with mild reaction conditions performed under ambient pressure and temperatures of ~70°C.[12] Furthermore, both bases are relatively cheap and commonly available. The downfall of using strong bases as catalysts is their high sensitivity to free fatty acids (FFAs) that can be found in many precursor oils, ultimately leading to saponification. Upon dissociation, Na^+ and K^+ ions interact with the free fatty acid to form a metal salt called "soap", a contaminant that can significantly lower the final biodiesel yields and increases purification steps and costs **(figure 3b)**.

Under basic conditions the reaction mechanism is as follows **(figure 4)**; the methoxide is formed through the deprotonation of methanol by NaOH/KOH, followed by a nucleophilic attack of the methoxide on the carbonyl of the triglyceride. This forms a tetrahedral intermediate and upon reformation of the carbonyl, the leaving group leaves, forming a FAME and a diglyceride. This mechanism repeats twice more until reaction completion resulting in a mixture of FAME and glycerol as the by-product.

(a)

(b)
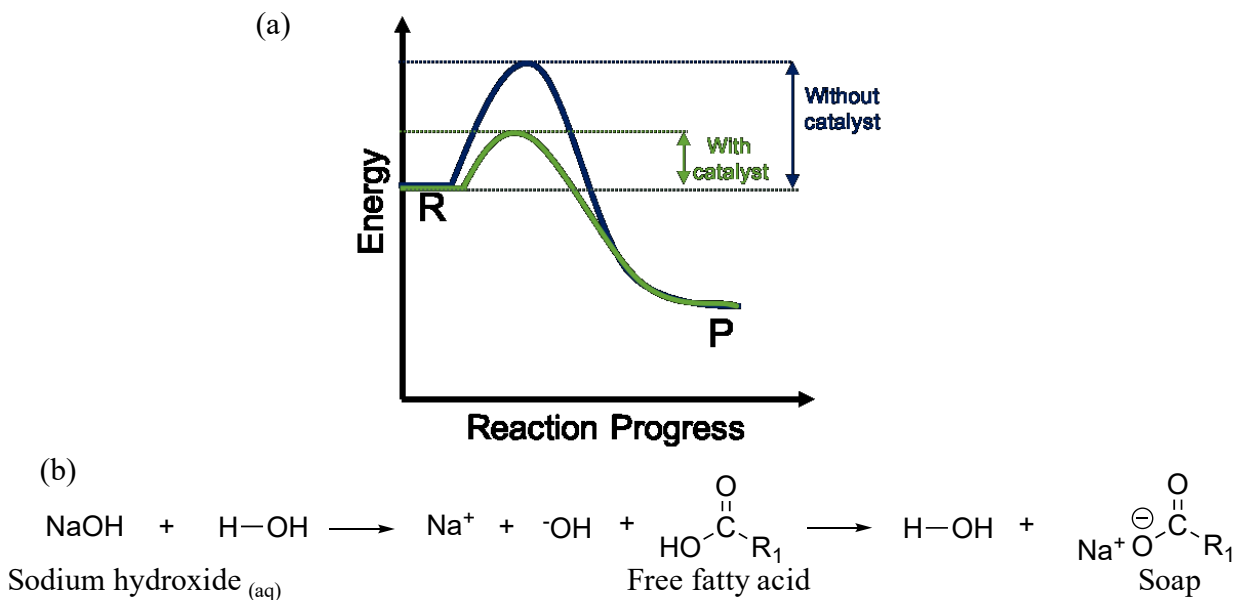
Figure 3. (a) Energy diagram showing the change in the activation energy barrier in the presence and absence of a catalyst. (b) Reaction scheme of sodium ions with free fatty acids forming "soap".
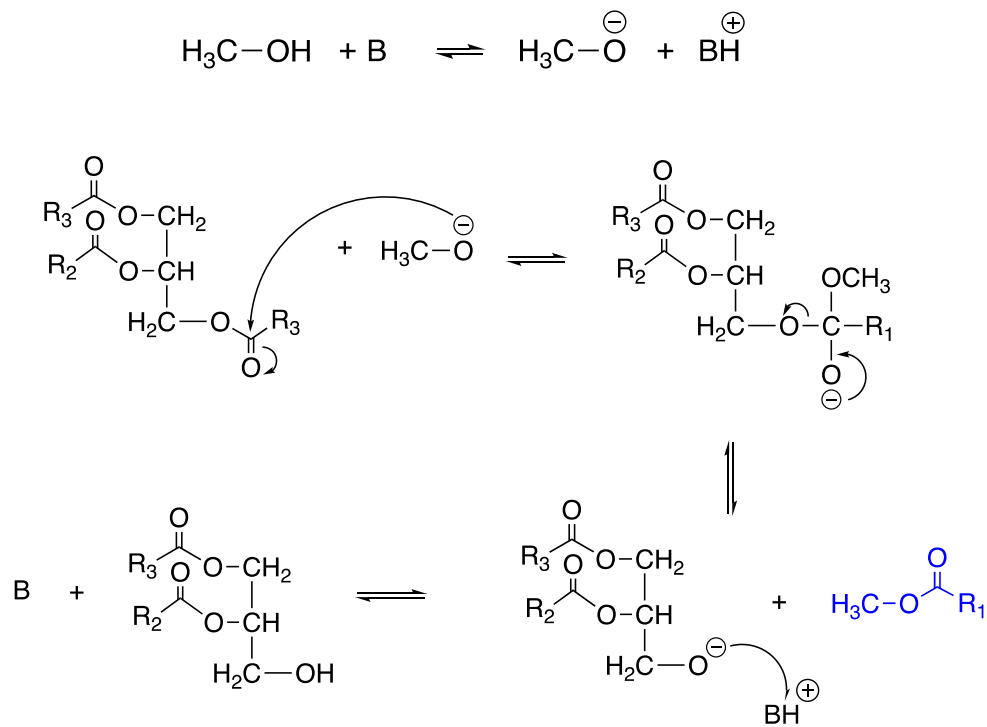
Figure 4. Homogeneous base-catalyzed transesterification reaction mechanism.

5

Strong acid homogeneous catalysts such as H_2SO_4 have the advantage of being insensitive to FFAs, therefore formation of the "soap" is not a concern. The downsides of using a strong acid are the slower reaction rates leading to longer reaction times, often up to 10 h or more, as well as higher temperatures and methanol content.[13,14] The use of homogeneous catalysts for the commercial production of biodiesel has become the norm; however, it also poses a significant restraint on the economic growth of biodiesel and has hindered its mass production and global acceptance. In order to circumvent these limitations, scientists are exploring the use of heterogeneous catalysts in order to render the biodiesel production process more sustainable and economically viable. Under acidic conditions, the reaction mechanism is as follows **(figure 5)**; the first step involves the protonation of the carbonyl oxygen by the acid catalyst, forming a tertiary carbocation through resonance. This allows for the nucleophilic attack of the methanol lone pairs on the positively charged carbon forming a tetrahedral intermediate. Upon a proton transfer
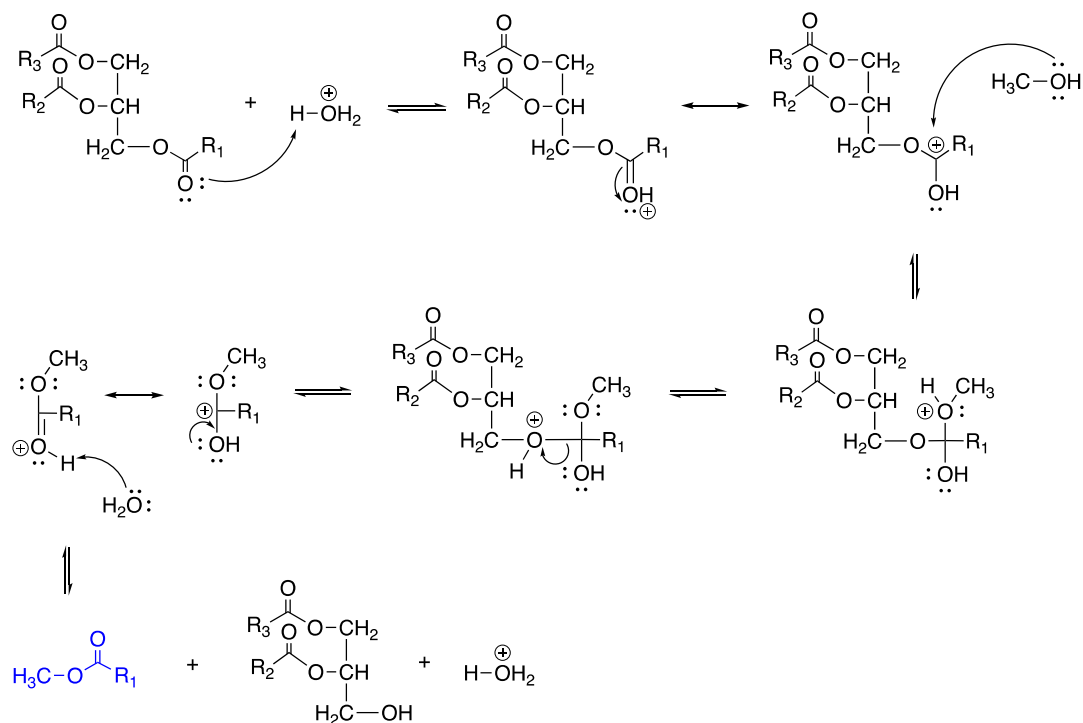
Figure 5. Homogeneous acid-catalyzed transesterification reaction mechanism.

followed by the removal of the leaving group, the carbonyl reforms to produce a FAME and a diglyceride. This mechanism repeats twice more until reaction completion resulting in a mixture of FAME and glycerol as the by-product.

FFAs are converted to methyl esters through the esterification reaction with a similar mechanism to the acid-catalyzed transesterification reaction, typically using H_2SO_4. In addition to the investigation of heterogeneous catalysts for the transesterification reaction, research is also being conducted on efficient solid acid catalysts that can replace strong homogeneous acids for the catalysis of the esterification reaction. This would allow the use of waste oils, high in FFA content, to be utilized and converted to biodiesel without the need of oil pre-treatment steps involving highly corrosive strong acids.

1.2.2 – Heterogeneous Catalysts Used for Biodiesel Production

Heterogeneous catalysts or *solid* catalysts are those which are considered to be in a separate phase of the reaction than the reactants. Therefore, heterogeneous catalysts are more easily separated and recuperated from the final reaction mixture and thus may be reused for subsequent catalytic reactions. This results in typically simpler purification requirements. Many acid- and base-heterogeneous catalysts have been proposed for biodiesel production, the most popular being, alkaline earth[15,16] or transition metal oxides[16], zeolites[11,17], and resins[18]. The most common example of a metal oxide catalyst is CaO, which mimics base catalysis due to the negative oxygen ions acting as Brønsted bases and therefore proton acceptors that can then form the methoxide ion necessary for the transesterification reaction.[19] Moreover, CaO catalysts are promising because they are considered to be cheaper than other metal-based catalysts and can be synthesized from a number of green and sustainable methods.[20] While metal oxides in general have relatively high

catalytic efficiency, multiple drawbacks persist. There is a higher possibility of metal leaching which not only causes catalyst active site deactivation, but also imposes further purification requirements and therefore increases overall costs. One other consequence to metal leaching is the probability that free metal cations can interact with FFAs found in the oil precursor to form the "soap" contaminant, as is the case of homogeneously-catalyzed reactions. While heterogeneous catalysts can be very beneficial in industrial processes and promote economic growth, they often require more energy intensive reaction conditions which can limit their application in industry. In terms of the transesterification reaction, heterogeneously-catalyzed reactions often require higher methanol content, with stoichiometric ratios between 1:9 – 1:275[16,21–23], catalyst loading of up to 15 wt%[21,24], and reaction times and temperatures of up to 20 h[16,23,25,26] and 300 °C[16,25], respectively.

The quality and physico-chemical properties of biodiesel is regulated and determined by a set of government standards, ASTM (American Society for Testing and Materials) D6751 and/or EN (European Standards) 14214. The product quality and attainment of these standards is directly affected by the biodiesel production process, taking into account reaction conditions such as amount and type of catalyst, oil precursor used, methanol content and energy input. These standards are to ensure that the biodiesel produced can safely and efficiently run in diesel engines without further purification and/or modification **(table 1)**. Most importantly, properties such as methanol content, metal content and acid value should be wisely considered when designing and using heterogeneous catalysts. Since higher methanol content is typically required for heterogeneously-catalyzed biodiesel production, it is expected that higher concentrations of residual methanol would be present in the final purified product thus, depending on how much methanol was initially used, this concentration may surpass the maximum allowed value of 0.20 % (m/m). Similarly, a maximum concentration of 5.0 mg/kg of alkali and alkaline earth metals is

allowed in the final biodiesel product. Therefore, heterogeneous catalysts that entail the incorporation of large amounts of these metals may increase the chances of metal leaching and incorporation in the final biodiesel product, consequently resulting in a higher concentration than the allowed value, regardless of extensive purification. The acid value is also an important property that may have significant impacts on biodiesel quality and is directly dependent on the content of free fatty acids left unreacted in the final product. If the oil precursor contains an abundance of FFAs and is used conversely with a catalyst that does not have high efficiency towards the esterification of FFAs to FAME, this could potentially result in a biodiesel product with a high acid value and has been shown to cause large engine deposits due to polymerization at high temperatures.[27] These examples illustrate the important on how the design of heterogeneous catalyst may not only have effects on reaction efficiency but how this ultimately translates to the quality of biodiesel being produced and therefore, its resulting engine performance and safety.

Table 1. ASTM and EN standards for B100 biodiesel.[28]

Property	Units	ASTM D6751	EN 14214
Ester content	% (m/m)	-	96.5
Density at 15 °C	(kg/m^3)	880	860-900
Viscosity at 40 °C	(mm^2/s)	1.9-6.0	3.5-5.0
Cetane number	-	Min. 47	Min.51
Acid value	(mg KOH/g)	Max. 0.50	Max. 0.50
Methanol content	% (m/m)	Max. 0.20	Max. 0.20
Free glycerol	% (m/m)	Max. 0.02	Max. 0.02
Total glycerol	% (m/m)	Max. 0.24	Max. 0.25
Monoglyceride	% (m/m)	Max. 0.40	Max. 0.70
Alkaline metals (Na^+, K^+)	(mg/kg)	Max. 5.0	Max. 5.0
Alkaline earth metals (Ca^{2+}, Mg^{2+})	(mg/kg)	Max. 5.0	Max. 5.0

1.3 – Towards Sustainable Biodiesel

While the concept of heterogeneous catalysis is in itself considered to be green and more sustainable than its homogeneous counterpart, the requirement of more energy intensive reaction conditions currently outweighs the benefits. Irrespective of the choice of catalysts used, there are some fundamental limitations to the current biodiesel production paradigm. Currently, the oil precursor used must be a refined vegetable oil such as canola oil, soybean oil, or palm oil, among others, due to the fact that these oils contain minimal free fatty acid content, and will not interact with Na^+ or K^+ ions causing saponification. In fact, 95% of the current oil feedstock stems from refined edible oils. Thus, the use of refined vegetable oil precursors accounts for 80% of the total biodiesel production cost, highlighting the importance of oil feedstock and its economic impact on the overall process.[29,30] Moreover, the use of refined vegetable oils also introduces the *food vs fuel* debate, where arguments concerning the ethics and viability of diverting and repurposing agricultural land for the production of biofuels arises. Furthermore, a large portion of the high cost of biodiesel stems from the extensive purification process needed for refined oil extraction and production. Another concern with the current processes focuses on the use of excessive amounts of water required to purify the crude biodiesel product. This is particularly the case for homogeneous catalysts, which remain dissolved in both the biodiesel product and the glycerol by-product. The purification process produces large amounts of waste, which must then be treated.

In order to circumvent the negative repercussions and the corresponding financial limitations of current biodiesel production approaches, research is now focusing on transforming the process towards a more sustainable and financially feasible approach. The principal modification would require the use of greener, or non-edible oils to produce biodiesel. These oils include, jatropha oil, castor oil, rubber seed, among others, as well as what is known as waste

edible oils, which comprise frying oil or grease trap oils. While the success of this vision can revolutionize biodiesel production, it also comes with its own limitations. The problem with using waste edible oils is that they have much higher water and free fatty acid content relative to refined vegetable oils and also typically have modified physical properties due to the frying process.[31] The current concerns are the need to find a novel catalytically efficient catalyst that can successfully convert these oils to biodiesel that is on par with the ASTM standards, all the while keeping the reaction conditions as minimally energy intensive as possible.

1.3.1 – Is the Biodiesel Production Process Green Chemistry?

The term *biodiesel* is associated with words like "green" and "environmentally friendly"; however, do the current industrial practices associated with biodiesel production adhere to the twelve green chemistry principles? The concept of green chemistry has increasingly become more pertinent to implement into the design and synthesis of chemicals and materials as scientists become more aware of the undesirable impacts that science may have on human health and the environment, including aquatic, animal and plant ecosystems. In 1998 the twelve green principles were created and are as follows; 1) prevention, 2) atom economy, 3) less hazardous chemical syntheses, 4) designing safer chemical, 5) safer solvents and auxiliaries, 6) design for energy efficiency, 7) use of renewable feedstocks, 8) reduce derivatives, 9) catalysis, 10) design for degradation, 11) real-time analysis for pollution prevention, 12) inherently safer chemistry for accident prevention.[32] While the chemicals comprising biodiesel, FAMEs, do not pose environmental risks upon combustion and do not contribute to greenhouse gases as their fossil fuel counterparts do, the production process and raw materials used for biodiesel synthesis must also be optimized to reduce its ecological footprint and implement the green chemistry principles to

lead to fully sustainable and environmentally benign practices. While the transesterification reaction is catalytically driven, implementation of principle 9 could be further optimized by using a sustainable heterogeneous catalyst derived from biomass and waste products. This would also aid in better implementing principle 1, prevention, by reducing the need for large amounts of chemically-contaminated waste water and concentrated acids that are currently used in abundant amounts during the biodiesel production process. Synthesizing a catalyst from renewable sources such as lignin would also aid in further implementing principle 7, use of renewable feedstocks, by utilizing biomass derived from forestry waste. It is estimated that only 25 % of the annual biomass produced every year would be needed to fuel a complete bio-based global economy.[33]

1.3.2 – The Abundance of Biomass

Biomass, including forestry waste and waste by-products from manufacturing processing, is widely used as a renewable source for bioenergy production, including heat and electricity, used to power industrial processes. Apart from the direct energy harvest from biomass, it can also be valorized into other products such as biochemicals[34–36] and biomaterials[37,38], which in turn can be used to increase the sustainability and greenness of other industrial processes and materials. The primary utilization of biomass in regards to biodiesel production is the extraction of lipids from microalgae as an oil feedstock.[39–41] Microalgae is an interesting approach as it grows rather rapidly, has a high lipid content and does not require the use of agricultural land. Johnson *et al.* investigated biodiesel production from the transesterification of algal oil from *schizochytrium limacinum* resulting in a biodiesel yield of 98.4%.[41] The drawback to using algae-derived oils is the extremely tedious and multi-step extraction method required to efficiently extract triglycerides from the algae, limiting its commercialization.[42] Alternatively, to integrate the utilization of biomass in the

biodiesel production cycle, the synthesis of biomass-derived heterogeneous catalysts is another avenue that may be explored as to increase the sustainability of current industrial practices. Uprety *et al.* investigated the catalytic efficiency of a heterogeneous catalyst derived from wood ash obtained from biomass sources.[21] The catalyst showed a promising biodiesel conversion of 88 % using relatively mild reaction conditions at 9 wt% loading catalyst and 9:1 methanol to oil ratio.[21] Pua *et al.* synthesized a solid acid catalyst by activating lignin with phosphoric and sulfuric acid, and demonstrated its high catalytic efficiency towards the esterification reaction with a biodiesel conversion of 96.1%.[43] The aforementioned works reveal the potentials to valorize biomass by integrating its use into the production of heterogeneous catalysts in order to increase the sustainability of biodiesel as a green fuel and lower its production costs.

1.3.3 – The Abundance of Crude Glycerol

With biodiesel production significantly increasing over the last 20 years, so has the production of crude glycerol. About 10% (w/w) of crude glycerol is formed as a by-product of the transesterification reaction for a given amount of FAME produced.[44] The production of increasing amounts of crude glycerol is affecting the pure glycerol industry by drastically lowering their sales costs. Thus, there exists a need to find a sustainable manner to reuse crude glycerol in other industries and applications. The utilization and processing of crude glycerol will also aid in balancing out the relatively high biodiesel production costs. Crude glycerol contains a number of impurities remaining from the transesterification reaction including, residual methanol, soap, FFAs and salts.[44,45] The presence of impurities limit the use of crude glycerol for applications in the cosmetic, pharmaceutical and food industries, which could otherwise lead to safety and health concerns.[45] Currently, crude glycerol is often used as animal feedstock due to its high energy

source and conversion to glucose upon metabolism however, concerns over the effects of excess glycerol on the animals' normal physiological metabolism has limited its use.[44,46] Alternatively, crude glycerol may be valorised and broken down to synthesize value-added chemicals such as 1, 3-propanediol and citric acid, as well as polymers and other materials.[44,47]

Newly emerging, researchers are shifting towards the utilization of glycerol to form glycerol-based heterogeneous catalysts for the esterification or transesterification reactions as means to re-integrate crude glycerol back into the biodiesel production process. Devi *et al.* synthesized a solid acid catalyst from the carbonization of glycerol with sulfuric acid to produce a solid glycerol-based catalyst with active sulfonic groups on the surface.[48] Upon esterification of palmitic acid, using 10 wt% loading catalyst, biodiesel conversions of 99% were achieved after 4 h and showed promising catalyst reusability studies of up to 8 reaction cycles.[48] Ferrero *et al.* reported a glycerol-enriched heterogeneous catalyst for the transesterification reaction through the synthesis of calcium glyceroxide with varying amounts of glycerol.[49] The results showed a considerable increase in biodiesel conversion upon the use of calcium glyceroxide when compared to calcium oxide, obtaining 91.6 % versus 69.8 %, respectively.[49]

With a myriad of materials being investigated for their application in heterogeneous catalysis for the transesterification reaction, nanomaterials are gaining considerable interest and attention. Nanomaterials, currently being explored as novel alternatives in the field of catalysis, have been touted as a versatile alterative to current homogeneous and heterogeneous catalysts in biodiesel production.

1.4 – Nanomaterials

Nanomaterials exhibit unique properties when compared to their bulk counterpart, rendering them attractive for a wide range of applications. A material is considered to be *nano* if it measures 1–100 nm in a single dimension and this definition encompasses materials such as polymers, dendrimers, quantum dots, upconverting nanoparticles and carbon nanotubes, among others. These nanoparticles possess unique physico-chemical properties, which scientists exploit to create innovations in applications to nanomedicine[50,51], bioimaging[52,53], environmental science[54], and catalysis[55,56]. Nanomaterials are especially interesting for catalysis applications due to an inherent property that all nanomaterials exhibit, which is their high surface area to volume ratio. In order to visualize this, consider a cube representing a bulk material where each side measures 1 µm, consequently having an area and volume of 6 µm^2 and 1 µm^3, respectively (**figure 6).** While maintaining an equivalent total volume, this same cube can be broken into 125 smaller cubes, representing nanoparticles, each with a side measuring 200 nm and consequently having a total surface area and volume of 30 000 µm^2 and 1 µm^3, respectively. Therefore, the nano cubes

	Area	Volume	Area:Volume
Bulk	6 µm^2	1 µm^3	1:1
Nano	30 000 µm^2	1 µm^3	5000:1
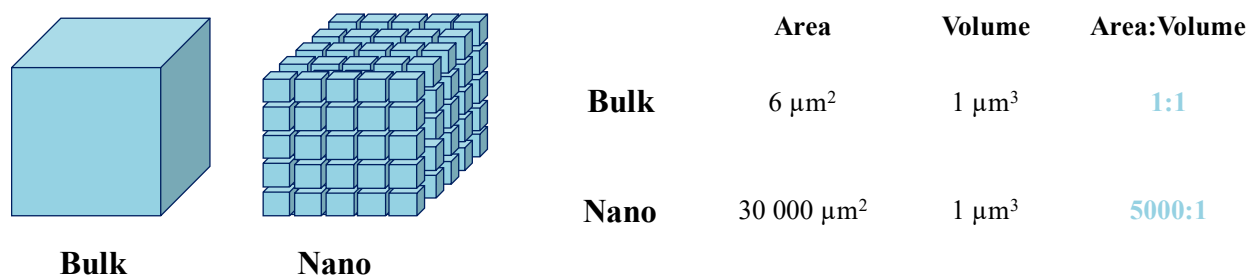
Figure 6. Visual representation of a cube comparing bulk and nanosized materials and the effect on surface area to volume ratio as one departs form the micron scale to the nanoregime.

will have an area to volume ratio 5000 times greater than its bulk counterpart. This leads to a higher degree of surface active groups for a given amount of material and allows for substrate molecules to adsorb to the surface while consuming less catalytic material.

It is no surprise that given the increase in surface area to volume ratio, several nanomaterials have been explored for biodiesel production. For example, enzyme-immobilized nanoparticles such as carbon nanotubes and nanofibers have been suggested as efficient catalysts for enzyme-catalyzed transesterification.[57] Although these catalysts were highly stable and reusable up to 15 reaction cycles, they require tedious synthesis and purification protocols and enzymes can be very costly. Thus, the search for novel heterogeneous catalysts persists. More recently, carbon dots have emerged as a potential alternative to metal-based systems owing to their versatile physico-chemical properties.

1.5 – What are Carbon Dots?

Carbon dots (CDs) are a member of the carbon nanomaterial family and are approximately 10 nm in size. They are quasi-spherical in shape, amorphous and their elemental composition comprises sp^2 and sp^3 hybridized carbon, along with oxygen and hydrogen. Furthermore their structure can be doped with heteroatoms such as nitrogen and sulfur **(figure 7a)**. CDs were accidentally discovered in 2004, when Xu *et al.* purified single-walled carbon nanotubes and noted fluorescent impurities during their purification protocol.[58] After characterization of this impurity, they coined the name *carbon dots.* CDs are well known for their versatile optical properties and tunable fluorescence from the UV to NIR regions of the electromagnetic spectrum. For this reason, their photoluminescent properties have been heavily exploited for applications in bioimaging[59–61] and sensing[59,62]. However, carbon dots also exhibit interesting chemical and structural properties

that render them interesting candidates for a myriad of other applications in biomedicine, electrocatalysis, and solar energy, amongst others **(figure 7b)**[63]. One notable feature of carbon dots is the fact that they can be synthesized from a number of easily accessible precursors. CDs are commonly synthesized from citric acid, amino acids, sugars and cheap simple molecules. This allows for facile and inexpensive synthesis procedures that would be beneficial for large scale productions necessary for large industrial processes such as biodiesel production. One field in which CDs have not been significantly explored is chemical catalysis. The chemical surface groups of CDs can be extensively tailored to feature carboxylic acids/carboxylates, alcohol, amine, amide and thiol moieties that can potentially act as catalytically active sites to participate in, or to catalyze various organic reactions. Thus far, a scarce number of CD-composite materials have been investigated as catalysts for oxidation[64] and reduction[65] reactions.
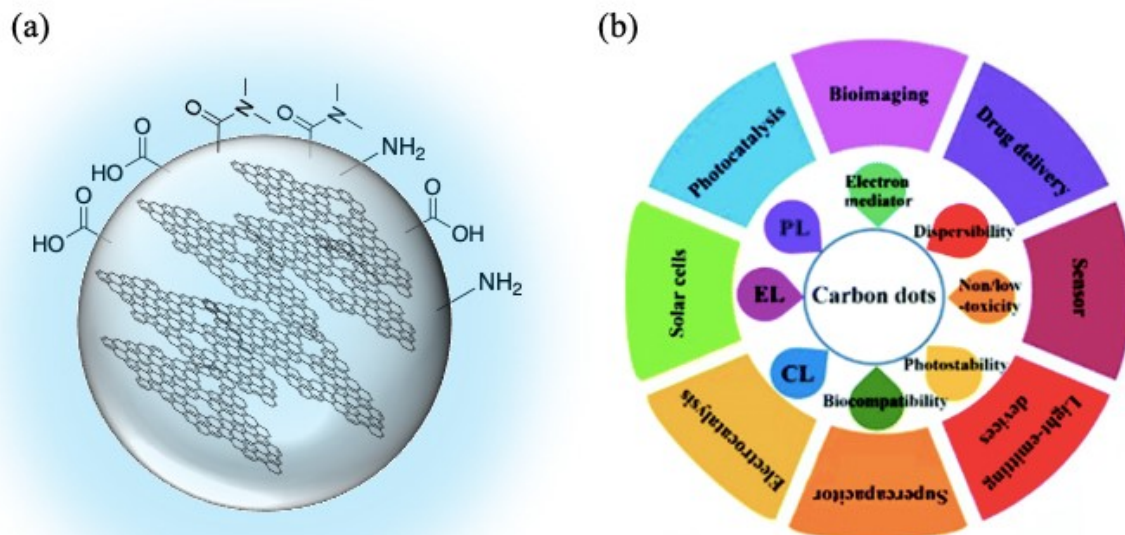
Figure 7. (a) Graphical representation of the structure of CDs. (b) The chemical-physical properties and applications of CDs (adapted from Kang *et al.*). [63]

1.5.1 – Synthesis of Carbon Dots

CDs can be synthesized *via* two approaches, namely top-down or bottom-up synthesis techniques **(figure 8)**[66]. Top-down techniques include arc discharge, laser ablation and electrochemical oxidation. This approach entails the breaking of carbon-based structures, such as graphite and carbon nanotubes, into smaller components and eventually leads to the formation of CDs. While this approach allows for high material yield and a CD structure that bears resemblance to the starting material, the resultant CDs often exhibit large size distributions and require post-synthesis modification to enhance their low fluorescence quantum yield. Alternatively, bottom-up techniques include microwave, hydrothermal and ultrasonic syntheses. This approach consists of simple molecules as starting materials such as citric acid, which is commonly used as a carbon rich backbone. Furthermore, synthesis modification can easily be implemented through addition of different precursors that possess heteroatoms that could be used to passivate the surface or the

Figure 8. Top-down and bottom-up approaches for the synthesis of carbon dots (figure adapted from De *et al*.). [66]
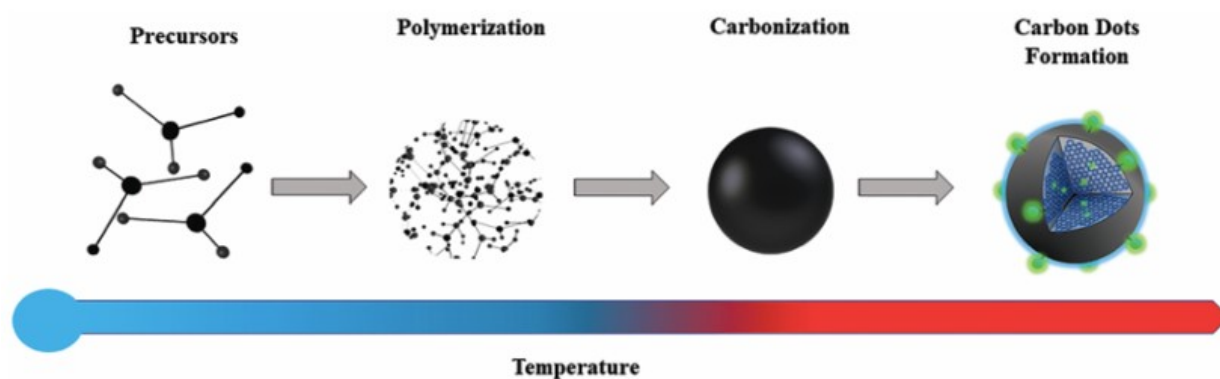
Figure 9. Series of steps for the formation of CDs *via* the bottom-up approach (figure adapted from de Medeiros *et al.*). [67]

internal structure of the CDs. This approach forms CDs through a series of steps that encompass condensation, cyclization, polymerization and carbonization **(figure 9)**.[67]

1.5.2 – Microwave-assisted Synthesis of Carbon Dots

Microwave-assisted syntheses offers several advantages over other synthetic approaches. CD formation typically occurs using rapid reaction times of 5-20 min, this being due to very efficient and uniform heating of starting materials by the microwave radiation **(figure 10a)**. Upon absorption of microwave radiation, chemical compounds will align their electric dipole with the electric field of the incoming radiation, this movement generates heat through molecular rotation. For the heating to be 100% efficient, laboratory microwaves require the usage of microwave transparent reaction vials as the reaction vessel in order to properly heat the substrates. This approach has some limitations, one being the need for polar molecules as the starting material or solvent since a dipole is necessary to efficiently absorb microwave radiation. Most synthesis microwaves also possess a pressure cut-off of ~300-500 psi, limiting the use of some low-boiling point solvents at high temperatures. Industrial usage of microwave synthesis does limit large-scale

production due to the small microwave radiation penetration depth, which significantly impacts the scale at which a reaction can be performed and thus limiting the yield obtained.

1.5.3 – Hydrothermal Synthesis of Carbon Dots

Hydrothermal synthesis of carbon dots is a much more robust process since pressures can reach as high as 3000 psi, 10-fold that of microwaves. This high pressure may promote some interesting chemical reactions and endow new properties that may be not be achievable through other synthetic methods. This process heats the starting material through thermal/bulk heating, which is nonuniform and occurs through a thermal gradient, thus increasing the chances of unreacted intermediates that will need to be purified post synthesis **(figure 10b)**. However, on an industrial scale this approach is much more feasible since large autoclaves are often used in industrial processes and would enable a large amount of material to be produced at once, limiting operational costs.

(a)   **(b)**
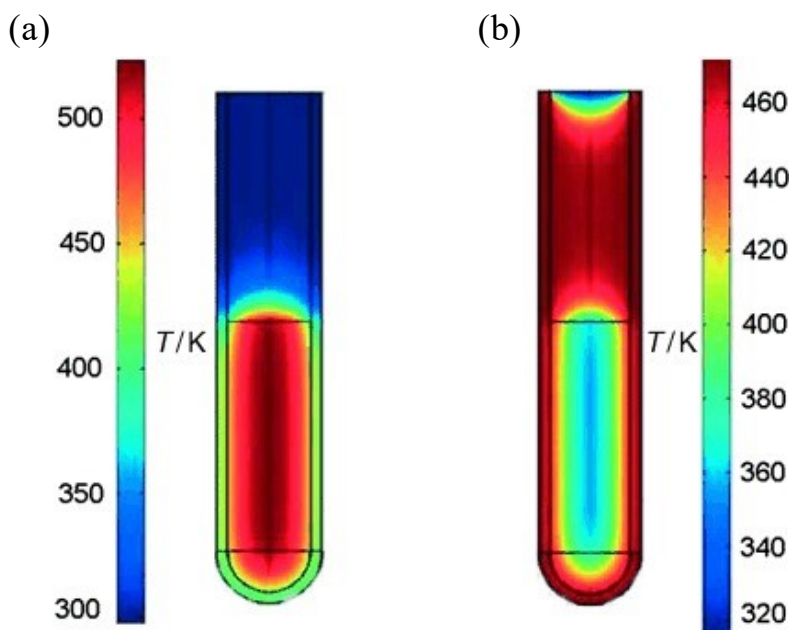
Figure 10. (a) Temperature gradient for microwave-assisted reactions, representing the uniform and efficient heating of the solution. (b) Temperature gradient for hydrothermal-assisted reactions, representing thermal heating where the vessel is heating first and then there is an inefficient heat transfer to the solution (figure adapted from Kappe *et al.*).[68]

1.5.4 – Biomass-derived CDs

In light of the versatile and facile synthetic procedures used for CD synthesis, many researchers are focusing on the synthesis of CDs using green and sustainable precursors such as orange[61] and lemon juice[69], honey[70], coal[71] and agricultural waste[72–74]. The goal is to produce CDs that have high fluorescence quantum yields along with distinct physical and structural properties. Biomass-derived CDs stemming from agricultural waste such as lignin and cellulose precursors are an interesting option that utilizes forestry waste and scraps that would alternatively remain unused and require costly disposal procedures. Rai *et al.* developed CDs through a microwave-assisted reaction using an aqueous dispersion of lignosulfonate lignin as the sole reactant. These lignin-derived CDs were determined to be a green, cost-effective and water soluble alternative for bioimaging applications and showed good biocompatibility and high photostability.[72] Chen *et al.* synthesized oxidized CDs via a hydrothermal-assisted reaction using Kraft lignin and hydrogen peroxide as a powerful oxidizing agent. These CDs were investigated for their potential in bio-imaging of HeLa cells and exhibited environmental friendliness, low toxicity and good water solubility while maintaining excellent bioimaging capabilities.[73] Souza *et al.* synthesized oxygenated CDs through carbonization of cellulose in a highly acidic media, resulting in a high degree of surface functionalization with carboxylic acids, lactones and phenols. Additionally, the carboxylic acid moieties were used to covalently modify the CD surface with PEG1500N resulting in an increase in amine and amide groups that passivated the surface and enhanced the quantum yield.[74] Utilizing biomass sources as CD precursors can greatly lower their production costs, as well as render them a sustainable and a viable option for green applications.

1.5.5 – Tailoring the CD Surface Chemistry

One of main advantages of CDs is the ease of surface modification, which allow for decoration with a myriad of functional groups. Modification of the CD structure and surface chemical properties can be altered during synthesis upon careful selection of precursors used during synthesis. Yu *et al.* produced amino acid-derived CDs through a microwave-assisted reaction and altered the degree of carbon and nitrogen content introduced in the CD structure by choosing amino acids with increasing amounts of carbon or nitrogen.[75] Through x-ray photoelectron spectroscopy (XPS) analysis, the authors confirmed that as the carbon or nitrogen content in the amino acid precursor increased so did the relative carbon or nitrogen contents present in the CDs.[75] Similarly, hydrophobic CDs were also synthesized via a microwave-assisted synthesis using a polaxamer, PF-68, and phosphoric acid as the reaction solvent. This endowed the surface of the CD with a hydrophobic nature that were dispersible in a range of hydrophobic solvents such as acetone, toluene, hexane, and THF.[76] Furthermore, CD surface chemistry can be altered by simply altering the precursor concentration used during the synthesis of the CDs. For example, while using citric acid and diethylenetriamine (DT3) as precursors for amine-passivated CDs, citric acid was added at a constant amount and the DT3 concentration was varied.[77] This variation in precursor concentration led to CDs with both carboxylic acid and amides present on the surface and as DT3 concentration increased, consequently so did the degree of amides present on the surface, as confirmed through FT-IR **(figure 11a)**. The same effect was observed when varying reaction temperature, noticing a decrease in carboxylic acid functionalization as temperature increased **(figure 11b)**. Alternatively, post-synthetic modifications can also be carried out to achieve a similar outcome. CDs have been synthesized *via* electrochemical oxidation of a graphite rod, which resulted in CDs with alcohols and carboxylic acids present on the surface.[78]

Post synthesis, the CDs were refluxed in a H_2SO_4 solution to endow acidic SO_3H groups on the surface and turn them into acid-catalysts for a room temperature ring-opening reactions.[78]

This being said, the surface and structural composition of CDs can easily be tuned and modified through pre- or post-synthesis modification in order to tailor their chemical properties and endow them with specific groups that can be used in a multitude of specific applications. Surface chemistry is extremely important in applications such as catalysis where the surface dictates if a substrate can efficiently be adsorbed or not.
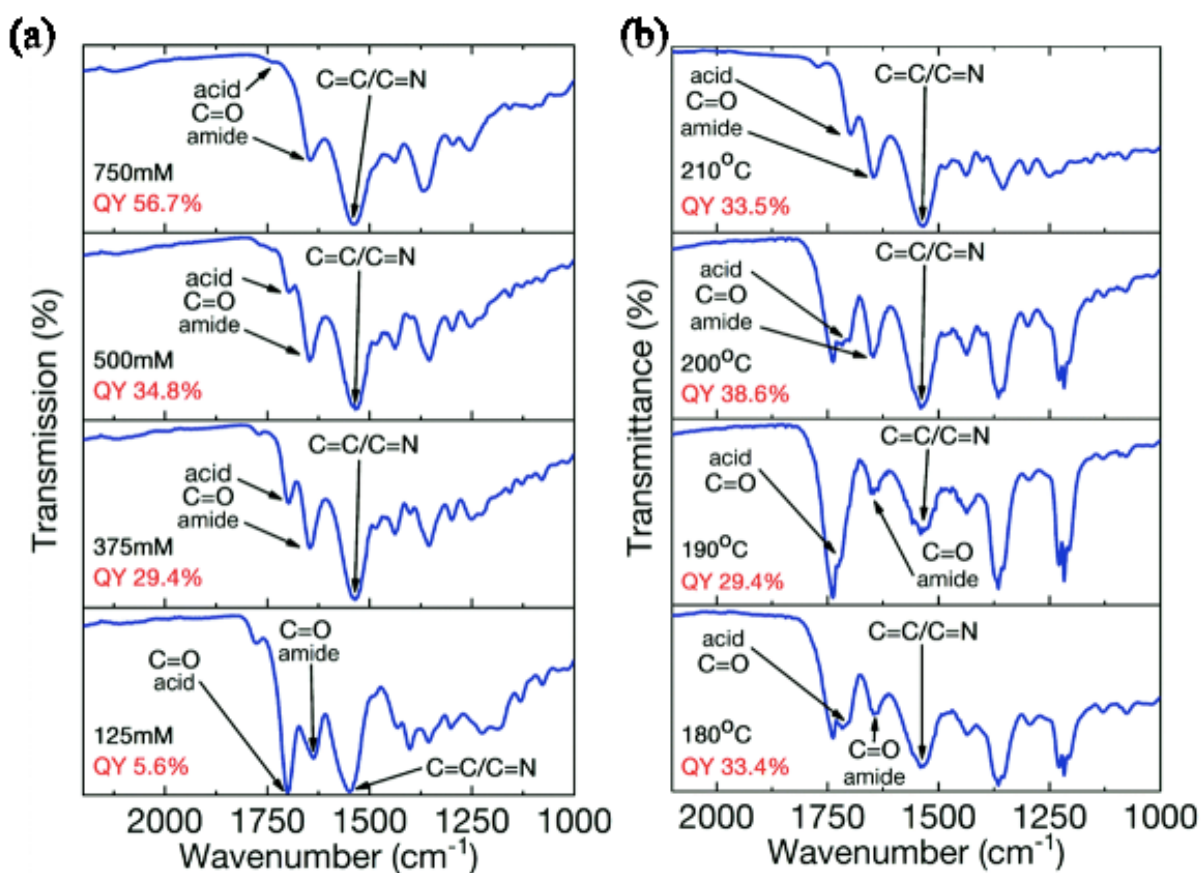
Figure 11. (a) Effect of [DT3] on the degree of CD surface functionalization with carboxylic acids/amides (figure adapted from Manioudakis et al.).[77] (b) Effect of reaction temperature on degree of CD surface functionalization with carboxylic acids/amides (figure adapted from Manioudakis et al.).[77]

1.5.6 – Carbon Dots as Heterogeneous Catalysts

Due to their versatile and tunable surface chemistry, CDs have recently garnered interest as heterogeneous catalysts for a multitude of different chemical reactions.[79] Their facile synthesis, ability to be synthesized from an abundance of chemicals and renewable materials allow CDs to be particularly advantageous in larger scale, robust industrial reactions.

CDs are most commonly used as photocatalysts due to their interesting optical properties and have been reported as photocatalysts for a number of reactions including water splitting[80,81], CO_2 reduction[82,83], and dye degradation[84,85]. Usually, for carbon dots to be rendered photo-catalytically active, they are often doped with heavy metals and/or are formed as hybrids with other materials such as carbon nitrides and carbon nanotubes. Recognizing the potential for metal-free and greener alternatives, carbon dots, containing no presence of heavy metals and little to no toxicity, are being explored as novel organocatalysts for multiple synthetic reactions. CDs can act as acid catalysts by containing Brønsted acid groups on the surface which inherently enhances the electrophilicity of the CD towards a nucleophilic moiety.[79] Majumdar *et al.* investigated the acidic surface properties stemming from surface carboxylic acid groups on CDs synthesized from b-carotene and their catalytic efficiency towards aza-Michael and condensation reactions.[86] CDs have also been reported as hydrogen bond catalysts between itself and the electrophilic substrate.[79] Mayank *et al.* synthesized CDs via pyrolysis of citric acid resulting in a highly hydroxyl-functionalized surface capable of acting as proton donors to successfully synthesize 4*H*-chromene derivatives.[87] Lastly, CDs have been reported as aminocatalysts due to high degrees of primary and secondary amine surface groups, capable of catalyzing aldol-type reactions. Pei *et al.* utilized amino functionalized CDs, synthesized from citric acid and diamine to catalyze Knoevenagel

condensation reactions and resulted in yields of up to 95.2% and 93.7% along with post catalyst reusability for 6 reaction cycles.[88]

The increasing interest into the catalytic applications of CDs as heterogeneous alternatives for organosyntheses has driven the scientific thrust for their investigation in a myriad of different chemical reactions. One avenue that remains rather unexplored is the catalytic potential of CDs towards the transesterification and esterification reactions; however, based on the aforementioned works, it remains a promising alternative to conventionally used homogeneous catalysts.

1.6 – Statement of Problem

Understanding the importance of dwindling fossil fuel reservoirs and the urgent search to find efficient and renewable sources of energy, biodiesel is a promising candidate that in itself is both sustainable and renewable. Currently, the biodiesel production process is not considered to be a viable and economically feasible alternative to petro-diesel and for this reason its production and application has been rather limited. While homogeneous catalysts are widely used for a number of industrial applications, their use as catalysts for the transesterification of refined vegetable oils to biodiesel leads to a very costly production and tedious purification process coupled to the inability to regenerate and reuse the catalyst for subsequent reactions. While many heterogeneous catalysts have been proposed, they often lack a sustainable arm to their synthesis and the catalyst often contains metals, which entails additional challenges.

In this work, the design and synthesis of CDs was conducted using simple and commercially available precursors in order to develop a cost-efficient and effective heterogeneous catalyst for the transesterification reaction of canola oil to biodiesel. Both microwave and hydrothermal -assisted reactions were used for CD synthesis and characterization techniques such

as FT-IR, zeta potential, and CHNS analysis were instrumental in understanding the catalytic mechanism of the CDs and to investigate how their surface chemical properties are playing a role in the transesterification reaction. Guided by mechanistic studies, an iterative approach is employed for the synthesis of the CD catalyst in order to fine tune its surface chemistry to ensure maximum biodiesel conversion. The work also investigates catalyst recovery and reusability and evaluate the potential for changes in catalytic activity. Lastly, we turn our focus to sustainable materials such as lignin and glycerol as CD precursors to show how the biodiesel production life cycle could be shifted to a fully sustainable paradigm.

Chapter 2 – Experimental Procedures

2.1 – Materials and Reagents

Glycine ($\geq$ 99.0%), citric acid ($\geq$ 99.5%), sodium citrate tribasic dihydrate ($\geq$ 99.0%), and lignin-alkali were purchased from Sigma-Aldrich. Sodium hydroxide solution, methanol and glycerol ($\geq$ 99.0%) were purchased from Fisher Scientific. Food grade canola oil was purchased from a grocery store. The cellulose dialysis membrane (molecular weight cut-off = 3.5-5.0 kDa) was purchased from Spectrum Labs. All the chemicals were used without further purification.

2.2 – The Thermal-Mediated Synthesis of CDs

2.2.1 – Synthesis of Glycine-Derived CDs (GlyCDs)

GlyCDs were synthesized *via* a one-step hydrothermal reaction. Briefly, 8.0 mL of sodium hydroxide solution (5 mM) was added to 2.4 g of glycine and gently stirred for 5 min. This was followed by the addition of 9.6 g of citric acid and 100.0 mL of deionized water to the reaction vessel and was stirred until it was clear and homogeneous. The solution was then transferred to the hydrothermal reactor and heated at 210 °C under stirring (550 rpm) for 4 h. The reaction was left to cool to room temperature and the CD solution was dialyzed for 4 days against water, changing the water once a day, to remove unreacted precursors and fluorophores. Next, the sample was washed multiple times with acetone (1:10 v/v) to remove any remaining impurities. After each wash, the precipitate was collected by centrifugation at 10 000 x g for 10 minutes. The brown precipitate was dried in an oven at 80 °C for 24 h with a reaction yield of approximately 10%.

2.2.2 – Synthesis of Lignin-Derived CDs (LCDs) and Base-Activated LCDs (LCDs-b)

LCDs were synthesis *via* a one-step microwave reaction. Briefly, a 1:1 molar ratio of sodium citrate and lignin were added to 10 mL of Milli-Q-purified water and 0.5 mL of H_2O_2 in a 35 mL microwave transparent vial. The reaction was heated at 210 °C for 10 minutes under rapid stirring using a CEM Discover SP microwave synthesis reactor. Upon cooling to room temperature, the reaction mixture was dialyzed for 4 days against 1L of Milli-Q water, changing the water every 12 hours, thus, allowing for the removal of unreacted precursors and polar impurities. Upon dialysis, the LCD mixture was placed in an oven at 85°C and allowed to concentrate down to 5 mL. Subsequently, the LCDs were further purified using three acetone organic washes (1:10 v/v), removing any remaining organic impurities. Upon addition of acetone, the sample was vortexed for approximately 30 seconds and centrifuged at 10 000 × g for 10 minutes. The supernatant was discarded, and the pellet was subjected to two more washes. Upon completion, the resulting black precipitate consisting of purified LCDs were dried in an oven at 80 °C for 24 hours, resulting in a dark brown fine powder with a yield of approximately 10%.

For the synthesis of LCDs-b, briefly, 0.5 g of LCDs were dispersed in 10 mL of Milli-Q water and sonicated for 10 minutes to ensure a homogeneous solution. A pH electrode was used to determine the initial pH of the aqueous LCD dispersion and a 0.1% NaOH solution was added dropwise to the samples under constant stirring until the pH of the solution was raised by approximately 2 pH units. The samples were further purified using three acetone organic washes, using the same procedure employed during the original purification protocol for LCDs (final pH ~ 12.8).

2.2.3 – Synthesis of Glycerol-Derived CDs (GCDs)

GCDs were synthesized *via* a one-pot microwave-assisted reaction. Briefly, 2.0 mL of glycerol was added to 0.3, 0.6 or 1.2 g of sodium citrate (GCDs-0.3, GCDs-0.6, GCDs-1.2) in 2.0 mL of Milli Q deionized water and gently stirred in the microwave reaction vessel for 5 min to ensure a homogeneous solution. This solution was then transferred to the CEM Discover SP microwave synthesis reactor and heated at 210 °C for 20 min under vigorous stirring. The crude CD solution was dialyzed for 3 days against water, changing the water once a day, to remove unreacted precursors and fluorophores. Next, the sample was washed multiple times with ethanol (1 : 10 v/v) to remove any remaining impurities and unreacted precursors. After each wash, the precipitate was collected by centrifugation at 10 000 × g for 10 minutes. The brown precipitate was dried in an oven at 80 °C for 24 h with a reaction yield of approximately 10%.

2.3 – Biodiesel Synthesis and Reusability Procedure

2.3.1 – Biodiesel Synthesis Using Solvothermal Approach

Varying amounts of CDs (0.1-20 wt% relative to oil), was added to methanol (molar ratio 1:18-1:60 oil to methanol) and sonicated for 5 min until a homogeneous dispersion was obtained. The CD/methanol solution was then added to 2.0 mL of canola oil and the mixture was transferred to a 25.0 mL hydrothermal reactor. The reactor was heated at 65-150 °C for 1-3 h, under vigorous stirring at 550 rpm. Following reaction completion, the reactor was cooled to room temperature and the reaction mixture was transferred to a 15 mL centrifuge tube and placed in a 70 °C oven to allow the residual methanol to evaporate. The top phase (i.e. the biodiesel) was separated by centrifugation at 10 000 × g for 5 minutes from the lower CDs-glycerol layer and was further used for ^{1}H NMR analysis.

2.3.2 – Biodiesel Synthesis Using Conventional Heating Approach

Varying amounts of CDs (1-3 wt% relative to oil), was added to methanol (molar ratio 1:9-1:72 oil to methanol) and sonicated for 5 min until a homogeneous dispersion was obtained. Subsequently, 2.0 mL of canola oil and the CD dispersion were simultaneously transferred to a 10 mL vial with a crimped cap. The vial was transferred to a reaction block heated at 90 °C for 2 - 6 h, under vigorous stirring at 550 rpm. Upon completion of the reaction, the vial was removed from the reaction block and cooled to room temperature. The reaction mixture was transferred to a 15 mL centrifuge tube and placed in an oven at 70 °C for 12 hours to ensure excess methanol evaporation and separation of the glycerol/CDs and biodiesel phases. The mixture was then centrifuged at 10 000 × g for 5 minutes to further separate the layers and the biodiesel layer was collected for ^{1}H NMR analysis.

2.3.3 – CD Recovery and Reusability Procedure

Upon layer separation by centrifugation, the biodiesel layer was removed and the CD/glycerol layer was subjected to three organic washes using hexanes in order to remove any excess biodiesel remaining in the glycerol phase. After each wash the sample was centrifuged at 10 000 × g for 5 minutes and the hexanes layer was decanted. The CD/glycerol layer was used for subsequent transesterification reactions by transferring it to a reaction vial with 2.0 mL of canola oil.

2.4 – Characterization Techniques

2.4.1 – Agarose Gel Electrophoresis Analysis

Aqueous CD dispersions, prepared at different concentrations, were loaded into the wells of a 1% agarose gel at pH 7.4. Electrophoresis was performed at a voltage setting of 90 V for 25 minutes using a Mini-Subs GT Cell and a PowerPact Basic power supply, both from Bio-Rad. Gel-separated CDs were visualized in a UV box at an λ_{ex} of 365 nm.

2.4.2 – Transmission Electron Microscopy

CDs were dispersed in MeOH at a concentration of 10.0 $mg.mL^{-1}$. TEM grids were prepared by pipetting 10.0 mL of the CD solution on a 300 Mesh Cu (Cu-300HD) coated with a holey/thin carbon film (Grid Tech). The solvent was allowed to evaporate prior to analysis. TEM analysis was carried out using an LVEM5 benchtop electron microscope operating at 5 kV. Size distribution analysis was carried out using Fiji imaging software.

2.4.3 – X-ray Diffraction

XRD spectra were acquired using a 2nd Gen D2 Phaser X-ray diffractometer (Bruker AXS). A Cu Kα source at a generator power of 30 kV/10 mA, a scan range from 10 to 80° (2θ) with a step size of 0.10° per 2 s, and a position sensitive detector opening of 4.79° were used during analysis. All data was processed using the Bruker DIFFRAC software.

2.4.4 – Thermogravimetric Analysis

Thermogravimetric analysis was carried out using a TGA Q500 analyzer from TA instruments. Samples were heated from 25 to 900 °C at a heating rate of 5 $°C.min^{-1}$ under an N_2 atmosphere with a flow rate of 50 $mL.min^{-1}$. Analysis was performed by Dr. Galyna Shul at Université du Québec à Montréal.

2.4.5 – X-ray Photoelectron Spectroscopy

XPS analysis of GlyCDs was acquired using a Thermo Scientific Kα X-ray photoelectron spectrometer. Each analysis was carried out on three different points of the sample, in triplicate, with 10 runs for each scan. The averages were plotted for both the survey and high-resolution scans. Analysis was performed by Dr. Lihong Shang at McGill University.

2.4.6 – Fourier-Transform Infrared Spectroscopy

FT-IR spectra were collected using a Thermo Scientific Nicolet iS5 equipped with an iD5 ATR accessory. Spectra were collected using 64 scans with a resolution of 0.4 cm^1, a gain of 1, an optical velocity 0.4747 and an aperture setting of 100. Data was processed using Omnic 9 software.

2.4.7 – ^{1}H Nuclear Magnetic Resonance Spectroscopy

Quantitation and composition of biodiesel was determined using a Bruker Fourier UltrashieldTM operating at 300 MHz. Sample analysis was carried out using the Mestrelab Mnova software. All samples were prepared in $CDCl_3$ for analysis. A calibration curve was obtained by preparing 10 known sample mixtures of methyl oleate and canola oil from 0% to 100% methyl oleate. The ratio between the integrated peaks at 3.7 ppm and 2.3 ppm were calculated and plotted against the known percentage of methyl oleate present in the sample. This method was also used to quantitate the conversion of biodiesel obtained through the CD-catalyzed transesterification reactions. In this case, the ratio of the integrated peaks (3.7 ppm/2.3 ppm) was calculated and the percent conversion value was obtained from the linear regression equation of the calibration curve **(figure 30c)**.

2.4.8 – Zeta Potential Analysis

Zeta potential measurements were carried out using a Zeta Sizer from the Malvern Instruments-Nano Series. The samples were dispersed in methanol at a concentration of 5.0 mg.L^{-1}. Twenty runs were performed for each measurement in triplicate, and the average result was used.

2.4.9 – Elemental Analysis

Elemental analysis was carried out using a vario MICRO cube elementar instrument (Elementar). Approximately 3.0 mg of each sample was weighted and subjected to the quantitative high-temperature decomposition under oxygen atmosphere. The gaseous components of the sample were separated and quantified using a direct Temperature Programmed Desorption (direct TPD) column. The samples were analyzed in triplicates and the results averaged. Analysis was performed by Dr. Anne-Laure Larroque at McGill University Health Centre – Research Institute.

2.4.10 – Gas Chromatography Analysis

For the GC-MS analysis, an Agilent 7890A instrument was used coupled to an Agilent 5975C mass spectrometer. A HP-5ms GC column was used, with a length of 30 m and diameter of 0.250 mm. Helium was used as the carrier gas. The column flow was 1.7 mL.min^{-1}.

Chapter 3 – Results and Discussion

3.1 – Synthesis and Characterization of Carbon Dots

3.1.1 – Synthesis and Characterization of Glycine-Derived CDs

The synthesis of Glycine-derived CDs (GlyCDs) was adapted from a protocol by Sarkar *et al.*[89] in which hydrophobic carbon dots were synthesized through a multi-step pyrolysis method and were used as micelle templating agents. GlyCDs were synthesized *via* a one-pot hydrothermal reaction, at 210 °C for 4 hours, using glycine, citric acid and sodium hydroxide as precursors. Upon reaction completion, the crude solution underwent purification protocols such as dialysis, to remove polar and membrane permeable precursors and intermediates, and subjected to organic washes using acetone to ensure removal of nonpolar impurities. Upon purification, the sample was then dried in an oven at 80 °C for 24 hours. The hydrothermal route offers several advantages namely as it is a one pot synthesis, can be used for larger sample volumes and is relatively inexpensive. While microwave syntheses provide more efficient heating and quicker reaction times, their adoption on an industrial scale is not completely feasible, corroborating the use of a hydrothermal approach. A schematic representation of the synthesis procedure for GlyCDs is given in **figure 12**. The addition of NaOH during synthesis was necessary to provide a basic environment in which the carboxylic acid groups of the precursors would become deprotonated, providing a
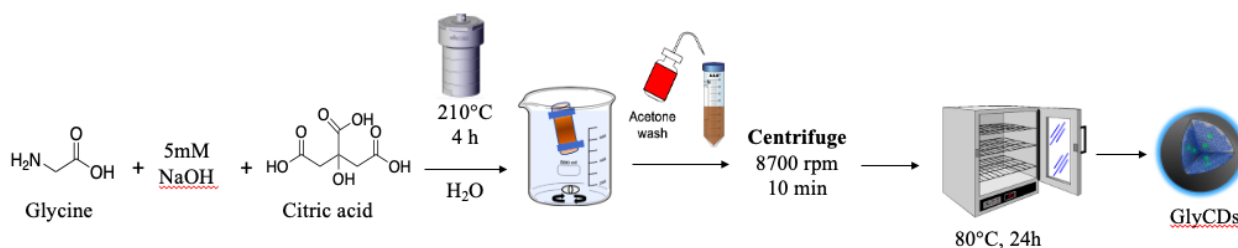
Figure 12. Schematic representation of the GlyCDs synthesis protocol.

negatively charged CD surface to act as the catalytic active site. The synthesized GlyCDs were a brown/orange color and consisted of a powdered texture. In order to confirm the formation of negatively charged nanoparticles, an agarose gel electrophoresis analysis was conducted on an aqueous solution of GlyCDs **(figure 13a)**. The gel was visualized under a UV box at an λ_{ex} of 365 nm, which showed the CD band migrating towards the positive electrode and confirming its negative surface charge. FT-IR analysis was performed on the precursors, glycine and citric acid, used to synthesize the GlyCDs **(figure 13b)**. When synthesizing CDs, the precursors chosen are used to endow the different types of functional groups that will be present on the surface of the CD. In the case of GlyCDs, a highly negatively charged and oxygenated surface was sought after and therefore citric acid was used as not only the rich carbon source but also as a carboxylic acid
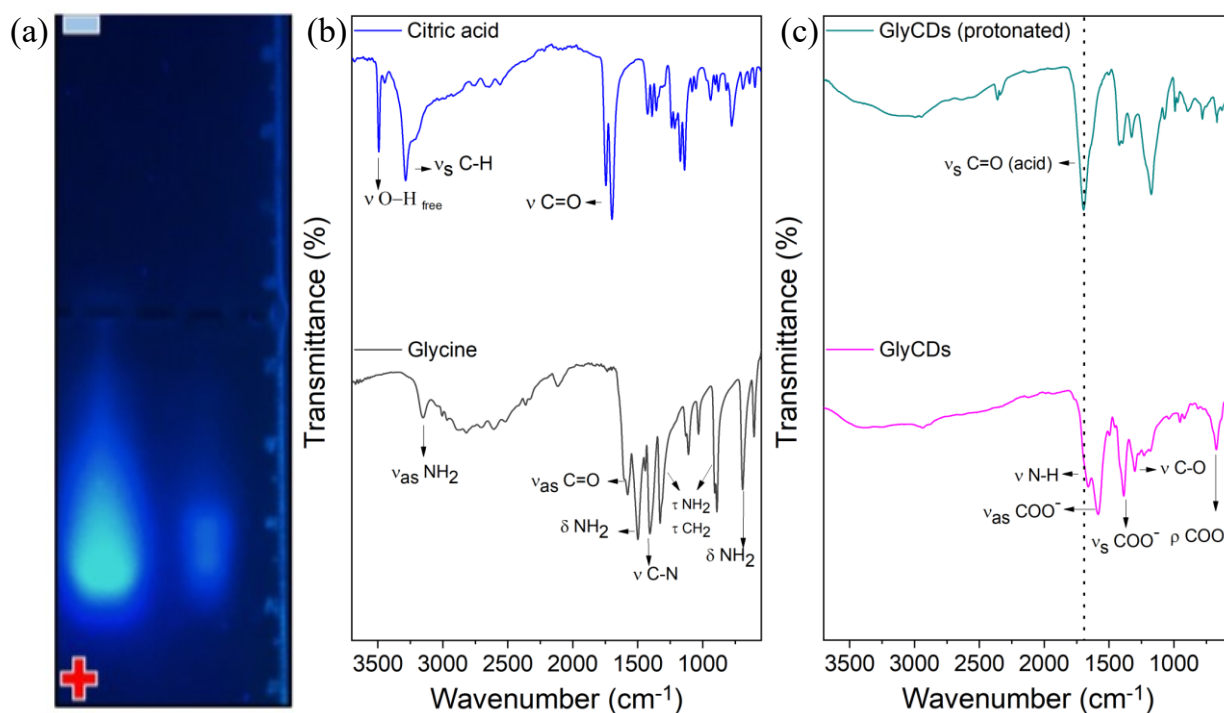
Figure 13. (a) 1% agarose gel electrophoresis conducted at pH 7.4 using two different concentrations of GlyCDs. The results show the GlyCDs migrating towards the positively charged anode indicating they are negatively charged. (b) FT-IR spectra of the precursors, citric acid and glycine, used to synthesize GlyCDs. (c) FT-IR spectra of GlyCDs (protonated) and GlyCDs, depicting the difference in surface chemistry upon addition of NaOH during synthesis.

and highly oxygenated source. Glycine was used as a small simple molecule that can be used as a nitrogen and oxygen source to aid in the structural formation of CDs, otherwise a synthesis consisting of only citric acid results in an extremely low yield after purification. FT-IR analysis was carried out for the GlyCDs and the protonated GlyCDs (+GlyCDs) in order to observe the difference in surface chemistry upon deprotonation with NaOH during synthesis **(Figure 13c)**. The principal difference illustrated was the disappearance of the symmetric stretching vibration at 1690 cm^{-1} associated with the carbonyl of the carboxylic acid for the +GlyCDs which, upon deprotonation, causes the formation of a carboxylate functional group, confirmed by the asymmetric and symmetric stretching vibrations at 1580 cm^{-1} and 1390 cm^{-1}, respectively. Furthermore, the GlyCDs also demonstrate the stretching vibration associated to the N-H and C-O groups at 1670 cm^{-1} and 1304 cm^{-1}, respectively. GlyCDs were further characterized according to their size and morphology. Transmission electron microscopy (TEM) allows for the visualization and size determination of a material through the transmission and diffraction of electrons. By TEM **(figure 14a)**, monodisperse quasi-spherical dots with an average size of 10.9 ± 2.8 nm are observed while particle size distribution analysis reveals a Gaussian size distribution **(figure 14a inset)** ranging from 6–16 nm. X-ray diffraction (XRD) was used in order to investigate the structural nature of GlyCDs. This technique involves the irradiation of the sample with a monochromatic source of x-rays from a copper K$_\alpha$ radiation source. Upon irradiation, the x-rays will interact with the sample at different angles which results in interactions with the electrons present in the material and results in coherent scattering of x-rays when constructive interference occurs at specific angles. XRD analysis confirmed the amorphous nature and the absence of significant long-range order for the GlyCDs **(figure 14b)**, as confirmed by the broad reflection centered at 30 °2θ. A lack of crystallinity is characteristic property for carbon dots and remains
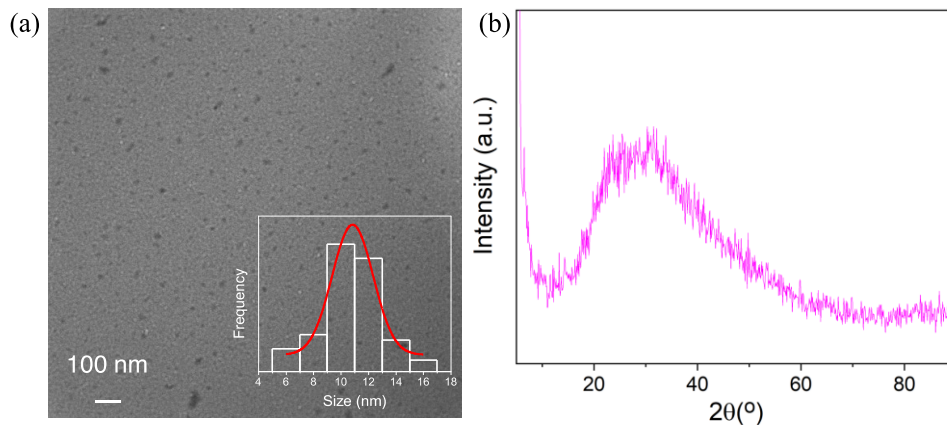
Figure 14. (a) TEM image of a 1 mg.mL^{-1} dispersion of GlyCDs dispersed in MeOH. (b) XRD diffraction pattern for GlyCDs, demonstrating their amorphous nature due to the broad pattern observed centered at 30 °2θ.

fairly consistent in the literature.[52,90,91]

In order to corroborate the FT-IR findings, X-ray photoelectron spectroscopy (XPS) was carried out on the GlyCDs **(figure 15)**. XPS analysis is an extremely useful technique for the chemical characterization of carbon dots. In brief, during the course of analysis, the material is irradiated with a monochromatic source of X-rays from a Mg K$_\alpha$ photon source. The x-ray irradiation results in the ejection of a core electron from the atoms comprising the material. Core electrons have characteristic binding energies and are not affected by the chemical composition of their environment, providing valuable information on the types of functional groups present on the surface of the material. The X-ray penetration depth in the sample is on the order of a micrometer; however, useful electron signals are usually obtained from a depth of up to 10 nm, therefore for most materials XPS is primarily a surface technique and would not provide much information about the core of a material. Considering the average size of a carbon dot is ~10 nm, XPS can provide valuable information on the types of functional groups present in the core and surface of the dots. The XPS survey scan revealed five binding energies at 1071.64, 532.39, 498.03, 399.63, and 286.94 eV corresponding to sodium (Na1s), oxygen (O1s), sodium (Na KLL), nitrogen (N1s)

37

and carbon (C1s), respectively. High resolution XPS (HR-XPS) analysis of the binding energies present in the survey spectrum and subsequent deconvolution of the observed peaks was used to determine the chemical states at the surface (and core) of the CDs. Upon deconvolution of the O1s peak, three binding energies are observed at 530.81, 531.87 and 535.29 eV, attributed to the presence of C=O, COOH functional groups and residual sodium. The residual sodium behaves as counter ions to stabilize the carboxylates present on the CD surface. Deconvolution of the N1s peak shows three binding energies observed at 398.19, 399.62, and 400.54 eV and are attributed to pyridinic nitrogen, benzenoid amines and graphitic nitrogen, respectively. Deconvolution of the C1s peak shows four binding energies at 284.66, 285.52, 286.10 and 287.79 eV and are attributed
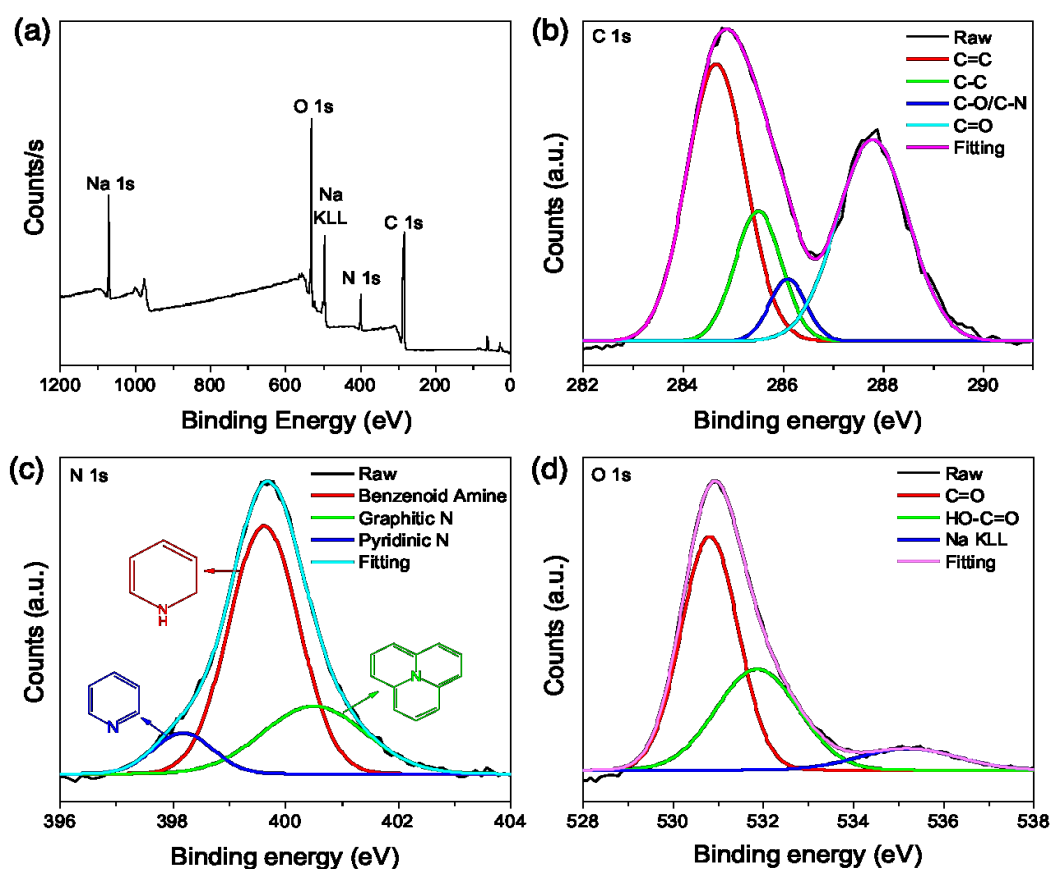
Figure 15. (a) XPS survey scan of GlyCDs revealing five binding energies ascribed to Na1s, O1s, Na KLL, N1s and C1s. Deconvoluted spectra of HR-XPS shows (b) C1s binding energy maxima at 286.94 eV; (c) N1s binding energy maxima at 399.63 eV; (d) O1s binding energy maxima at 532.39 eV.

to C=C, C–C, C–O/C–N and C=O functional groups, respectively.

As the transesterification reaction is carried out at temperatures of nearly 150 $^\circ$C, thermogravimetric analysis (TGA) was carried out to determine the thermal stability of the carbon dots. The TGA thermogram shows a three-step decomposition profile **(figure 16)**. The initial 9.2% weight loss observed at 140 $^\circ$C can be attributed to the removal of water molecules adsorbed on the surface of the carbon dots. The second weight loss (36.2%) was noted at 385 $^\circ$C and attributed to the onset of decomposition of the surface moieties. The third weight loss step occurs at 795 $^\circ$C and accounts for 42.6% of the total weight loss, indicating that the CD core has decomposed. The residual weight at 900 $^\circ$C is due to the Na^+ ions present on the surface of the carbon dots, due to the use of NaOH during CD synthesis thus causing the Na^+ ions to interact electrostatically with the negatively charged carboxylates surface groups. The presence of Na^+ ions is in accordance
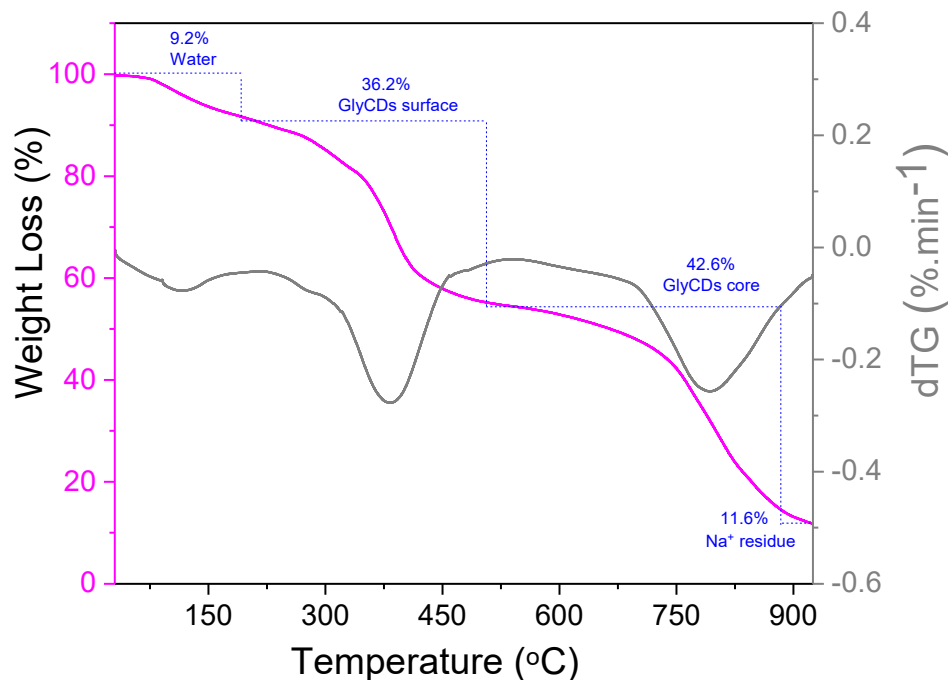
Figure 16. Thermogravimetric analysis of GlyCDs showing a three-step decomposition weight loss pattern. The first weight loss (9.2%) occurs at 140°C, the second weight loss (36.2%) occurs at 385°C, and the third weight loss (42.6%) occurs at 795°C.

39

with the XPS data that shows the presence of Na KLL and 1s electron orbitals. The elemental composition of the GlyCDs was investigated through elemental CHNS analysis in order to gain more insight on the atomic composition of the CDs. **Table 2** summarizes the results, indicating a rather high oxygen content approximately equal to carbon, which may seem surprising; however, it is not unexpected when taking into account the precursor used during synthesis, citric acid, not only a rich source of carbon but also of oxygen.

Table 2. Elemental composition analysis for GlyCDs.

C (%)	H (%)	N (%)	S (%)	O (%)
38	4	6	0	40

3.1.2 – Synthesis and Characterization of Lignin-Derived CDs

One of the most positive attributes of CDs is the ability to prepare them from a variety of raw and waste materials. A unique and fully sustainable process for biodiesel production would be the use of a catalyst that was synthesized solely from renewable and raw materials such as lignin and cellulose for example. Lignin is an aromatic biopolymer derived from forestry waste and by products of the pulp and paper industry. Its structure is primarily composed of three main monomers, coniferyl alcohol, sinapyl alcohol and *p*-coumaryl alcohol **(figure 17a)**, to form a large polymeric structure rich in carbon primarily linked by ether linkages with some hydroxyl groups that may be used for covalent functionalization **(figure 17b).**[92] For this reason, its use as a rich carbon source for the production of CDs is an interesting route to be investigated as it would
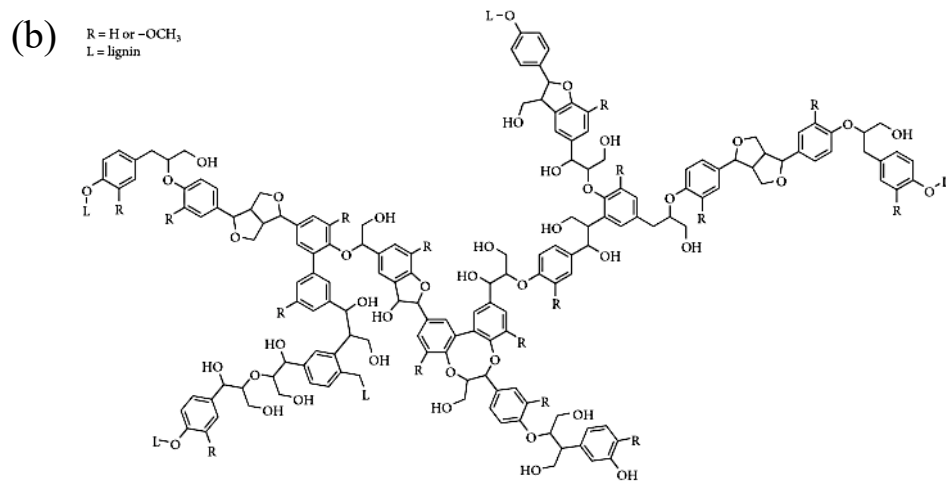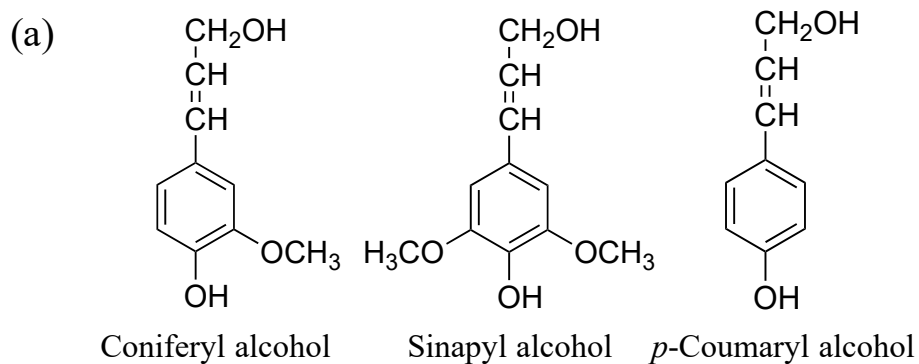
Figure 17. (a) Monomeric units used to compose the polymeric structure of lignin. (b) Representation of the highly aromatic network composing lignin's structure (figure adapted from Lu *et al.*).[92]

provide the possibility for environmentally benign design and synthesis of sustainable CDs. Guo *et al.* synthesized a lignin-derived carbonaceous catalyst in which the material underwent an acidic treatment with sulfuric acid in order to functionalize the surface with sulfonic acid groups and endow the material with strong acidic properties with the ability to catalyze the esterification reaction.[93] Pua *et al.* also synthesized a lignin-derived heterogeneous catalyst by treating Kraft lignin with phosphoric acid and sulfuric acid at high temperatures to endow the surface of the catalytic material with strong acidic groups that would participate in the esterification of FFAs.[43]

The abovementioned works demonstrate promising results on the utilization of lignin for a more sustainable production of biodiesel and shows how lignin's structure can be chemically altered to for a specific application.

Lignin-derived CDs (LCDs) were synthesized *via* a microwave-assisted reaction of alkali lignin and sodium citrate in a 1:1 molar ratio and hydrogen peroxide **(figure 18)**. The crude CD reaction mixture underwent significant purification through dialysis to remove water soluble intermediates or remaining unreacted sodium citrate and organic washes using acetone to remove hydrophobic impurities and unreacted lignin. The precipitate obtained after the washing and centrifugation steps was dried in an oven to allow for acetone evaporation.

LCDs were expected to have similar surface chemistry as the GlyCDs. FT-IR confirms the presence of carboxylate moieties, introduced due to sodium citrate, as shown by the asymmetric and symmetric stretching vibrations associated with the COO$^-$ groups at 1580 cm^{-1} and 1390 cm^{-1}, respectively, as well as the symmetric stretching vibration ascribed to C-O bonds at 1135 cm^{-1} **(figure 19a)**. There were no significant stretches pertaining to amine or amide functional groups, suggesting that the elemental composition of the LCDs is predominantly composed of carbon and
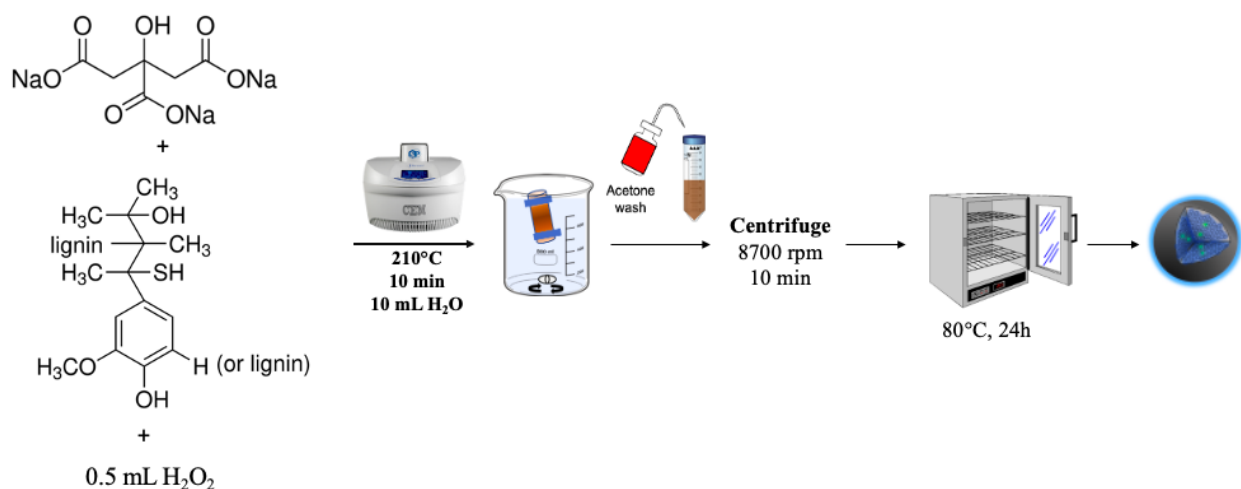
Figure 18. Schematic representation of the synthesis and purification protocol for LCDs.

oxygen, similar to the GlyCDs. The role of hydrogen peroxide during the synthesis of LCDs is to introduce oxygen groups to the surface and the overall structure of the CD and endow them with active sites that can efficiently catalyze the transesterification reaction of canola oil to biodiesel.[94] Hydrogen peroxide is known to be a strong oxidizing agent and a report by Chen *et al.* described the hydrothermal synthesis of carbon dots using lignin and H_2O_2 as a method to oxygenate the surface and render the CDs more hydrophilic for potential uses in biological applications.[73] As a control, LCDs without the addition of H_2O_2 were also synthesized to investigate the change in surface properties as well as their effect on catalytic efficiency towards the transesterification reaction. Upon analysis *via* FT-IR, there was no significant change to the surface of the CD;
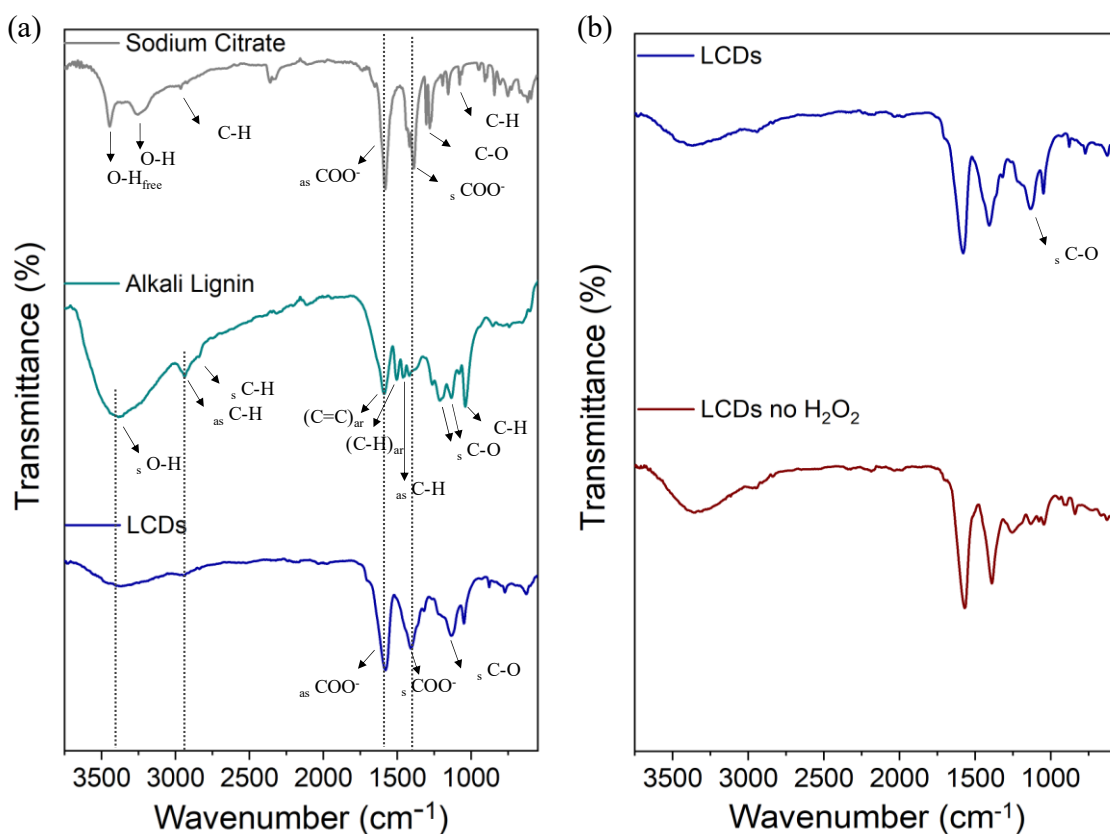
Figure 19. (a) FT-IR spectra of the precursors used to synthesize LCDs, sodium citrate and lignin, and LCDs showing characteristic stretching for carboxylate functional groups. (b) FT-IR spectra of LCDs and LCDs synthesized in the absence of H_2O_2, demonstrating the decrease in oxygen content due to the lack of the symmetric stretching vibration associated to C-O bonds.

however, the increase in oxygen content can be confirmed through the disappearance of the symmetric stretching vibration associated with the C-O bond at 1135 cm^{-1} which is much more prominent for the LCDs prepared using H_2O_2 **(figure 19b)**.

TEM analysis was carried out to confirm the presence of CDs. While some larger nanoparticles are observed, CDs with a size distribution of 10.6 ± 2.5 nm are also predominantly present **(figure 20a)**. TEM analysis for the LCDs with no H_2O_2 shows the formation of large particle aggregates with average sizes of ~ 50-200 nm, as well as some CDs with a size distribution of 12.7 ± 2.5 nm **(figure 20b)**.
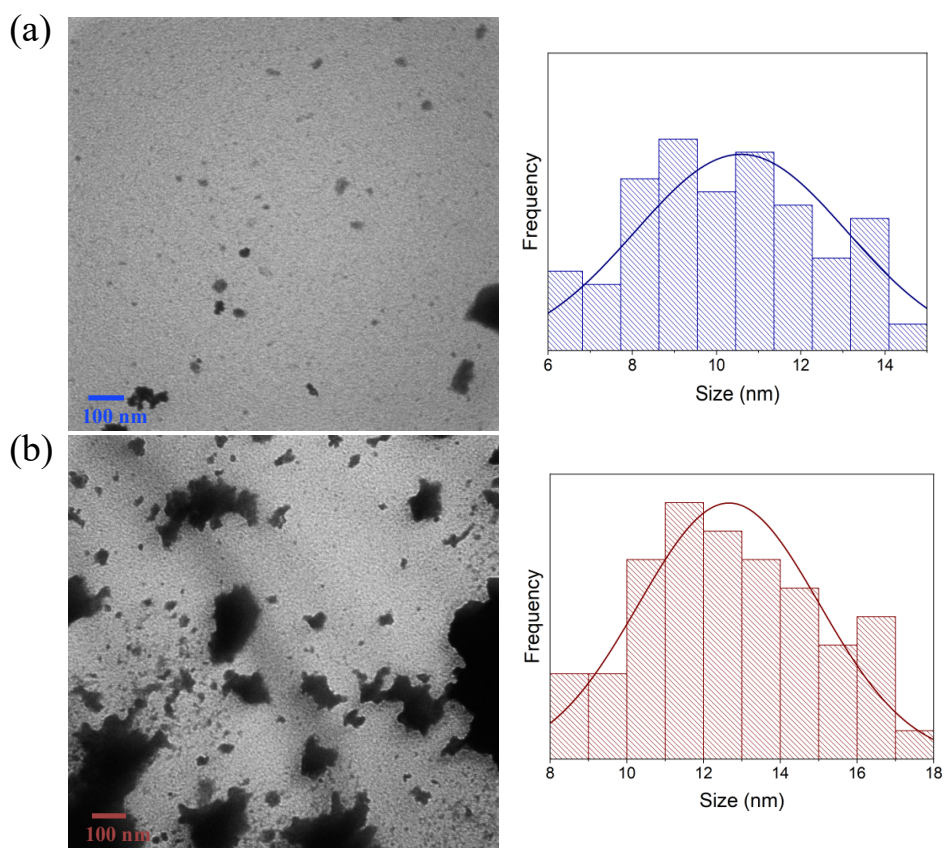
Figure 20. (a) TEM micrograph of LCDs dispersed in methanol illustrating quasi spherical nanoparticles with a size distribution of 10.6 ± 2.52 nm. (b) TEM micrograph of LCDs synthesized in the absence of H_2O_2 showing minimal quasi spherical nanoparticles with a size distribution of 12.7 ± 2.45 nm, as well as the presence of large agglomerates with sizes of ~ 50-200 nm.

To confirm the formation of amorphous CDs, XRD analysis was carried out on the LCDs. Its amorphous nature was confirmed by the broad feature spanning 15-50 °2θ **(figure 21a)**. The appearance of a small crystalline peak was observed at 23 °2θ assigned to the 002 plane for graphitic carbon structures, a feature that is not present in sodium citrate or alkali lignin, confirming that upon synthesis of LCDs, a new graphite-like organized structure is partially formed.[95] The major crystalline peaks associated with sodium citrate, at 12 and 18 °2θ are not present in the diffractogram for the LCDs, indicating that sodium citrate was purified from the CD product. Pure alkali lignin also presents an amorphous character due to the disorganized and random polymerization of its structure, presenting two distinct broad features between 15-30 °2θ and a small shoulder spanning 35-60 °2θ. This shoulder is not present for the LCDs suggesting that unreacted lignin was purified from the final CD product.

Made up of an extensive sp^2 hybridized aromatic network, lignin offers high thermal stability making it an excellent raw material for use in industrial processes. Pure lignin presents its largest degradation step at ~400 °C, due to the breakdown of aromatic structures into monomeric counterparts.[96] TGA analysis was carried out on the LCDs to ensure high thermal stability and robustness and the thermograph **(figure 21b)** presents four main weight loss steps. The first two weight losses of 4.3 % and 10.4 % were observed at 50 °C and 160 °C, respectively, pertaining to the evaporation of residual acetone left over from the purification process and adsorbed water molecules present on the CD. The third weight loss step of 22.2 % was observed starting at 225 °C and ending at 640 °C. This broad weight loss step is associated to the decomposition of oxygenated surface functional groups present on the CD surface as well as the breakdown of aromatic structures, prevalent in lignin's structure.[96] The final and largest weight loss step of 30.1 % beginning at 640 °C is not present in the decomposition profile of pure alkali lignin and is typical
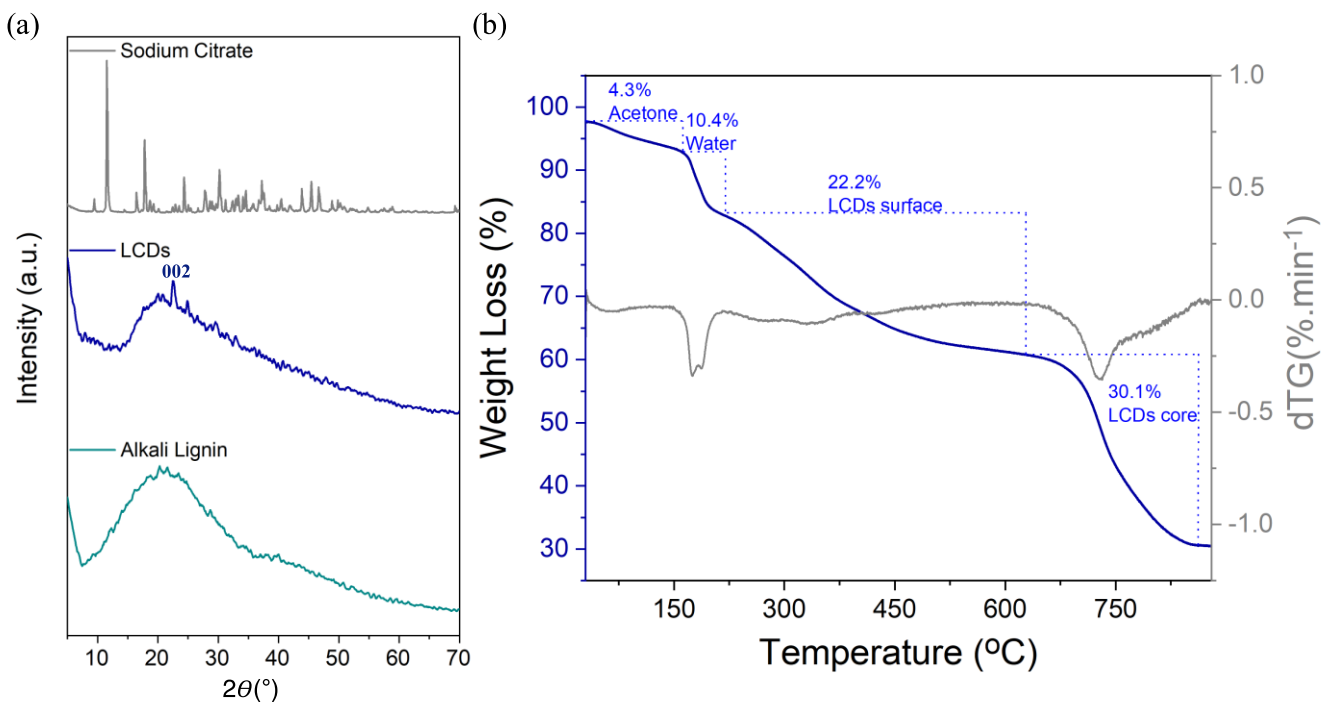
Figure 21. (a) XRD spectra for LCDs, demonstrating the amorphous nature of the LCDs based on the broad feature centered at 20 °2θ and the appearance of the 002 place associated to graphitic carbon confirms a partial graphitic nature upon CD synthesis. Alkali lignin, also demonstrating its amorphous polymeric structure to the broad feature centered at 20 °2θ and a smaller shoulder at 40 °2θ. (b) TGA thermogram of LCDs demonstrating their high thermal stability with the first weight loss step at 40 °C and the last weight loss step at 750 °C, pertaining to the CD surface and core, respectively.

of the decomposition of the CD core, comprised of a highly sp^2 hybridized network including some graphitic nature as observed by XRD analysis.[97] At 900 °C, 33 % of material is left over, typically seen in the decomposition profile of alkali lignin, presumably from the formation of highly thermally-stable aromatic structures.[98] Additionally for the LCDs, some of the left over undecomposed material at 900 °C pertains to residual Na$^+$ ions present on the surface of the CD due to the incorporation of sodium citrate during synthesis.

3.1.3 – Synthesis and Characterization of Glycerol-Derived CDs

Glycerol-derived CDs (GCDs) were synthesized *via* a microwave-assisted reaction of glycerol and sodium citrate in 2 mL of H_2O **(figure 22)**. The reaction mixture resulted in a dark brown homogeneous solution that was then subjected to dialysis against water and multiple organic washes using ethanol in order to remove any unreacted glycerol or sodium citrate remaining in the mixture.

While the most common solvent for organic washes is acetone, in this case ethanol was more efficient at removing the excess unreacted glycerol as seen *via* FT-IR analysis **(figure 23)**, where the GCDs washed with ethanol no longer evidenced the stretching vibration pertaining to O-H at 3290 cm^{-1}, the asymmetric and symmetric stretching vibrations associated with the C-H bonds at 2930 cm^{-1} and 2880 cm^{-1}, respectively, as well as by the absence of the C-O stretching vibration at 1032 cm^{-1}. The absence of these vibrations, typically observed for glycerol, following several organic washes with ethanol confirms the removal of any unreacted material that may decrease the catalytic efficiency of the GCDs. Following centrifugation, the precipitate was collected and upon drying, a brown powdered sample of CDs was obtained. The GCDs were synthesized using increasing amounts of sodium citrate, 0.3 g, 0.6 g, and 1.2 g to investigate the catalytic efficiency of the resulting GCDs. FT-IR analysis of the GCDs presents two intense
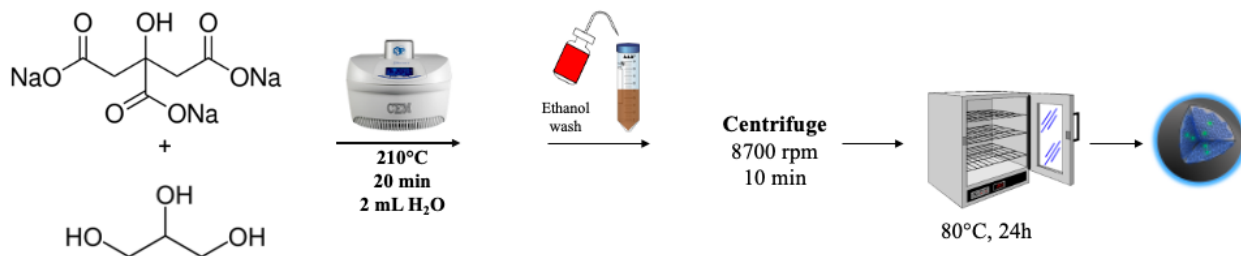
Figure 22. Schematic representation of the microwave-assisted synthesis protocol for GCDs.
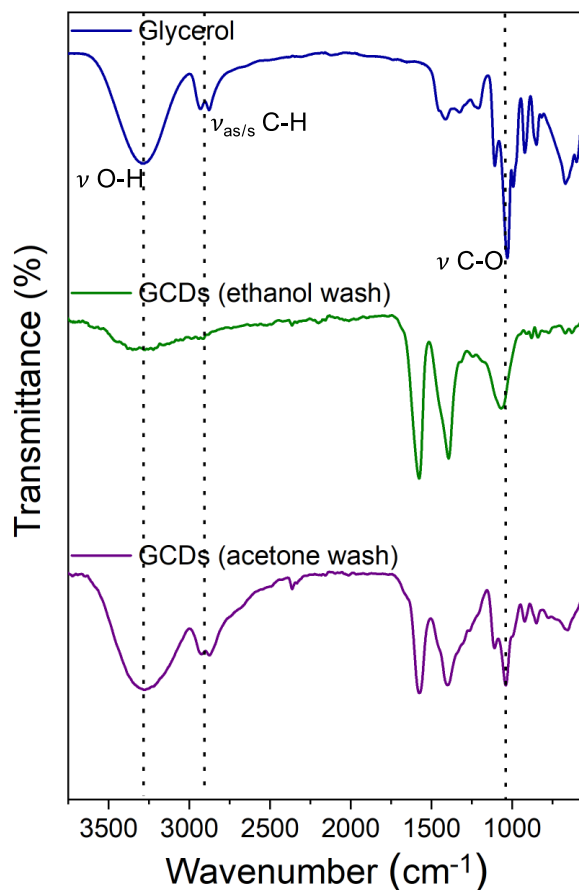
Figure 23. FT-IR spectra of pure glycerol and GCDs after acetone washes and ethanol washes. The absence in vibrations associated to glycerol after the ethanol washes confirms the removal of unreacted glycerol.

stretching vibrations associated with the asymmetric and symmetric COO⁻ functional groups at 1580 and 1390 cm⁻¹, respectively, as well as the stretching for the C-O bond at 1070 cm⁻¹ **(figure 24a)**. The carboxylate moieties stem from sodium citrate used as the precursor, which also present the stretching vibrations ascribed to the COO⁻ groups. Varying the sodium citrate content used during the synthesis of GCDs (denoted GCDs-0.3, GCDs-0.6, and GCDs-1.3 for the synthesis using 0.3g, 0.6g, and 1.3 g of sodium citrate, respectively) did not have a significant effect in terms of the types of groups present on the surface of the dots. FT-IR analysis shows the three characteristic stretching vibrations for all three samples **(figure 24b)** noting no significant differences.

48
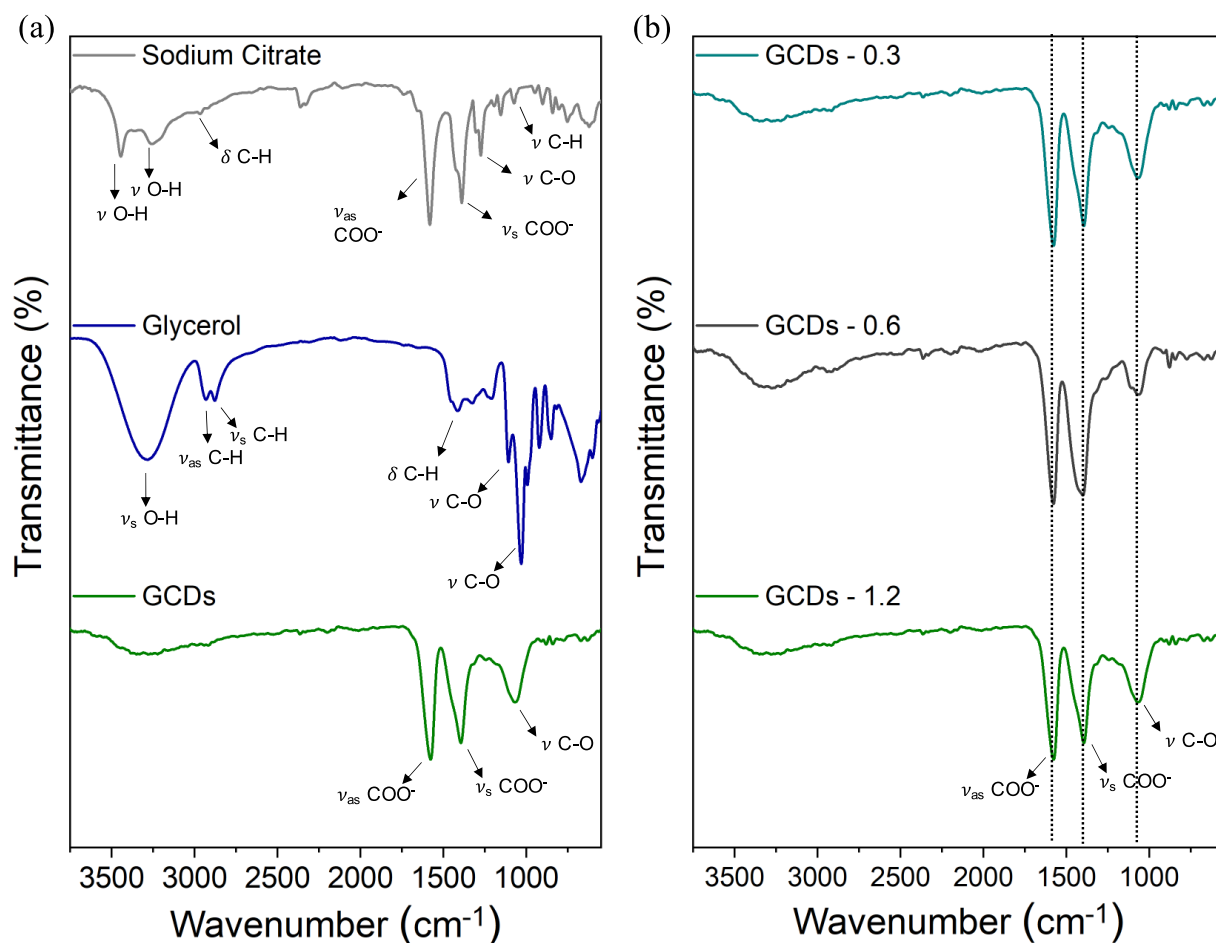
Figure 24. (a) FT-IR spectra of GCDs and precursors used to synthesize, sodium citrate ad glycerol. (b) FT-IR spectra of GCDs synthesized using varying amount of sodium citrate, 0.3 g, 0.6 g, 1.2 g. The results do not show difference in the types of functional groups present on the surface of the CDs

TEM analysis was carried out to confirm the formation of CDs. The GCDs-0.3 presented monodisperse quasi spherical nanoparticles with a size distribution of 11.6 ± 2.5 nm with no sign of aggregation **(figure 25a)**. The GCDs-1.2 presented fairly monodisperse quasi-spherical nanoparticles with a size distribution of 13.9 ± 2.7 nm **(figure 25b)**. While some agglomeration of the CDs is present, this is believed to be due to sample preparation and solvent effect.

XRD analysis was carried out on all the GCDs to investigate their crystallinity **(figure 26a)**. The diffractogram for GCDs-1.2 shows a broad feature spanning 15-60 °2θ confirming the
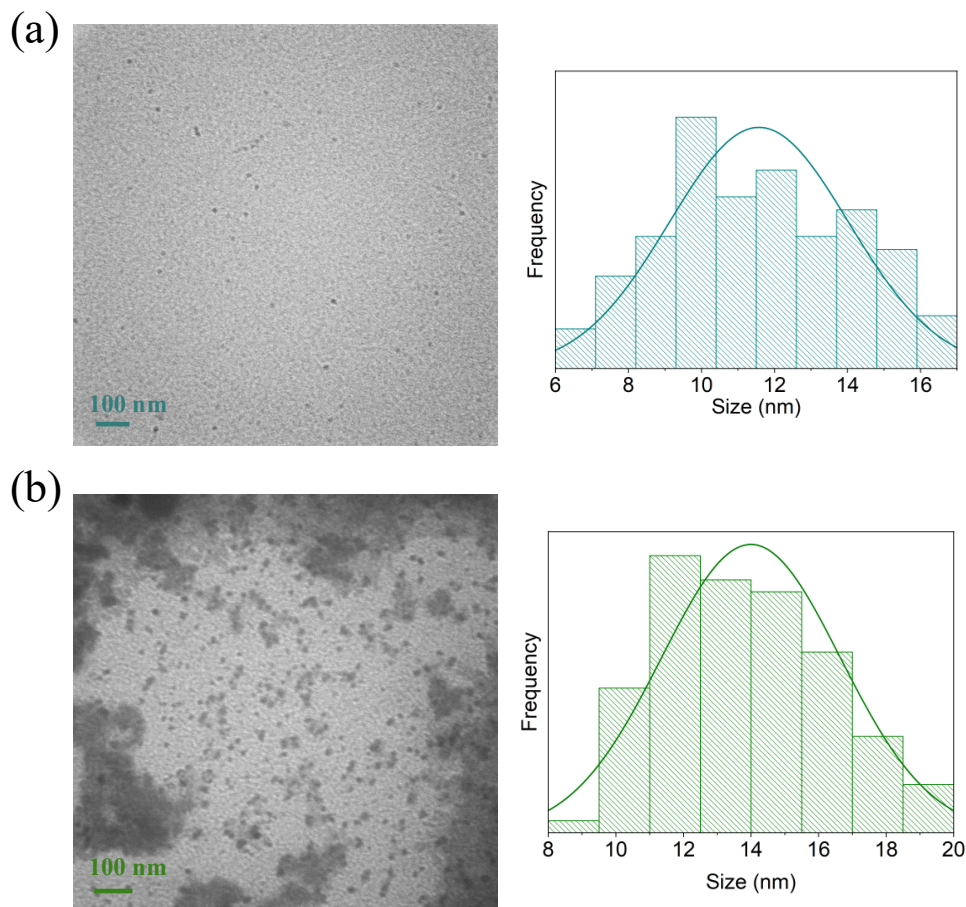
Figure 25. (a) TEM micrograph of GCDs-0.3 dispersed in methanol illustrating quasi spherical nanoparticles with a size distribution of 11.6 ± 2.5 nm. (b) TEM micrograph of GCDs-1.2 dispersed in water illustrating quasi spherical nanoparticles with a size distribution of 13.9 ± 2.7 nm.

amorphous nature of the GCDs however, the appearance of some ordered character is observed between 30-45 °2θ indicating some ordered structure possibly attributed to the 101 and 100 planes of graphite. This effect is brought upon by the addition of increased amounts of sodium citrate, evidently increasing the amount of organized sp^2 hybridized structure in the core of the CDs. The crystallinity decreases with a decrease in sodium citrate content as observed for the GCDs-0.3 where there were no significant diffraction peaks and solely a broad feature spanning 15-60 °2θ indicating it is completely amorphous. The crystalline reflections present between 30-45 °2θ are not ascribed to sodium citrate, noting that the major reflections present in the diffractogram of
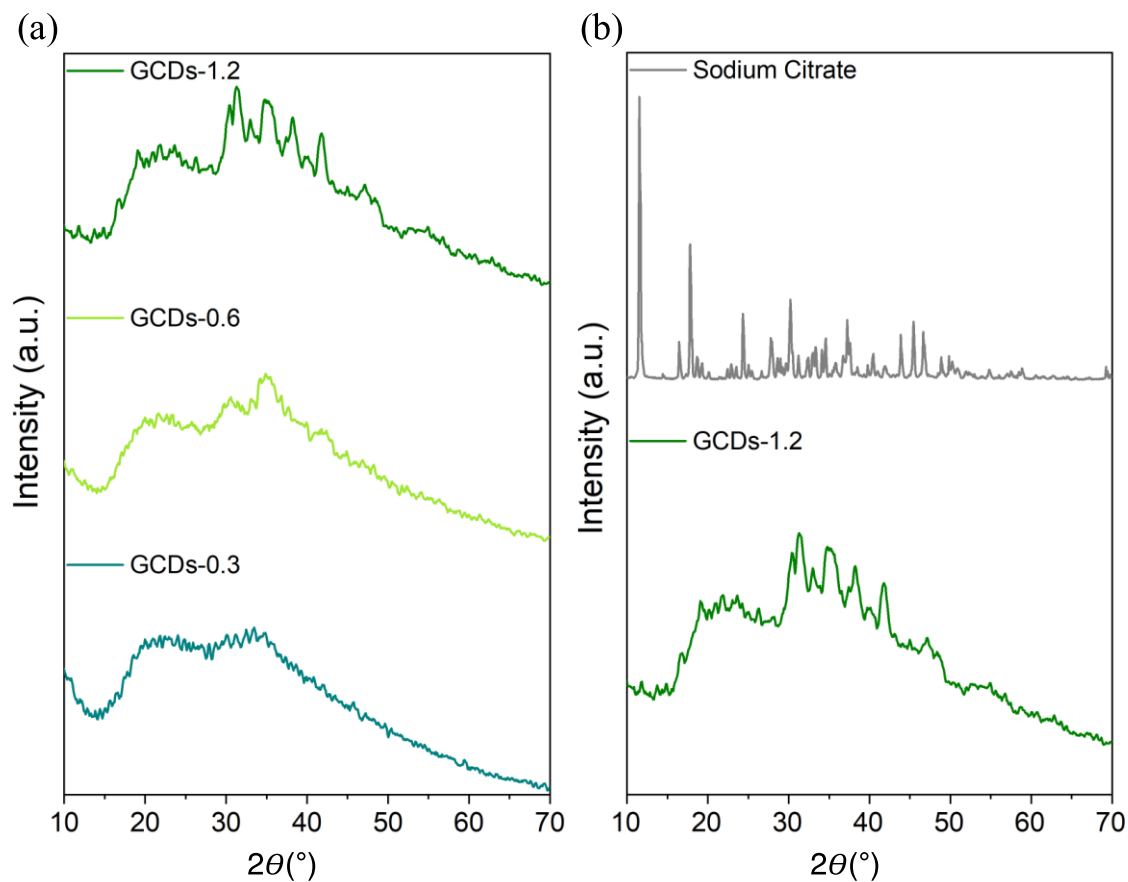
Figure 26. (a) XRD spectra of all GCDs synthesized using different amounts of sodium citrate. The results show that as sodium citrate content increases so does the crystallinity of the dots. (b) XRD diffractogram of GCDs-1.2 and sodium citrate, confirming adequate purification of GCDs due to the absence of key crystalline features of sodium citrate.

sodium citrate **(figure 26b)** are not present for the GCDs, indicating that the crystalline character stems from the CDs.

Glycerol-derived CDs were successfully synthesized *via* a microwave-assisted approach. In order to confirm if increased concentrations of sodium citrate correspondingly increases the oxygen content in the dots, elemental analysis would have to be performed as a future work. Further characterization including XPS and surface titrations would be needed to harvest information on the types of chemical groups present on the surface and core of the CD.

3.2 – Can Carbon Dots Catalyze the Transesterification Reaction?

The search for an efficient, robust and financially viable heterogeneous catalyst for the transesterification reaction has been ongoing for quite some time and numerous materials have been investigated as alternatives; however, carbon dots remain virtually unexplored in this field. Upon initial scouring of the literature, one report by Tangy *et al.*, investigated the use of carbon dot-functionalized SrO composites as heterogeneous catalysts for the transesterification of *Chlorella vulgaris,* a microalgae, to FAME.[99] The role of the polyethylene glycol derived CDs was to catalyze the esterification of the high degree of FFAs present in the oil derived from *Chlorella vulgaris* while the SrO provided the basic groups necessary to catalyze the transesterification reaction, resulting in a 2.5-fold increase in biodiesel conversion compared to bare SrO.[99] The aforementioned work demonstrated how the surface of the CD could be tuned to mimic homogeneous acids used to catalyze the esterification reaction, in this case, by designing a CD with a high degree of carboxylic acid and phenolic groups.[99]

Knowing the role of the hydroxide ion in the conventional base-catalyzed transesterification reaction mechanism where, step 1 **(figure 27a)** involves the deprotonation of the methanol proton by the strong base, NaOH, allowing for the methoxide to undergo a nucleophilic attack on the carbonyl of the triglyceride in step 2 **(figure 27b)**, we set our goal to mimic this mechanism using CDs. CDs were synthesized with an inherently negatively charged surface chemistry, to act as a proton sponge, and imitate the first step in the conventional homogeneous base-catalyzed reaction mechanism.

Following the synthesis and physico-chemical characterization of the CDs, the following step was to investigate their catalytic efficiency towards the transesterification reaction of canola oil to biodiesel. However, before beginning any transesterification reactions, a means to

(a) *Step 1*

$$NaOH + H_3C-OH \rightleftharpoons H_3C-O^{\ominus} + H_2O$$

(b) *Step 2*

$$R_3COO-CH_2$$
$$R_2COO-CH \qquad + \qquad H_3C-O^{\ominus}$$
$$H_2C-O-C-R_2$$
$$\overset{||}{O}$$
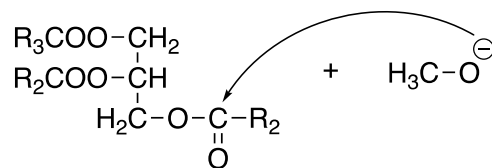
Figure 27. (a) Step 1 of the base-catalyzed transesterification reaction involving the methanol deprotonation. (b) Step 2 of the base-catalyzed transesterification reaction involving the methoxide nucleophilic attack on the carbonyl of the triglyceride.

characterize the conversion efficiency of triglycerides to FAME of the obtained biodiesel product must be established. In this work, a ^{1}H NMR protocol was chosen as a straightforward technique to accurately measure biodiesel conversion as opposed to industry used GC analysis.

3.3 – Biodiesel Characterization

According to industry practices and ASTM standards, the efficiency of the transesterification reaction is typically characterized by measuring the percent conversion of triglycerides to FAME using gas-chromatography (GC). While GC analysis can accurately determine the amount of triglycerides and FAME, as well as diglyceride and monoglyceride reaction intermediates, analysis usually requires sample derivatization, tedious calibrations, use of external standards and is generally considered to be time consuming.[100,101] Furthermore, from an academic standpoint, the availability of specific GC columns allowing for clear separation of FAMEs, often resulting in co-elution, may limit accurate characterization thus, requiring a more versatile characterization method. This limitation was confirmed to be of issue during preliminary transesterification reactions where upon GC analysis, using an Agilent HP5-ms column,
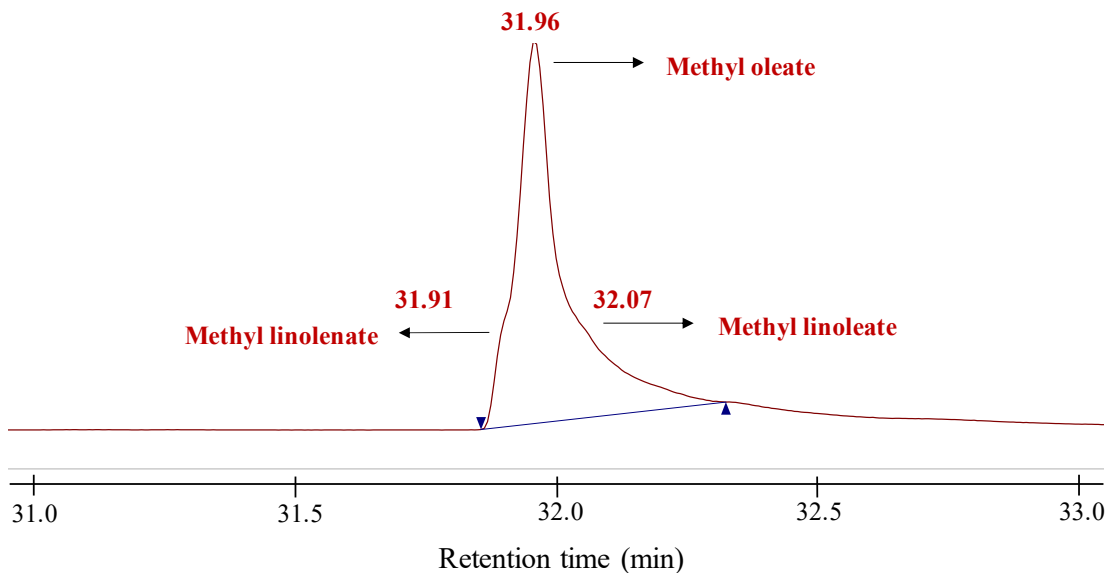
Figure 28. GC chromatogram for a representative sample of biodiesel obtained through the transesterification of canola oil. The three primary fatty acid methyl esters comprising biodiesel, synthesized from canola oil, co-eluted at approximately 32 minutes.

characterization of a biodiesel sample obtained from the transesterification of canola oil results in the co-elution of the three primary FAMEs comprising the biodiesel sample **(figure 28)**.[102] It was not possible to clearly separate the bands despite extensive method development and discussion with the column manufacturer.[102]

3.3.1 – Quantitative Characterization of Biodiesel *via* ^{1}H NMR

The use of ^{1}H NMR to quantify FAME content and % biodiesel yield has been used for lab-scale biodiesel production as it is a quick and robust analysis, does not require sample derivatization, presents accurate measurements with minimal error and is a non-destructive method.[101,103] ^{1}H NMR is a technique often used to determine the molecular structure of organic compounds. The basis of this technique is dependent on how protons, in a specific electronically charged environment, respond to an applied magnetic field, resulting in specific resonant frequencies that give information about specific chemical environments. Upon the

transesterification of a triglyceride to FAME, the glyceridic backbone is broken down and replaced with a methoxy group, giving rise to three equivalent protons in a new chemical environment which will appear on a ^{1}H NMR spectrum at 3.7 ppm, while the methylene protons remain at 2.3 ppm **(figure 29a)**. The biodiesel conversion is determined by taking the ratio of the areas under two specific chemical shifts illustrated in the NMR spectrum of biodiesel (**figure 29b**). Upon formation of biodiesel, a singlet at 3.7 ppm appears and is ascribed to the three methoxy protons
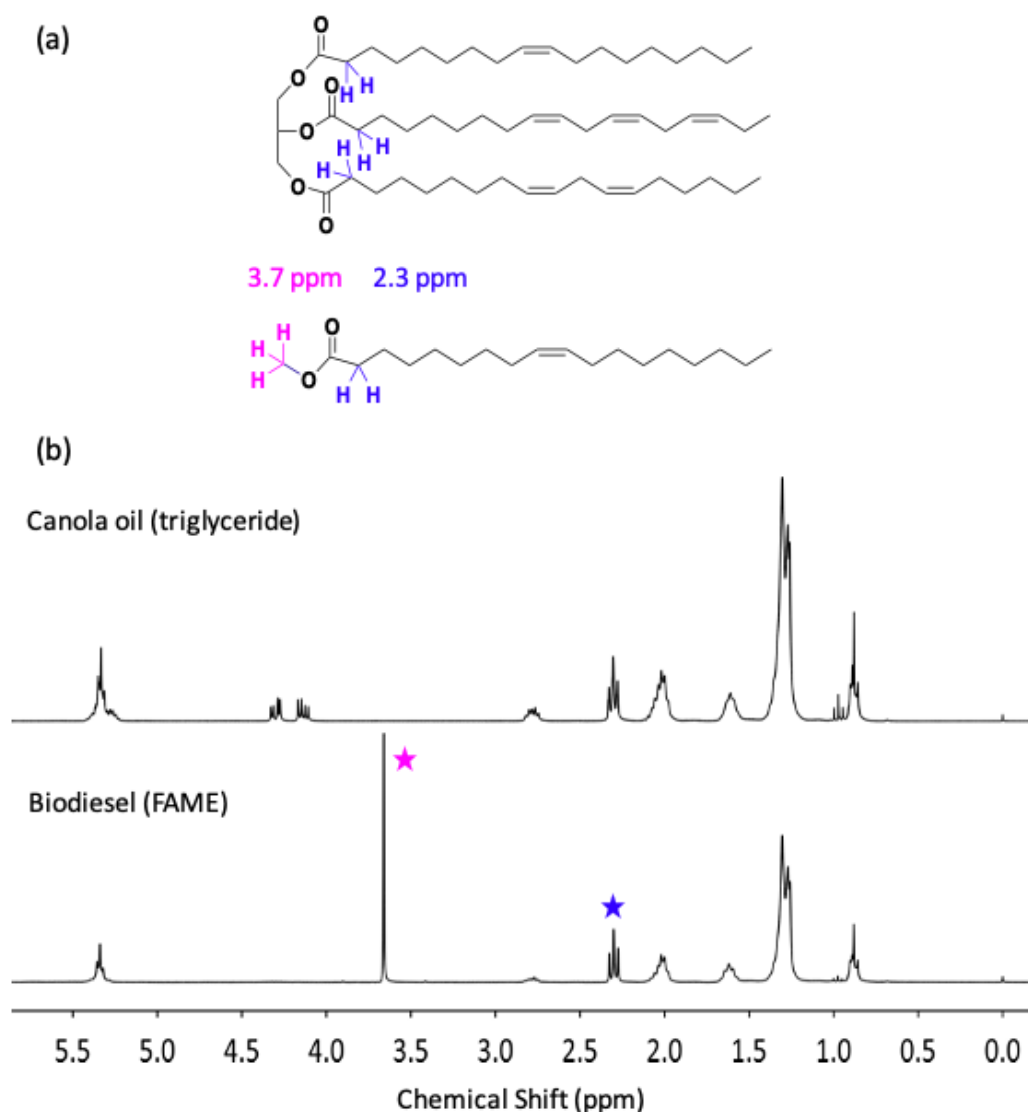
Figure 29. (a) Structures of triglyceride and FAME depicting the alpha-methylene and methoxy protons. (b) ^{1}H NMR spectra of canola oil and biodiesel illustrating the singlet at 3.7 ppm pertaining to the methoxy protons of FAME.

present in the methyl ester structure. This is coupled to the disappearance of the doublet of doublets at 4.3 ppm pertaining to the glyceridic protons of the triglyceride.[104] Simultaneously, a change in the area under the triplet at 2.3 ppm, pertaining to the α-methylene protons of both triglycerides and biodiesel, is observed following biodiesel formation.[104] To determine the % biodiesel conversion, a calibration curve was constructed with known weights of canola oil and varying amounts of methyl oleate between 0-100 %. Methyl oleate was chosen as the representative methyl ester since biodiesel produced from canola oil is ~60 % methyl oleate. The oil samples were then analyzed via ^{1}H NMR and the peak area ratios (3.7 ppm : 2.3 ppm) were measured **(figure 30a,b)**. A standard curve was built by plotting the peak area ratios and the percentage of methyl oleate in each sample **(figure 30c)**. Based on the equation of the standard curve, subsequent biodiesel containing samples could be quantified.

Alternatively, equation 1 could be used to estimate the conversion of canola oil to FAME:

$$Conversion \ (\%) = \frac{2A_{CH_3}}{3A_{CH_2}} \times 100$$

Where A_{CH3} is the integrated area for the methyl protons belonging to FAME and the coefficient of 2 pertains to the number of methylene protons, while A_{CH2} is the integrated area for the methylene protons and the coefficient of 3 pertains to the number of methoxy protons.[103,105]
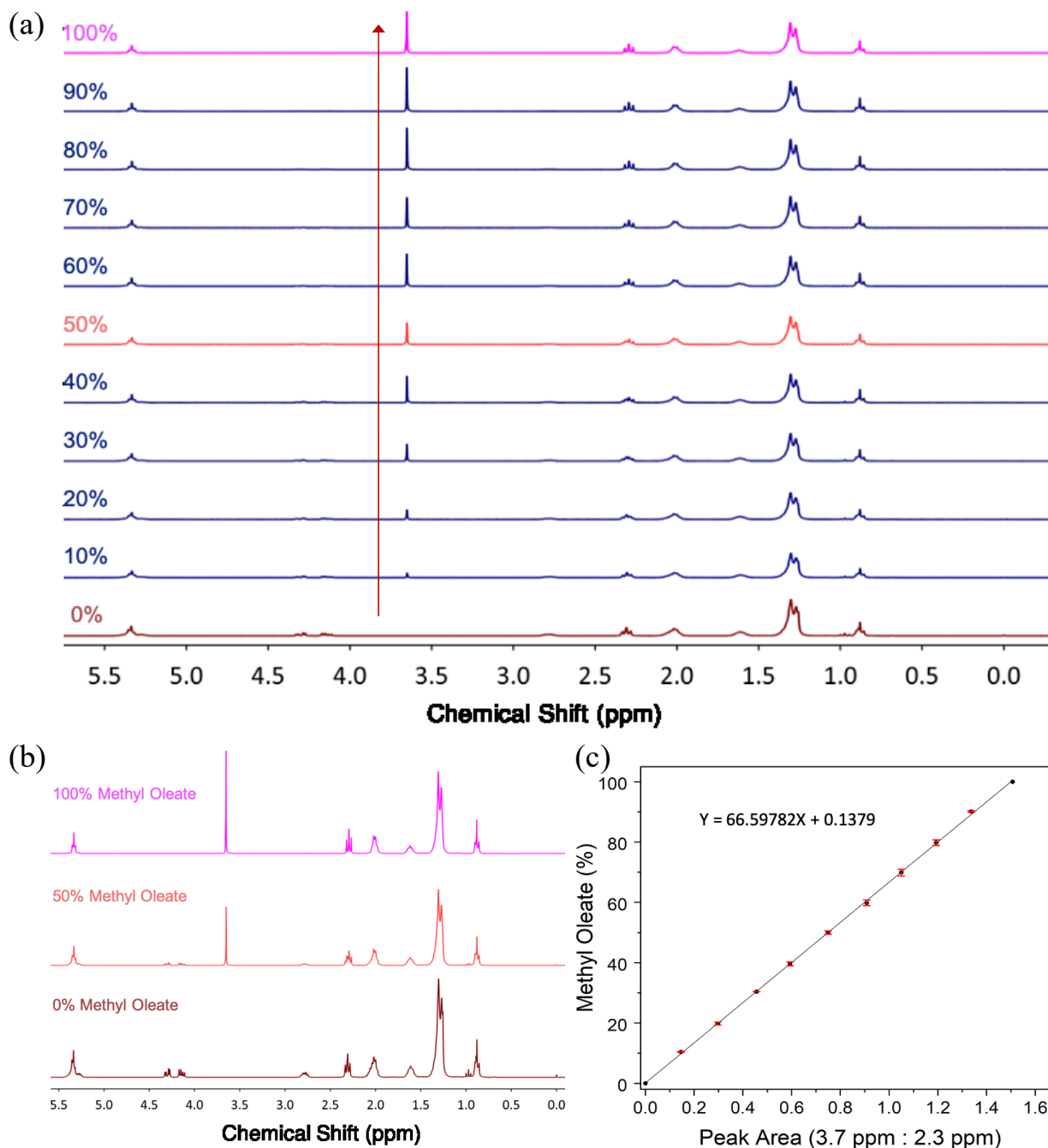
Figure 30. (a) ^{1}H NMR spectra for all samples ranging between 0-100% methyl oleate content. The arrow depicts the increase in the singlet at 3.7 ppm as methyl oleate content increases. (b) ^{1}H NMR spectra for 0, 50 and 100 % methyl oleate standard samples, illustrating the formation of a singlet at 3.7 ppm and the disappearance of the doublet of doublets at 4.3 ppm as the methyl oleate content in the sample increases. (c) Standards curve and equation used to determine the biodiesel conversion. The curve was constructed using known amounts of canola oil and methyl oleate.

3.3.2 – Qualitative Characterization of Biodiesel *via* FT-IR

A qualitative analysis of the transesterification reaction and biodiesel production can be conducted using Fourier-Transform infrared spectroscopy by monitoring two specific spectroscopic vibrations. Upon analysis of both canola oil and biodiesel, the FTIR spectra **(figure 31)** reveal the characteristic asymmetric and symmetric stretching vibrations at 2922 cm^{-1} and 2852 cm^{-1} associated with the C-H bonds of the methylene groups, as well as the stretching vibration associated with the =C-H groups, respectively. Moreover, it is possible to monitor the high intensity asymmetric stretching vibration associated with the carbonyl group at 1740 cm^{-1}, present in both triglycerides and FAME.[104,106] Characteristic bands for biodiesel are present at
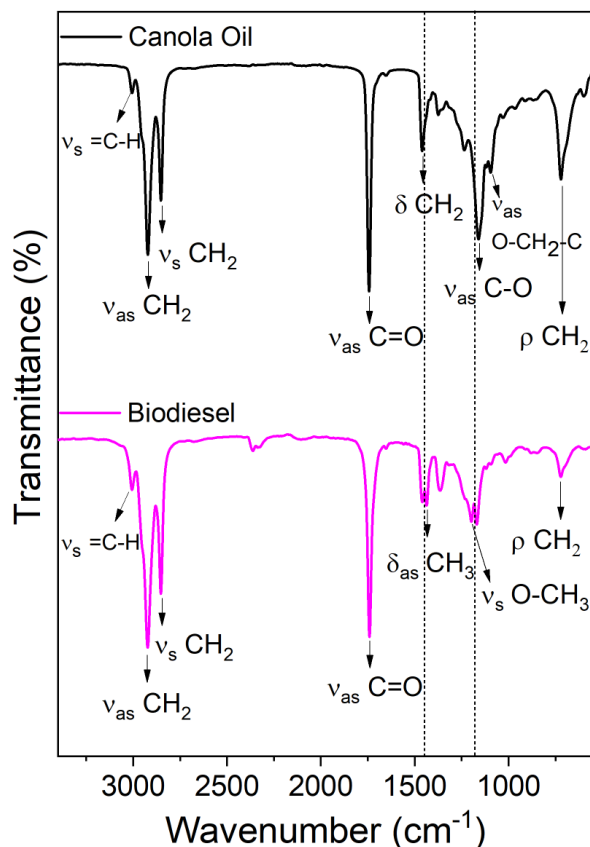
Figure 31. FTIR spectra of canola oil and biodiesel, representing the characteristic vibrations associated with each materials.

1441 cm^{-1} corresponding to the asymmetric bending vibration of the CH$_3$ moiety of the methoxy group, and at 1196 cm^{-1} corresponding to the symmetric stretching of the O-C bond of the methoxy group.[104,106] Canola oil presents a characteristic asymmetric stretching vibration at 1100 cm^{-1} pertaining to the O-C bond of the methylene groups, as well as the CH$_2$ bending vibration at 1455 cm^{-1} and the asymmetric stretching vibration associated to the C-O bond at 1160 cm^{-1}.[104,106]

3.4 – CD-Catalyzed Transesterification Reactions

3.4.1 – GlyCDs-Catalyzed Transesterification of Canola Oil and Reusability Studies

In order to optimize the reaction conditions, we investigated several parameters including catalyst loading, reaction time and temperature **(figure 32a)**. The transesterification reaction was carried out at various reaction conditions as summarized in **table 3**. The amount of homogeneous (e.g. KOH) catalyst required to catalyze the transesterification of canola oil to biodiesel, under conventional heating, has been reported to be ~1 wt% of the oil precursor used. In contrast, higher loadings are required when using heterogeneous catalysts typically ranging from 3-15 wt%. The transesterification reactions were carried out varying the GlyCD catalyst in the range of 0.1-20

Table 3. Reaction parameters varied in order to determine optimal conditions for the transesterification of canola oil using GlyCDs.

GlyCD loading (wt%)	Temperature (°C)	Reaction time (hrs)	Canola Oil:MeOH
0.1	150	3	1:60
0.25	150	3	1:60
1.0	65	3	1:60
1.0	100	3	1:60
1.0	125	3	1:60
1.0	150	3	1:18
1.0	150	3	1:60
1.0	150	2	1:18
1.0	150	2	1:60
1.0	150	1	1:60
10	150	3	1:60
20	150	3	1:60

wt%. In order to isolate the effect of catalyst loading, all other parameters were kept constant at 150 °C with a 3 hour reaction time and an oil : methanol ratio of 1 : 60. It is interesting to note that even at low catalyst loading values, such as 0.1%, a significant conversion of 34% is obtained. At 1.0 wt% GlyCDs, the conversion from canola oil to biodiesel reaches a plateau, with a yield of 98.3 ± 0.2%. For that reason, this amount of catalyst was selected and maintained for subsequent optimization steps. As for any catalyzed reaction, temperature plays a significant role in driving the reaction rate. Conventionally heated reactions, using homogeneous base catalysts such as NaOH, are usually carried out at 65-70 °C. Nevertheless, heterogeneous catalysts often require higher temperatures to increase their catalytic efficiency. To evaluate the effect of temperature, the transesterification reaction using GlyCDs was carried out at 65 °C, 100 °C, 125 °C and 150 °C. At the highest temperature tested (150 °C), a biodiesel conversion yield of 98.3 ± 0.2% was obtained. We note that conversion to biodiesel was found to be significantly lower at temperatures below 150 °C. Conversions of 0, 0.7 ± 0.1 and 9.2 ± 1.9 % were obtained at 65 °C, 100 °C and 125 °C, respectively. Thus, it was deemed that a temperature of 150 °C is the optimum temperature for the GlyCD-catalyzed transesterification of canola oil. Subsequently, the effects of reaction time on biodiesel conversion were investigated at 1 h, 2 h and 3 h, while maintaining all other parameters constant. At the 1 h time point, a modest conversion of canola oil to biodiesel is observed with a value of 15.6 ± 2.8%; however, increasing the reaction time to 2 h significantly influences the reaction with an observed conversion of 97.6 ± 0.2%. The stoichiometric ratio required for the transesterification reaction is one molecule of oil to three molecules of alcohol. However, this reaction occurs at an equilibrium, and an excess of the alcohol is added to drive the reaction in the forward direction. Normally, when a homogeneous catalyst is used to produce biodiesel, an oil to methanol ratio of 1:6 is used. In the case of heterogeneous catalysts, often higher methanol is

required, reaching 1:9-1:275.[16,21,22,107] The ratio of canola oil to methanol was investigated at 1:18

and 1:60 to determine the ideal ratiometric volume of excess methanol required for the

transesterification reaction **(figure 32b)**. At a 2 h reaction time and using a 1:18 oil to methanol

ratio, low biodiesel conversions of 44.2 ± 8.2 % were observed. However, using a 1:18 oil to

methanol ratio and increasing the reaction time to 3 h, we observe biodiesel conversions of 97.6 ±
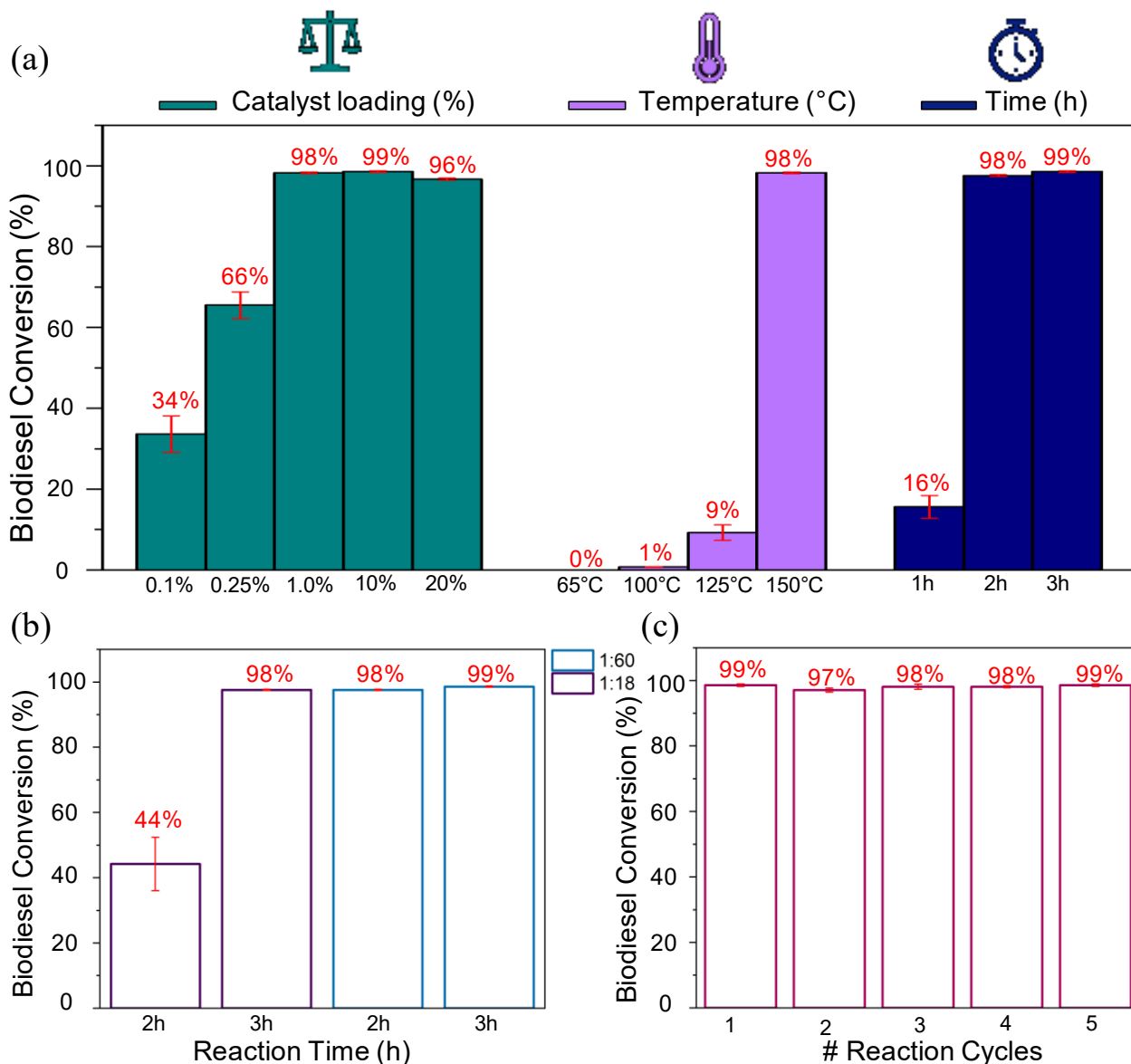
Figure 32. (a) Reaction optimization of catalyst loading (wt%), reaction temperature (°C), reaction time (h). (b) Oil : methanol optimization. (c) Reusability and stability studies of GlyCDs. Reaction conditions were kept constant for each cycle.

61

0.2 %, this being the highest biodiesel conversion obtained under our optimized conditions. Shorter reaction times can be used to achieve the same conversion yields; however, the oil to methanol ratio must be increased to 1:60. One of the primary benefits of using a heterogeneous catalyst is the possibility of recuperating and reusing the catalyst in subsequent reactions. Following optimization efforts, the reusability of the GlyCDs was investigated **(figure 32c)**.

Upon completion of each reaction, the mixture of biodiesel oil, glycerol and carbon dots was left in the oven at 70 °C to remove the excess methanol. Following centrifugation of the mixture, separation of the biodiesel from the glycerol/GlyCD mixture was achieved. The second transesterification reaction was carried out using the exact same conditions as the previous and a biodiesel conversion of 97.1% was obtained. This procedure was repeated for 5 catalytic cycles and what is remarkable is that there appears to be no decrease in biodiesel conversion with each subsequent reaction. Following each reaction, we confirmed the separation of the biodiesel and glycerol phases using FT-IR where it was clear that the glycerol phase shows a similar spectrum relative to pure glycerol **(figure 33a)**. Some residual biodiesel is also present in the glycerol-GlyCD layer confirmed by the stretch at 3007 cm^{-1} representing the symmetric stretching of the sp^2 C-H in biodiesel. To further purify the glycerol layer containing the GlyCDs, the layer was subjected to three organic washes using hexanes to remove any remaining biodiesel and then placed in an oven at 70 °C. We see characteristic stretches of glycerol at 2935 cm^{-1} and 2879 cm^{-1}, pertaining to the symmetric and asymmetric C- H stretching, however the sp^2 C-H stretch found in biodiesel is no longer present confirming the efficacy of the purification protocol. The presence of GlyCDs is confirmed through the symmetric stretching vibrations pertaining to N-H and COO$^-$ at 1670 cm^{-1} and 1390 cm^{-1}, respectively, as well as the asymmetric stretching vibration for COO$^-$
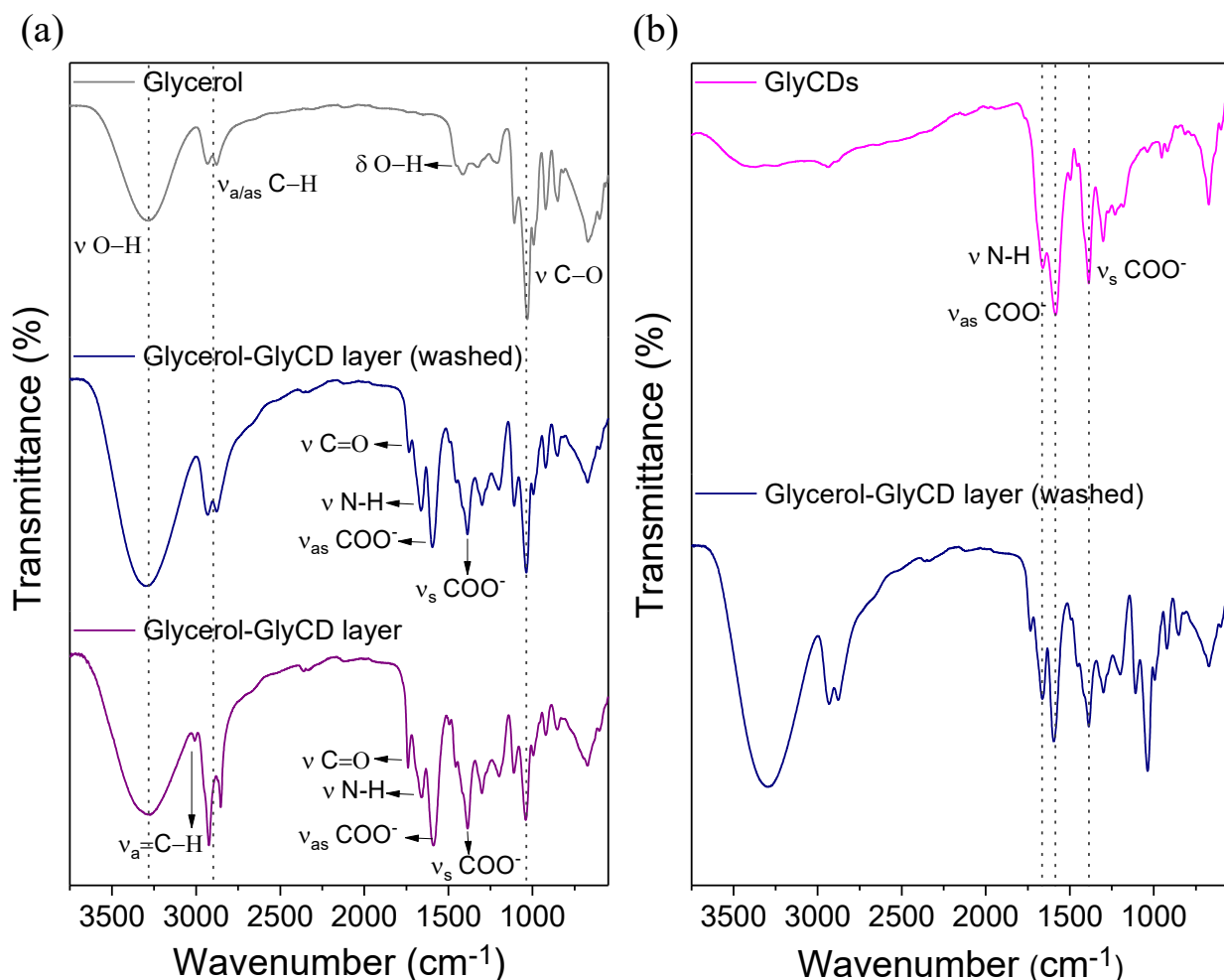
Figure 33. (a) FT-IR spectrum of the glycerol-GlyCD layer after the transesterification reaction with the presence of biodiesel contamination, glycerol-GlyCD layer post organic wash using hexanes, and pure glycerol. (b) FT-IR spectrum of GlyCDs and glycerol-GlyCD layer (hexane washed) to confirm the presence of GlyCDs.

at 1580 cm^{-1} **(figure 33b)**. The results show sustained catalytic efficiency of the GlyCDs while maintaining biodiesel conversions above 96.7%.

In order to ascertain the effects of the GlyCD catalyst, we carried out control reactions. This was especially important since the reaction is being carried out under high pressures that can drive reactions forward without the use of a catalyst. A reaction of solely canola oil and methanol was carried out in the hydrothermal reactor at 150 °C for 3 h using an oil to methanol ratio of 1:60 and showed that in the absence of the GlyCDs, no conversion to biodiesel can be obtained **(figure**

34a). In fact, the ¹H NMR spectrum was identical to that of the starting canola oil. Additionally,

we investigated the use of +GlyCDs, which were synthesized in the exact same way except for the

deprotonation of the carboxylic groups. The transesterification reaction was carried out using 20

wt% of +GlyCDs at 150 °C for 3 h using an oil to methanol ratio of 1:60. A slight singlet peak

was observed by ¹H NMR at 3.7 ppm indicating an 8% conversion to biodiesel had occurred

(figure 34b). Lastly, a control using pure glycine was carried out to confirm that unreacted glycine

was not playing a role in biodiesel synthesis and in fact, the ¹H NMR spectrum was identical to

that of the starting canola oil, indicating no reaction had taken place. **(figure 34c)**. Thus, with a 1

wt% catalyst loading at 150 °C, a short reaction time of 3 h, and an oil to methanol ratio of 1:18,

our system is a promising candidate for biodiesel production in comparison to already-reported

heterogeneously catalyzed systems. We hypothesize that the catalytic mechanism works in a

similar way to homogeneous base-catalyzed transesterification reactions. In the conventional
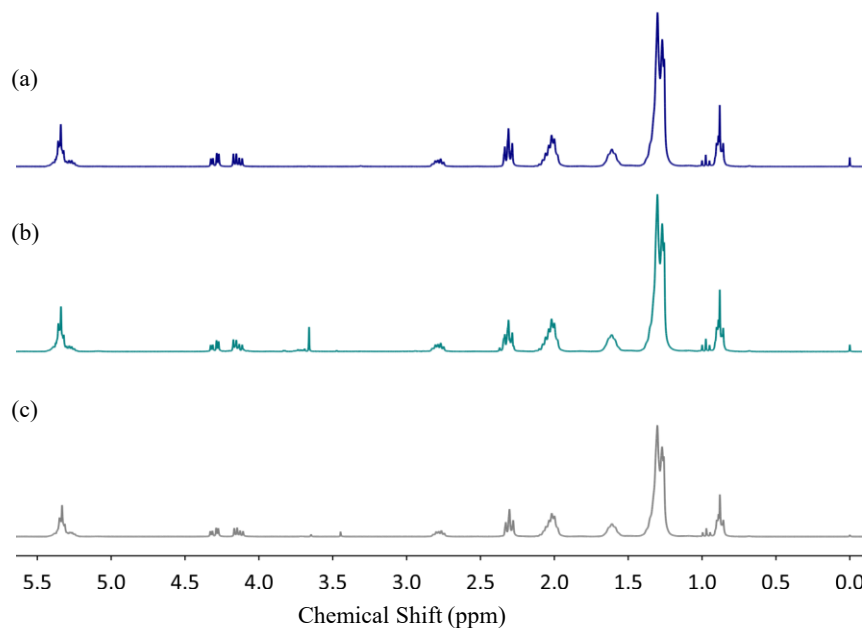
Figure 34. (a) ¹H NMR results for the transesterification reaction of canola oil and MeOH, no catalyst present. (b) ¹H NMR results for the transesterification reaction using GlyCDs (protonated) as the catalyst. (c) ¹H NMR results for the transesterification reaction of pure glycine as the catalyst.

reaction, deprotonation of methanol occurs due to the use of a strong base (e.g. KOH, NaOH), followed by the methoxide attack on the carbonyl of the triglyceride. It has been reported that some organic compounds such as amino-containing molecules can act as non-ionic bases and catalyze the transesterification reaction. The control experiment where protonated +GlyCDs were used for the transesterification reaction resulted in negligible biodiesel conversion obtained, which can be attributed to the amino groups on the CD surface that may play a small role in the catalyzed reaction. In this case, the amino group deprotonates the methanol, and the methoxide formed attacks the ester. The transesterification mechanism can also occur with weak bases, such as carboxylates. However, higher pressures and reaction temperatures are needed to overcome the energy barrier to allow the reaction to move forward. This validates our findings where temperatures of 150 °C in the hydrothermal reactor were necessary in order to ensure biodiesel conversion. As both amino and carboxylate groups are present on the surface of GlyCDs, both mechanisms are likely to occur. However, the carboxylates are believed to play a major role in the transesterification reaction mechanism. Therefore, the proposed mechanism for the GlyCDs-catalyzed transesterification reaction **(figure 35)** starts with the methanol attack on the ester, forming a tetrahedral intermediate zwitterion, which collapses, and a proton transfer by the carboxylates on the CD surface will occur and shift the reaction equilibrium. Subsequently, the
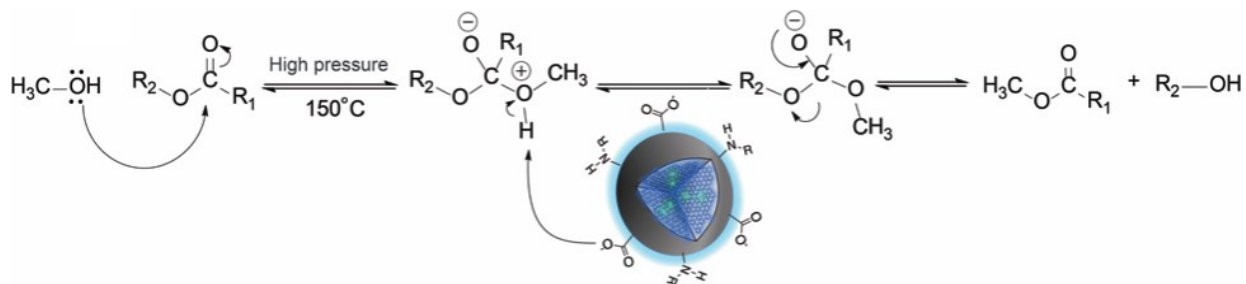
Figure 35. Proposed transesterification mechanism using GlyCDs catalyst.

reaction follows the normal transesterification mechanism, forming glycerol as a by-product.

In order to corroborate this proposed mechanism, additional studies were carried out on the GlyCDs. The deprotonation step using NaOH during the synthesis procedure of GlyCDs was believed to be an integral part in rendering the GlyCDs catalytically efficient for the transesterification reaction. In order to further assess the important of the deprotonation step, the degree of deprotonation was altered to see if this modification would have an effect on biodiesel conversion. According to the original protocol, the pH of the glycine-citric acid aqueous solution prior to NaOH addition was 2.50 and post NaOH addition was 3.50. The amount of NaOH was added at 25%, 50% and 75% of the original amount, being 8 mL, corresponding to pH values of 2.78, 3.01, and 3.24, respectively. Following the synthesis of the dots, they were further purified and isolated using acetone and dried in an oven at 80 °C. The CDs were characterized according to their surface properties in order to investigate the effect of varying the degree of deprotonation. Zeta potential is a characterization tool frequently used to investigate the surface potential of a nanoparticle. The surface charge is calculated according to a common model that utilizes a known applied electric field and a measured particle velocity. **Table 4** summarized the zeta potential experimental results, demonstrating the increase in negative potential as the percentage of deprotonation increases.

Table 4. Zeta potential analysis results for the GlyCDs at different degrees of NaOH addition.

Deprotonation (%)	Surface potential (mV)
0	-3.7
25	-5.2
50	-6.5
75	-8.1
100	-10.8

FT-IR analysis was also carried out to investigate the degree of carboxylic acid vs carboxylate formed upon the different deprotonation degree **(figure 36)**. As the percentage of deprotonation increases, the intensity of the symmetric stretching vibration associated to the COO⁻ group at 1580 cm⁻¹ increases. The CDs were then used as catalysts for the transesterification reaction. The same biodiesel synthesis protocol used for GlyCDs was followed and the biodiesel product was analyzed via ^{1}H NMR where an increase in intensity of the chemical shift at 3.7 ppm pertaining to the methoxy protons of the fatty acid methyl ester was observed as the percentage of deprotonation of the CDs increases **(figure 37a)**. The results show a clear correlation between the amount of NaOH used upon synthesis and conversion to biodiesel. At 0% deprotonation, the
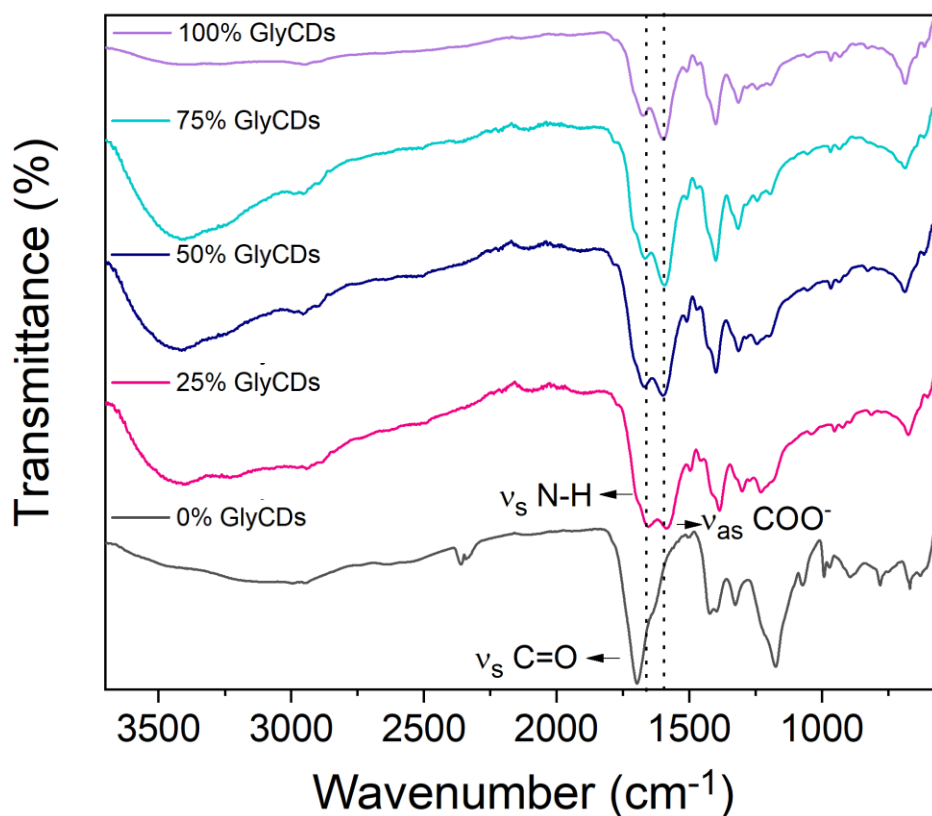
Figure 36. FT-IR analysis of 0-100% deprotonated GlyCDs, confirming the increase in carboxylate moieties on the surface of the CD due to the increase in the intensity of the asymmetric stretching vibration pertaining to the COO- group.

transesterification reaction results in a biodiesel conversion of 8%, most probably due to the low amount of amine groups on the CD surface. Upon 25%, 50% and 75% deprotonation, the transesterification reaction results in biodiesel conversions of 11%, 29% and 54%, respectively **(figure 37b)**. To further validate the that the formation of carboxylate surface groups was essential
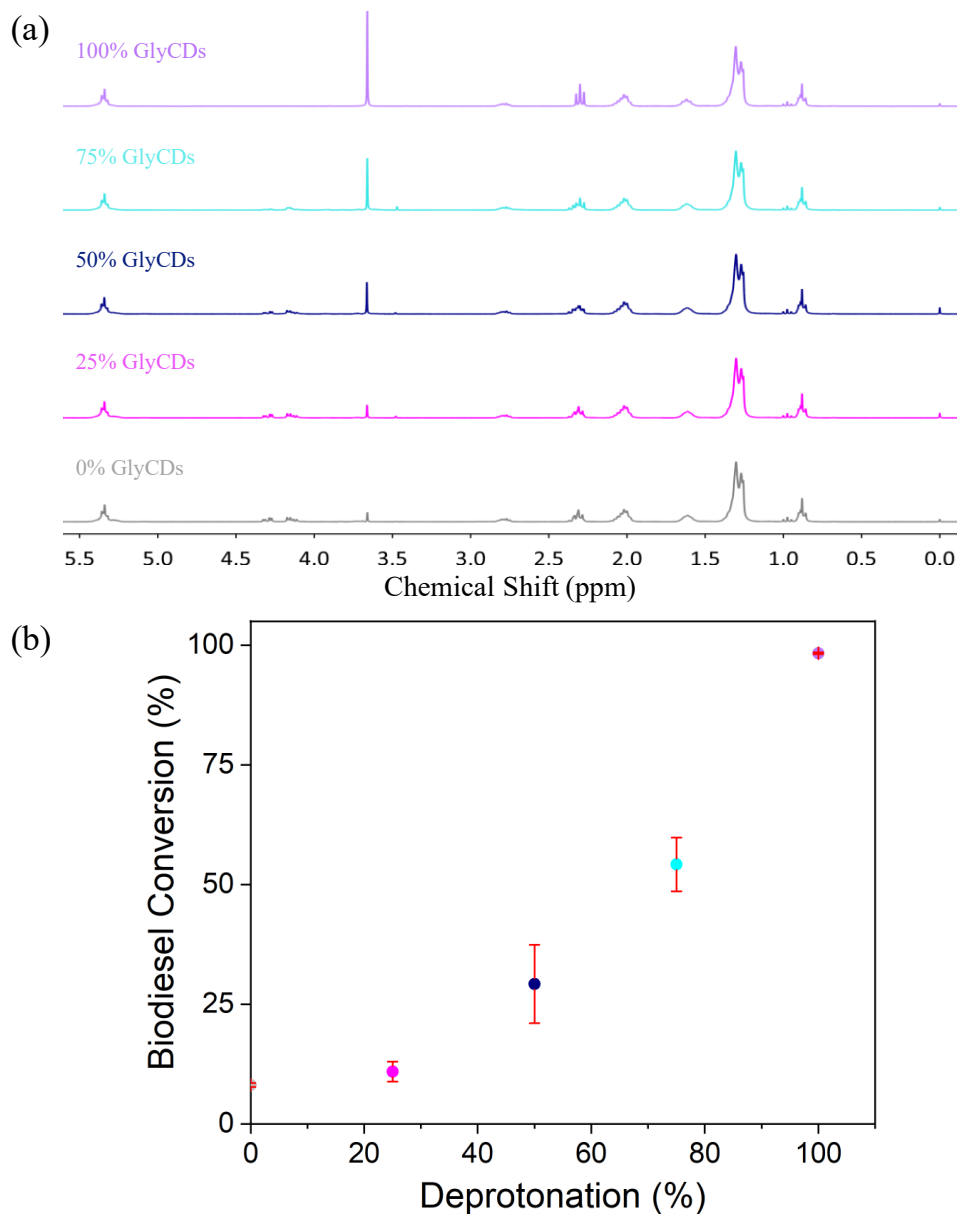
Figure 37. (a) ^{1}H NMR spectra of biodiesel product for 0-100% deprotonated GlyCDs. (b) Correlation between the percentage of deprotonation and biodiesel conversion.

for catalytic efficiency of the transesterification reaction, GlyCDs were synthesized using sodium citrate tribasic dihydrate instead of citric acid, the difference being the presence of no carboxylic acids in the former. If successful, this would also eliminate a step during the synthesis protocol, rendering the whole catalyst preparation method more sustainable. In theory, this may also increase the amount of Na^+ ions electrostatically interacting on the surface of the dots and therefore may increase the amount of Na^+ leaching in the final biodiesel product; however, according to the ASTM and EN standards a maximum concentration of 5 mg/kg is allowed and thus more characterization such as ICP-MS is needed. As expected, the use of GlyCDs synthesized using sodium citrate as the carbon/oxygen and carboxylate source resulted in a biodiesel conversion of 97% **(figure 38a)**.Furthermore, zeta potential analysis was carried out to assess their surface potential which resulted in a potential of -26.7 mV. The surface potential for the GlyCDs synthesized using sodium citrate was significantly higher than the original GlyCDs synthesized
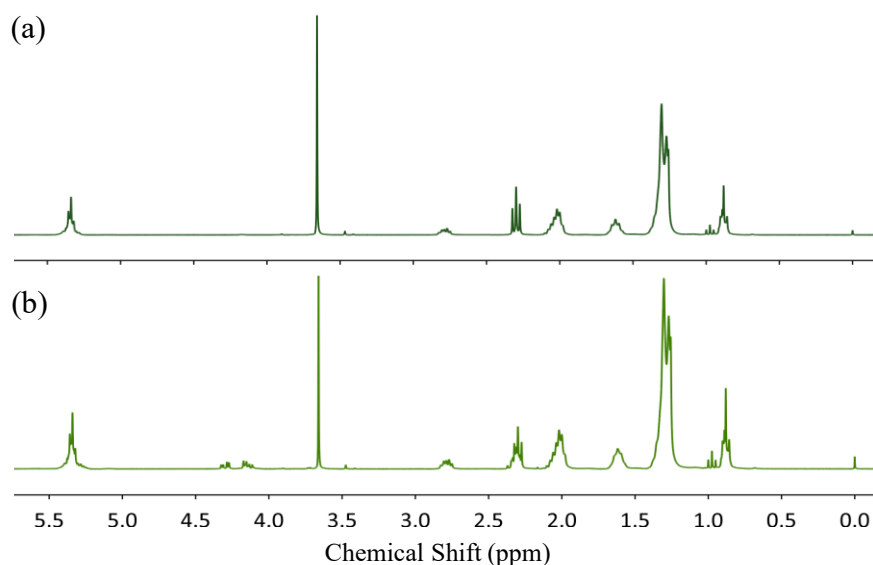
Figure 38. (a) ^{1}H NMR spectrum for the biodiesel product obtained from the use of GlyCDs synthesized using sodium citrate, an intense chemical shift at 3.7 ppm is obtained, resulting in a biodiesel conversion of 97%. (b) ^{1}H NMR spectrum for the biodiesel product obtained after a conventional heating transesterification reaction, using GlyCDs synthesized using sodium citrate, a singlet is observed at 3.7 ppm is obtained, resulting in a biodiesel conversion of 49%.

using citric acid and NaOH, confirming that the use of sodium citrate results in a CD with a higher degree of negative surface character. Ergo, these sodium citrate-derived GlyCDs were used as catalysts for the transesterification reaction of canola oil under conventional heating. The reaction was carried out using similar reaction conditions as the previous GlyCDs at 1 wt% loading catalyst, 1:18 oil to methanol ratio, 3 h reaction time and at a reaction temperature of 90 °C. This resulted in a biodiesel conversion of 49%, demonstrating that the increased negative surface potential of the CD does in fact increase its catalytic efficiency towards the transesterification reaction however since the reaction did not obtain $\geq$ 96.5% at a rather long reaction time, this CD would still not be the most efficient and energy-friendly option **(figure 38b)**. Nevertheless, these results confirm the necessity for a highly negative surface potential to render a CD nanocatalyst to be catalytically efficient towards the transesterification reaction. In order to ascertain that the excess of Na$^+$ ions were not playing a role in the catalytic efficiency, control studies were conducted using equivalent molar amounts of NaCl as compared to the amount of NaOH added. It is clear from the absence of the singlet chemical shift at 3.7 ppm that no FAME was formed and therefore there was 0% biodiesel conversion **(figure 39)**.
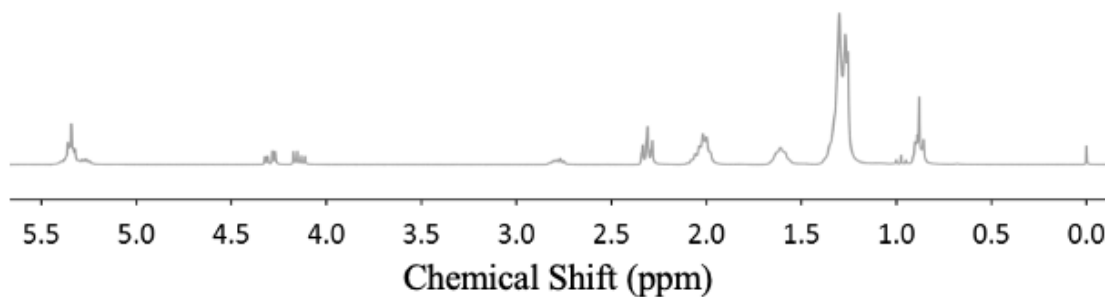
Figure 39. ^{1}H NMR spectrum for the oil product obtained from the use of NaCl as the catalyst. The absence of an intense singlet chemical shift at 3.7 ppm is observed, resulting in no biodiesel conversion.

In the present biodiesel industrial process, one of the greatest limitations to using homogeneous base catalysts such as NaOH and KOH is their high sensitivity to FFAs commonly found in waste oil. The alkali metal ions, Na^+ and K^+, will react with the FFA to form a salt contaminant called *soap*, which needs to be extensively purified from the final biodiesel product. There are several alternative methods to producing biodiesel that is high in FFA content depending on the percentage of FFAs present in the oil. If the FFA content is between 3-4%, extra homogeneous base catalyst is added to actively convert the FFAs to soap without having an effect on the degree of biodiesel conversion and purify the soap post reaction. For FFA content between 5-15%, common practice in industry is to use vacuum distillation to separate the FFAs from the triglycerides, the triglycerides undergo regular transesterification and the FFAs are usually sold as animal feedstock. For FFA content > 15%, acid pre-treatment is a common practice, which entails the addition of a homogeneous acid catalyst, commonly H_2SO_4, in order for the FFAs to undergo esterification which converts FFAs to FAME. Once the FFA content is < 1%, the regular base-catalyzed transesterification reaction is applied. Recognizing the current limitations of using oils high in FFA content, surface tuneability would allow for the design of catalysts that are able to efficiently catalyze the esterification and transesterification reactions simultaneously, eliminating the need for corrosive strong acids and bases. Due to this ongoing drawback, the search for a catalytically efficient bifunctional heterogeneous catalyst is ongoing and would be the most sustainable and cost-effective method to using oils high in FFA content.

In order to investigate the potential use of CDs as heterogeneous acid catalysts for the esterification reaction, the +GlyCDs were investigated owing to the presence of carboxylic acids on the CD surface, which endow acidic properties potentially strong enough to catalyze the esterification reaction. The reaction was carried out by mixing oleic acid as the model FFA,
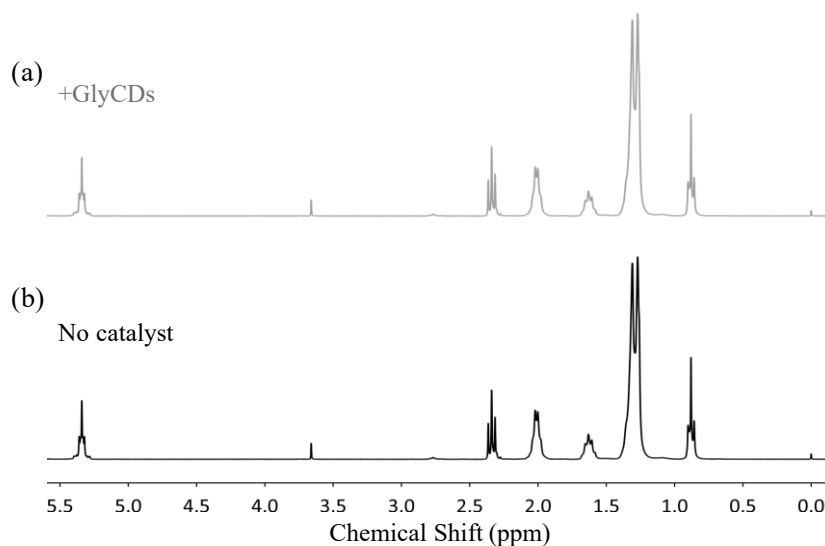
Figure 40. (a) ^{1}H NMR spectrum of oil product after the +GlyCD-catalyzed esterification reaction, no significant singlet is observed at 3.7 ppm confirming no biodiesel conversion. (b) ^{1}H NMR spectrum of the control reaction in the presence of no catalyst, the slight singlet at 3.7 ppm confirms some auto-catalysis occurred.

methanol and 3wt% of +GlyCDs and a 1:6 oil to methanol ratio. The reaction was heated under vigorous stirring at 80 °C for 3 h. The biodiesel conversion was then obtained by ^{1}H NMR **(figure 40a)**. A control was conducted to confirm that there was no significant auto-catalysis of solely oleic acid and methanol **(figure 40b)**. The ^{1}H NMR results show a negligible biodiesel conversion for the +GlyCD catalyzed reaction and that the same conversion is observed for the control reaction without the use of a catalyst indicating auto-catalysis. Based on these results, there is no direct evidence that CDs can catalyze the esterification reaction and future work needs to be carried out for the design and synthesis of CDs with stronger acidic properties as a possible alternative to using sulfuric acid to pre-treat oils high in FFA content in current industrial practices.

This work illustrates the potential for CDs, made from inexpensive precursors and simple synthetic procedures, to be used as a basis for the synthesis of catalytically efficient CDs to be used as heterogeneous catalysts for biodiesel production.

3.4.2 – LCDs-Catalyzed Transesterification of Canola Oil to Biodiesel

Following extensive characterization of the LCDs, their catalytic efficiency towards the transesterification reaction was investigated. Previous work on the GlyCDs relied on high reaction pressure and temperature to aid in product formation. This was done to drive the reaction forward and aid the GlyCDs by increasing their catalytic efficiency, providing a basis for the CD-catalyzed transesterification reaction that has been otherwise unexplored in the literature. The purpose of using lignin-derived CDs was to render the biodiesel production life cycle fully green and sustainable. While biodiesel is green, biodegradable and possesses tremendous environmental benefits over fossil fuel-derived oils, its production process is not green and it not only impacts its economic feasibility but also its environmental footprint. In order to drive the catalytic reaction forward relying on lignin-derived CDs to catalyze the transesterification reaction using conventional heating, the oil to methanol molar ratio was increased to 1:72, a rather elevated content of methanol compared to the conventional ratio of 1:6. The reaction temperature was set to 90 °C, slightly higher than the conventional temperature used at 65-70°C. The reaction time was set to 6 h, much higher than the conventional reaction time of 1-2 h and a loading catalyst of 1 wt% was used in order to keep one reaction parameter equal to the homogeneous catalysis counterpart. Both LCDs synthesized without and with the addition of H_2O_2 were investigated and respectively resulted in 58% and 97% biodiesel conversion, while the control groups, lignin and sodium citrate, were confirmed to have no catalytic efficacy **(figure 41)**. Upon confirmation that the LCDs can efficiently catalyze the transesterification reaction, the reaction parameters were optimized to reduce the energy and methanol required **(figure 42)**. The reaction time was first decreased to 4h, keeping an oil to methanol content of 1:72, a reaction temperature of 90 °C and loading catalyst of 1 wt%, resulting in a biodiesel conversion of 97%. However further decreasing

73

the oil to methanol content to 1:36 at reaction times of 6 h and 4 h resulted in biodiesel conversions of 53% and 41% respectively, indicating that a rather higher methanol content is required to drive the reaction forward. One of the main limitations to the implementation of heterogeneous catalysts
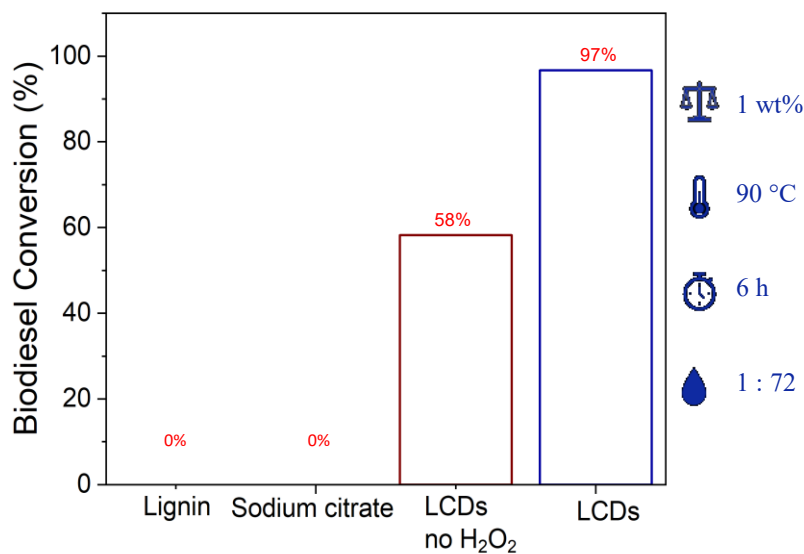
Figure 41. Biodiesel conversion results for LCDs synthesized without and with the addition of H2O2 and control reactions using the synthesis precursors, lignin and sodium citrate, to ensure no catalytic efficiency from unreacted precursors.
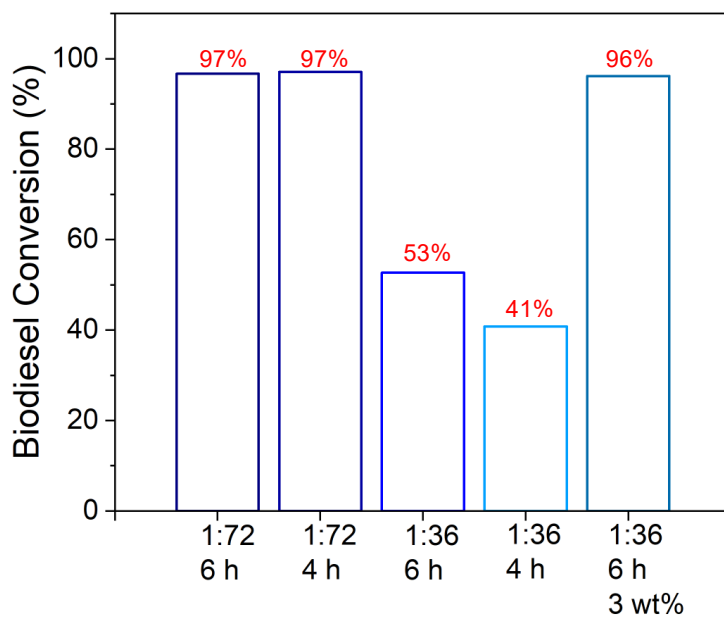
Figure 42. Reaction optimization results for the LCD-catalyzed transesterification reaction.

in current industrial practices is their general need for higher methanol contents. In order to drive the reaction forward using a 1:36 oil to methanol content, the loading catalyst for the LCDs was increased to 3 wt%, resulting in a biodiesel conversion of 96%. Increasing the catalyst loading of a lignin-derived catalyst in order to use half the methanol required would be a reasonable trade-off since the production of methanol does stem from fossil fuels.

Based on previous work conducted with GlyCDs where addition of NaOH to enable a base activation/modification to take place, the LCDs were subjected to a 1% NaOH solution under stirring for 5 minutes. Upon further washing with acetone to remove the Na^+ and ^-OH ions, the LCDs-b were dried in an oven at 80 °C and subsequently used as catalysts for the transesterification of canola oil. The reaction conditions were set to more closely resemble current industry reaction conditions, this included a reaction temperature of 90 °C, reaction time of 2 h, an oil to methanol content of 1:9 and a catalyst loading of 1 wt%. This reaction resulted in a biodiesel conversion of 90.5 %, as seen by the prominent singlet at 3.7 ppm on the ^1H NMR spectrum **(figure 43)**.

Studies have shown that upon treatment with strong bases such as NaOH and KOH, biomass-derived materials have shown increased surface area due to an increase in porosity of the material and also generates strong basic sites on the surfaces of the material.[108,109] The basic sites generally act like proton absorbers, similar to the partially negative oxygen of metal oxides like CaO, a common basic heterogeneous catalyst used for transesterification reactions.[108] The LCDs-b achieved >90 % biodiesel conversion upon NaOH treatment for only 5 minutes. It is proposed that with prolonged treatment times, catalytic efficiency of the LCDs-b will be increased and be able to catalyze the transesterification of canola oil without the need for highly energy intensive conditions. Future analysis and characterization must be carried out on the LCDs and LCDs-b
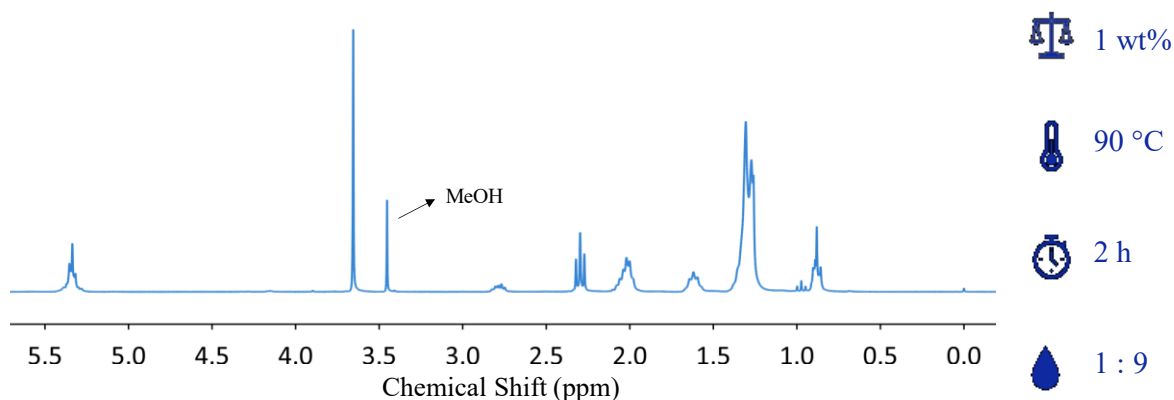
Figure 43. ^1H NMR spectrum of the transesterification reaction of canola oil catalyzed by LCDs-b, resulting in a biodiesel conversion of 90.5 %.

in order to ascertain the effects of the NaOH treatment. BET (Brunauer, Emmett and Teller) N_2 adsorption analysis would provide vital information regarding surface area and porosity and CO_2 adsorption experiments would be carried out to measure the number of basic sites present on the surface of the CDs.

Further work must be carried out to optimize both the synthesis of lignin-derived CDs and their possible application towards heterogeneous catalysis for biodiesel production. However, this work provides preliminary insights on the facile and simple synthesis of biomass-derived materials rendered catalytically efficient without the need for strong acids and tedious/energy intensive synthetic procedures, as often seen in previously reported biomass-derived heterogeneous catalysts for biodiesel production. The valorization of biomass is a key component in biodiesel production that would greatly increase the process' sustainability and greenness by adhering to the 7th green chemistry principle namely the use of renewable feedstocks.

3.4.3 – GCDs-Catalyzed Transesterification Reaction of Canola Oil to Biodiesel

The catalytic efficiency of GCDs towards the transesterification reaction of canola oil to biodiesel was investigated using conventional heating methods and ambient pressure. The loading

catalyst was kept at 1 wt%, on par with homogeneous catalyst counterparts; however, the reaction temperature was set to 90 °C in order to aid the catalyst in driving the reaction forward. Initially, the reaction was carried out using a relatively high methanol content of 1:72 and a reaction time of 6 h in order to determine if GCDs catalyzed the formation of biodiesel. This resulted in a biodiesel conversion of 98% and the result was maintained upon further optimization of the methanol ratio and reaction time. A decrease in biodiesel conversion to 42% was noted at an oil to methanol ratio of 1:9 at a reaction time of 30 min **(figure 44)**.

The effects of altering the sodium citrate concentration during synthesis on biodiesel conversion was investigated using the optimized reaction conditions of an oil to methanol content of 1:9, reaction time of 2 h, a catalyst loading of 1 wt% and a reaction temperature of 90 °C **(figure 45)**. The resulting biodiesel conversions were 67%, 82%, and 97% for GCDs-0.3, GCDs-0.6, and GCDs-1.2, respectively, indicating a clear correlation between the amount of sodium citrate required during GCD synthesis and catalytic efficiency. Furthermore, control experiments were conducted using the precursors used to synthesize GCDs, sodium citrate and glycerol, with both transesterification reactions resulting in 0% conversion. This indicated that unreacted precursors were not responsible for the catalytic activity observed. These results show extremely promising results while maintaining similar reaction conditions to current industrial practices and while using a CD heterogeneous catalyst made from glycerol, a by-product of the vegetable oil transesterification reaction.

Zeta-potential analysis **(table 5)** was carried out on the GCDs do investigate the effect of sodium citrate concentration used during CDs synthesis on the surface potential of the CD, a characteristic deemed essential in high catalytic efficiency for the transesterification reaction. As expected, as the amount of sodium citrate added during GCD synthesis increases, so does the
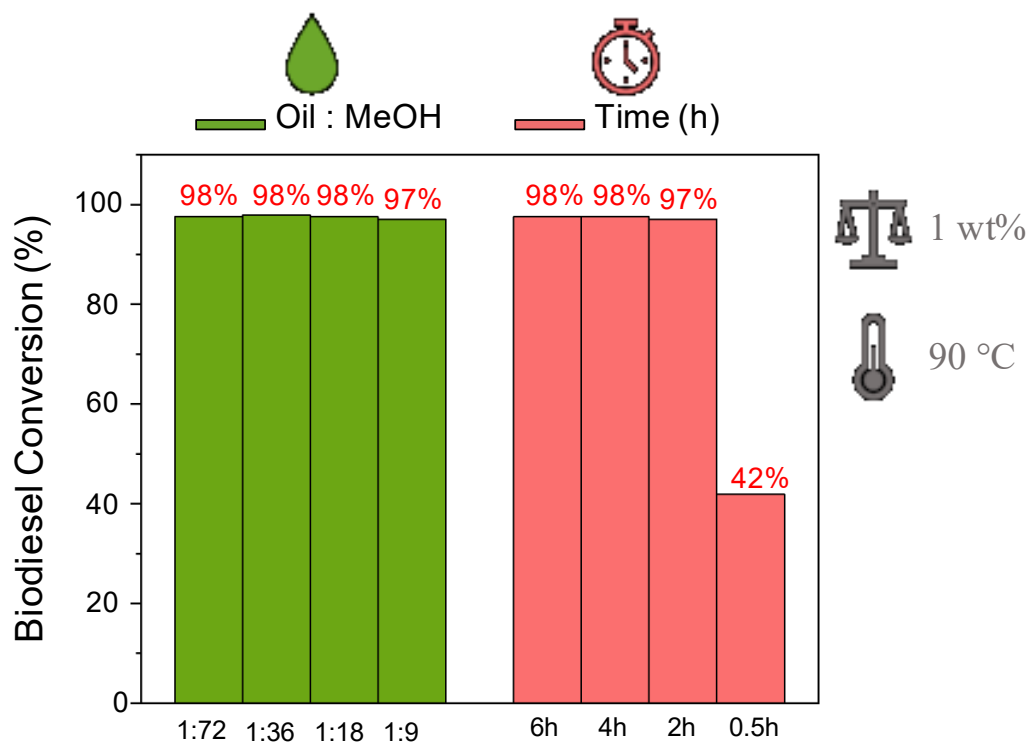
Figure 44. Summary of biodiesel conversion results upon reaction optimization of oil to methanol content and reaction time, keeping a loading catalyst of 1 wt% and reaction temperature of 90 °C constant.
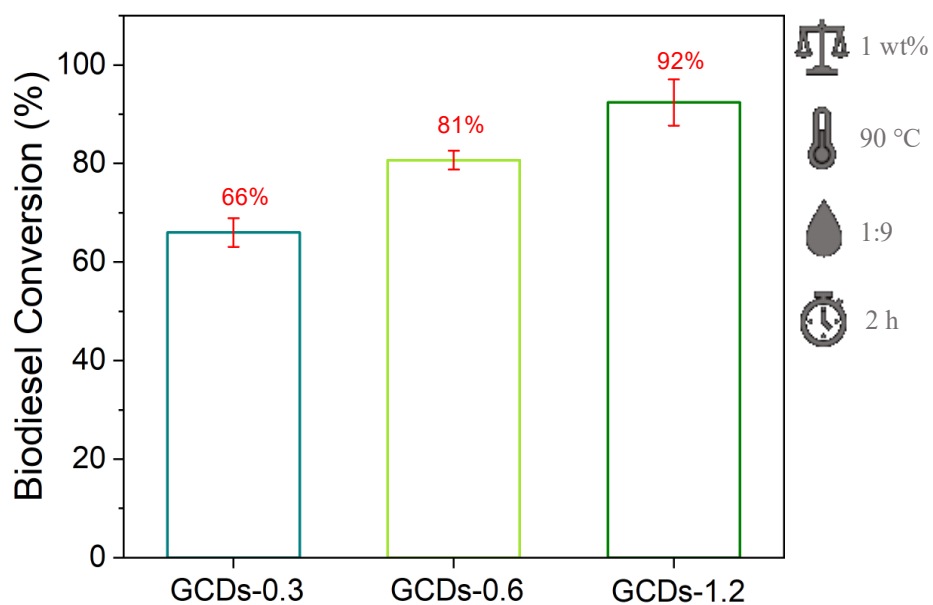
Figure 45. Biodiesel conversion for all GCDs. Results indicate an increase in biodiesel conversion as the content of sodium citrate is increased during synthesis of GCDs.

the negative surface potential. As seen with the GlyCDs, the surface potential has a significant impact on their catalytic efficiency towards the transesterification reaction of canola oil.

Table 5. Zeta potential analysis on GCDs. As the amount of sodium citrate added during synthesis increases so does the negative surface potential.

Amount of sodium citrate	Surface potential (mV)
0.3 g	-16.7
0.6 g	-17.8
1.2 g	-22.0

The GCDs-1.2's recovery and reusability was studied. The glycerol layer, containing both the glycerol by-product and the GCDs, was separated from the biodiesel layer by centrifugation and then washed with hexanes three times to remove any residual biodiesel. To isolate the GCDs and remove the glycerol by-product, the glycerol layer was washed three times with ethanol. The isolated GCDs were placed in an oven at 70 °C to dry before using them for a subsequent transesterification reaction. The dried GCDs were analyzed by FT-IR to investigate if there had been any changes to the surface chemistry upon catalyst washing and isolation and to ensure that the glycerol by-product was efficiently removed upon washing **(figure 46)**. FT-IR analysis of glycerol layer-post transesterification reaction one showed significant amount of glycerol as expected, due to the prominent stretching vibrations associated to the O-H groups at 3300 cm^{-1} and the C-O stretching vibration at 1030 cm^{-1} however, the presence of GCDs is confirmed by the appearance of the asymmetric stretching vibration pertaining to the COO$^-$ groups at 1580 cm^{-1}. The GCDs-1.2 upon washing with ethanol showed more prominent stretching vibrations
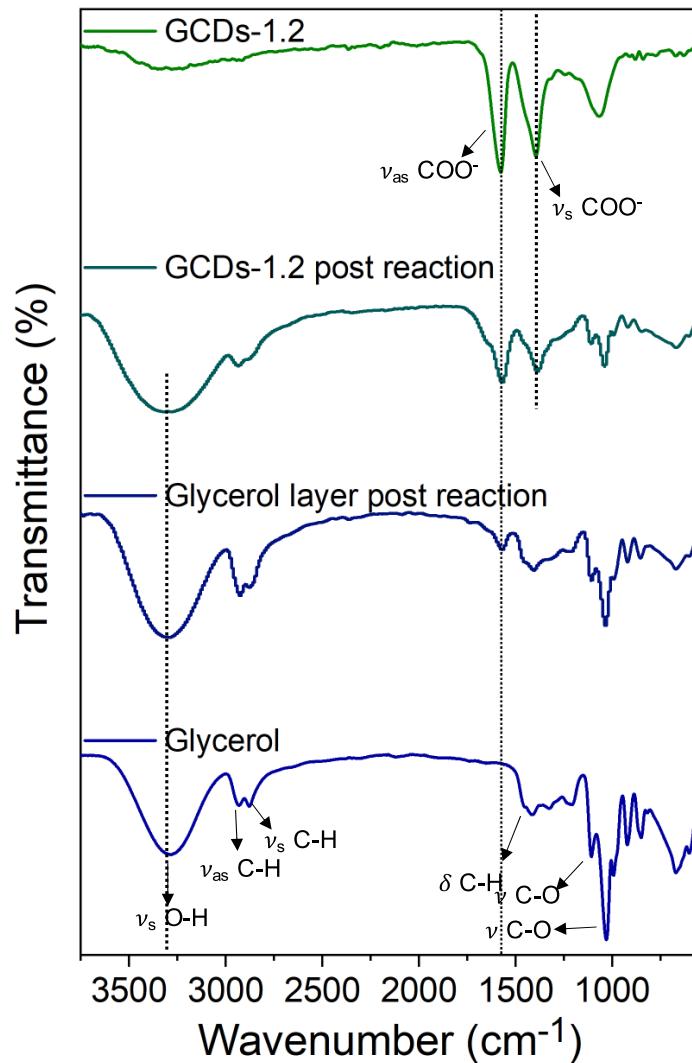
Figure 46. FT-IR analysis of the glycerol layer-post transesterification reaction, confirming the presence of GCDs due to the asymmetric stretching vibration at 1580 cm^{-1} pertaining to the COO$^-$ groups on the surface of the GCDs. The GCDs post transesterification and upon washing with ethanol show more prominent COO$^-$ asymmetric and symmetric stretching vibrations at 1580 cm^{-1} and 1390 cm^{-1} however the presence of residual glycerol is still present as confirmed by the symmetric stretching vibration associated to the O-H groups in glycerol.

associated to the COO$^-$ groups present on the surface of the CDs, further confirming their presence, however, residual glycerol was also confirmed through the prominent stretching vibration associated to the O-H groups of glycerol.

The dried GCDs-1.2 were dispersed in 0.75 mL, equivalent to 1:9 oil to methanol molar ratio, added to 2 mL of canola oil and then reacted for 2 h at 90 °C. Following ^{1}H NMR analysis

(figure 47), biodiesel conversion of 0 % was observed, indicating that the GCDs were not reusable possibly due to catalyst inactivation or decomposition during the transesterification reaction. FT-IR analysis previously showed a considerable presence of residual glycerol which may have inhibited activity. Further analysis and characterization of the GCDs must be carried out, primarily TGA analysis in order to determine their decomposition temperature and analyze their thermal stability.

Although the GCDs were not deemed reusable after one transesterification reaction, the preliminary results concerning the synthesis of glycerol-derived carbon dots as an alternative use for the crude glycerol by-product produced during the reaction opens other avenues into designing promising and useful materials from waste products in order to circumvent the limitations and costs associated with their generation during industrial processes.
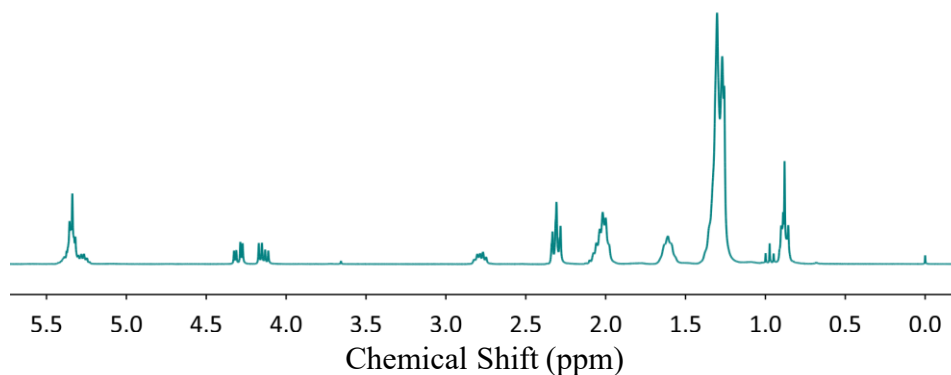
Figure 47. ^{1}H NMR spectrum of the oil phase post transesterification reaction indicating 0 % biodiesel conversion, confirming that the GCDs cannot be reused for subsequent reactions.

Chapter 4 – Conclusion and Future Works

4.1 – Conclusion

In this work, CDs prepared using glycine, lignin and glycerol were successfully synthesized and their physico-chemical properties were investigated for development as heterogeneous transesterification catalysts in the conversion of canola oil to biodiesel. GlyCDs were successfully used as catalysts and resulted in biodiesel conversions of > 96% while maintaining efficiency over at least five reaction cycles. However, high temperatures and pressure were required to drive the reaction forward and the GlyCDs were not successful at catalyzing the reaction at ambient pressures and lower temperatures.

These first findings provided the knowledge foundations that a highly negative surface potential was essential for achieving high biodiesel conversions. As such, two other carbon dot systems were investigated. The dots derived from a biomass precursor, lignin, were successfully used to achieve high biodiesel conversions of > 96% at ambient pressures and lower reactions temperature. For these catalysts, higher methanol content and longer reaction times were required limiting the overall desirability of these catalysts. However, the use of biomass as a CD precursor increases the overall greenness and financial attractiveness of biodiesel production and involves the valorization of forestry waste, which would also be beneficial in terms of cost and sustainability.

The utilization of crude glycerol, the by-product generated from the biodiesel production process, as a precursor for CDs would allow the transesterification by-product to re-enter the production process making it a truly sustainable practice and lowering the costs associated with glycerol purification. With that in mind, GCDs synthesized from glycerol and sodium citrate were extremely efficient, even at fairly mild reaction conditions, using an oil to methanol ratio of 1:9, a

loading catalyst of 1 wt%, a reaction temperature of 90 °C and a reaction time of only 2 h. These conditions were all comparable to their homogeneous catalyst counterparts. The ability to separate crude glycerol from biodiesel and subsequently use it to synthesize heterogeneous catalysts to produce more biodiesel would significantly decrease production costs and waste water currently required for biodiesel and glycerol purification.

This work provides preliminary insights on the design and synthesis of CDs with high catalytic efficiency towards the transesterification reaction of canola oil to biodiesel. The use of CDs as heterogeneous catalysts can be potentially advantageous due to their large surface area to volume ratio, their versatile surface chemistry, ability to synthesize from a number of inexpensive, raw and waste materials. Put together, this renders them an economically viable option for industrial practices such as biodiesel production.

4.2 – Future works

Further investigation into the synthesis and optimization of the LCDs and GCDs must be carried out. Reusability studies for both systems must also be studied in order to define their potential as true heterogeneous catalysts. Further characterization including elemental analysis, XPS, surface potentiometric titrations and CO_2 TPD analysis would be useful in obtaining key information regarding the structure of the CDs and ultimately provide insights into their catalytic mechanism. Furthermore, a move towards the use of waste oil precursors is necessary to increase the sustainability and reduce the costs associated to biodiesel production. Furthermore, the quality of the biodiesel product being produced through CD-catalyzed reactions must be evaluated. Properties such as residual glycerol and methanol content, sodium ion content, density, and viscosity are all important in determining the oil quality and effectiveness for use in diesel engines.

83

References

(1)   *World Energy Outlook 2019*; Paris, 2019.

(2)   *Key World Energy Statistics 2019*; 2019.

(3)   CO2 Emissions by fuel, World https://ourworldindata.org/grapher/co2-emissions-by-fuel-line%0A (accessed Apr 14, 2020).

(4)   Shafiee, S.; Topal, E. When Will Fossil Fuel Reserves Be Diminished? *Energy Policy* **2009**, *37* (1), 181–189. https://doi.org/10.1016/j.enpol.2008.08.016.

(5)   *BP Statistical Review of World Energy 2016*; 2016.

(6)   BP. BP Statistical Review of World Energy https://ourworldindata.org/grapher/biofuels-production-by-region.

(7)   Gerpen, J. H. Van; Peterson, C. L.; Goering, C. E. Biodiesel : An Alternative Fuel for Compression Ignition Engines. *2007 Agric. Equip. Technol. Conf.* **2007**, No. 31, 1–22. https://doi.org/913C0107.

(8)   *The Biodiesel Handbook*, 2nd ed.; Knothe, G., Krahl, J., Gerpen, J., Eds.; Academic Press and AOCS Press, 2010.

(9)   Yusoff, M. F. M.; Xu, X.; Guo, Z. Comparison of Fatty Acid Methyl and Ethyl Esters as Biodiesel Base Stock: A Review on Processing and Production Requirements. *JAOCS, J. Am. Oil Chem. Soc.* **2014**, *91* (4), 525–531. https://doi.org/10.1007/s11746-014-2443-0.

(10)   Vyas, A. P.; Verma, J. L.; Subrahmanyam, N. Effects of Molar Ratio, Alkali Catalyst Concentration and Temperature on Transesterification of Jatropha Oil with Methanol under Ultrasonic Irradiation. *Adv. Chem. Eng. Sci.* **2011**, *01* (02), 45–50. https://doi.org/10.4236/aces.2011.12008.

(11)   Shu, Q.; Yang, B.; Yuan, H.; Qing, S.; Zhu, G. Synthesis of Biodiesel from Soybean Oil and Methanol Catalyzed by Zeolite Beta Modified with La3+. *Catal. Commun.* **2007**, *8* (12), 2159–2165. https://doi.org/10.1016/j.catcom.2007.04.028.

(12)   Tasić, M. B.; Stamenković, O. S.; Veljković, V. B. Cost Analysis of Simulated Base-Catalyzed Biodiesel Production Processes. *Energy Convers. Manag.* **2014**, *84*, 405–413. https://doi.org/10.1016/j.enconman.2014.04.044.

(13)   Ataya, F.; Dubé, M. A.; Ternan, M. Acid-Catalyzed Transesterification of Canola Oil to Biodiesel under Single- and Two-Phase Reaction Conditions. *Energy and Fuels* **2007**, *21*

(4), 2450–2459. https://doi.org/10.1021/ef0701440.

(14)   Gebremariam, S. N.; Marchetti, J. M. Biodiesel Production through Sulfuric Acid Catalyzed Transesterification of Acidic Oil: Techno Economic Feasibility of Different Process Alternatives. *Energy Convers. Manag.* **2018**, *174* (June), 639–648. https://doi.org/10.1016/j.enconman.2018.08.078.

(15)   Lee, A. F.; Bennett, J. A.; Manayil, J. C.; Wilson, K. Heterogeneous Catalysis for Sustainable Biodiesel Production via Esterification and Transesterification. *Chem. Soc. Rev.* **2014**, *43* (22), 7887–7916. https://doi.org/10.1039/c4cs00189c.

(16)   Di Serio, M.; Tesser, R.; Pengmei, L.; Santacesaria, E. Heterogeneous Catalysts for Biodiesel Production. *Energy and Fuels* **2008**, *22* (1), 207–217. https://doi.org/10.1021/ef700250g.

(17)   Carrero, A.; Vicente, G.; Rodríguez, R.; Linares, M.; Del Peso, G. L. Hierarchical Zeolites as Catalysts for Biodiesel Production from Nannochloropsis Microalga Oil. *Catal. Today* **2011**, *167* (1), 148–153. https://doi.org/10.1016/j.cattod.2010.11.058.

(18)   Shibasaki-Kitakawa, N.; Honda, H.; Kuribayashi, H.; Toda, T.; Fukumura, T.; Yonemoto, T. Biodiesel Production Using Anionic Ion-Exchange Resin as Heterogeneous Catalyst. *Bioresour. Technol.* **2007**, *98* (2), 416–421. https://doi.org/10.1016/j.biortech.2005.12.010.

(19)   Refaat, A. A. Biodiesel Production Using Solid Metal Oxide Catalysts. *Int. J. Environ. Sci. Technol.* **2011**, *8* (1), 203–221. https://doi.org/10.1007/BF03326210.

(20)   Chen, G.; Shan, R.; Shi, J.; Yan, B. Ultrasonic-Assisted Production of Biodiesel from Transesterification of Palm Oil over Ostrich Eggshell-Derived CaO Catalysts. *Bioresour. Technol.* **2014**, *171*, 428–432. https://doi.org/10.1016/j.biortech.2014.08.102.

(21)   Uprety, B. K.; Chaiwong, W.; Ewelike, C.; Rakshit, S. K. Biodiesel Production Using Heterogeneous Catalysts Including Wood Ash and the Importance of Enhancing Byproduct Glycerol Purity. *Energy Convers. Manag.* **2016**, *115*, 191–199. https://doi.org/10.1016/j.enconman.2016.02.032.

(22)   Teo, S. H.; Taufiq-Yap, Y. H.; Rashid, U.; Islam, A. Hydrothermal Effect on Synthesis, Characterization and Catalytic Properties of Calcium Methoxide for Biodiesel Production from Crude Jatropha Curcas. *RSC Adv.* **2015**, *5* (6), 4266–4276. https://doi.org/10.1039/c4ra11936c.

(23)   Chouhan, A. P. S.; Sarma, A. K. Modern Heterogeneous Catalysts for Biodiesel Production:

A Comprehensive Review. *Renew. Sustain. Energy Rev.* **2011**, *15* (9), 4378–4399. https://doi.org/10.1016/j.rser.2011.07.112.

(24) Zabeti, M.; Wan Daud, W. M. A.; Aroua, M. K. Activity of Solid Catalysts for Biodiesel Production: A Review. *Fuel Process. Technol.* **2009**, *90* (6), 770–777. https://doi.org/10.1016/j.fuproc.2009.03.010.

(25) Melero, J. A.; Iglesias, J.; Morales, G. Heterogeneous Acid Catalysts for Biodiesel Production: Current Status and Future Challenges. *Green Chem.* **2009**, *11* (9), 1285–1308. https://doi.org/10.1039/b902086a.

(26) Lam, M. K.; Lee, K. T.; Mohamed, A. R. Homogeneous, Heterogeneous and Enzymatic Catalysis for Transesterification of High Free Fatty Acid Oil (Waste Cooking Oil) to Biodiesel: A Review. *Biotechnol. Adv.* **2010**, *28* (4), 500–518. https://doi.org/10.1016/j.biotechadv.2010.03.002.

(27) Mahajan, S.; Konar, S. K.; Boocock, D. G. B. Determining the Acid Number of Biodiesel. *JAOCS, J. Am. Oil Chem. Soc.* **2006**, *83* (6), 567–570. https://doi.org/10.1007/s11746-006-1241-8.

(28) Ramos; Dias; Puna; Gomes; Bordado. Biodiesel Production Processes and Sustainable Raw Materials. *Energies* **2019**, *12* (23), 4408. https://doi.org/10.3390/en12234408.

(29) Lam, M. K.; Lee, K. T.; Mohamed, A. R. Homogeneous, Heterogeneous and Enzymatic Catalysis for Transesterification of High Free Fatty Acid Oil (Waste Cooking Oil) to Biodiesel: A Review. *Biotechnol. Adv.* **2010**, *28* (4), 500–518. https://doi.org/10.1016/j.biotechadv.2010.03.002.

(30) Atabani, A. E.; Silitonga, A. S.; Badruddin, I. A.; Mahlia, T. M. I.; Masjuki, H. H.; Mekhilef, S. A Comprehensive Review on Biodiesel as an Alternative Energy Resource and Its Characteristics. *Renew. Sustain. Energy Rev.* **2012**, *16* (4), 2070–2093. https://doi.org/10.1016/j.rser.2012.01.003.

(31) Gui, M. M.; Lee, K. T.; Bhatia, S. Feasibility of Edible Oil vs. Non-Edible Oil vs. Waste Edible Oil as Biodiesel Feedstock. *Energy* **2008**, *33* (11), 1646–1653. https://doi.org/10.1016/j.energy.2008.06.002.

(32) Anastas, P.; Warner, J. *Green Chemistry: Theory and Practice*; Oxford University Press, 1998.

(33) American Chemical Society. 12 Principles of Green Chemistry.

(34) Kohli, K.; Prajapati, R.; Sharma, B. K. Bio-Based Chemicals from Renewable Biomass for Integrated Biorefineries. *Energies* **2019**, *12* (2). https://doi.org/10.3390/en12020233.

(35) Corma Canos, A.; Iborra, S.; Velty, A. Chemical Routes for the Transformation of Biomass into Chemicals. *Chem. Rev.* **2007**, *107* (6), 2411–2502. https://doi.org/10.1021/cr050989d.

(36) Tong, X.; Ma, Y.; Li, Y. Biomass into Chemicals: Conversion of Sugars to Furan Derivatives by Catalytic Processes. *Appl. Catal. A Gen.* **2010**, *385* (1–2), 1–13. https://doi.org/10.1016/j.apcata.2010.06.049.

(37) Zhang, L.; Liu, Z.; Cui, G.; Chen, L. Biomass-Derived Materials for Electrochemical Energy Storages. *Prog. Polym. Sci.* **2015**, *43*, 136–164. https://doi.org/10.1016/j.progpolymsci.2014.09.003.

(38) Satoh, K.; Sugiyama, H.; Kamigaito, M. Biomass-Derived Heat-Resistant Alicyclic Hydrocarbon Polymers: Poly(Terpenes) and Their Hydrogenated Derivatives. *Green Chem.* **2006**, *8* (10), 878–888. https://doi.org/10.1039/b607789g.

(39) Tangy, A.; Kumar, V. B.; Pulidindi, I. N.; Kinel-Tahan, Y.; Yehoshua, Y.; Gedanken, A. In-Situ Transesterification of Chlorella Vulgaris Using Carbon-Dot Functionalized Strontium Oxide as a Heterogeneous Catalyst under Microwave Irradiation. *Energy and Fuels* **2016**, *30* (12), 10602–10610. https://doi.org/10.1021/acs.energyfuels.6b02519.

(40) Scott, S. A.; Davey, M. P.; Dennis, J. S.; Horst, I.; Howe, C. J.; Lea-Smith, D. J.; Smith, A. G. Biodiesel from Algae: Challenges and Prospects. *Curr. Opin. Biotechnol.* **2010**, *21* (3), 277–286. https://doi.org/10.1016/j.copbio.2010.03.005.

(41) Johnson, M. B.; Wen, Z. Production of Biodiesel Fuel from the Microalga Schizochytrium Limacinum by Direct Transesterification of Algal Biomass. *Energy and Fuels* **2009**, *23* (10), 5179–5183. https://doi.org/10.1021/ef900704h.

(42) Taher, H.; Al-Zuhair, S.; Al-Marzouqi, A. H.; Haik, Y.; Farid, M. Effective Extraction of Microalgae Lipids from Wet Biomass for Biodiesel Production. *Biomass and Bioenergy* **2014**, *66*, 159–167. https://doi.org/10.1016/j.biombioe.2014.02.034.

(43) Pua, F.; Fang, Z.; Zakaria, S.; Guo, F.; Chia, C. Direct Production of Biodiesel from High-Acid Value Jatropha Oil with Solid Acid Catalyst Derived from Lignin. *Biotechnol. Biofuels* **2012**, *5* (1), 66. https://doi.org/10.1186/1754-6834-5-66.

(44) Yang, F.; Hanna, M. A.; Sun, R. Value-Added Uses for Crude Glycerol–a Byproduct of Biodiesel Production. *Biotechnol. Biofuels* **2012**, *5* (1), 1–10.

https://doi.org/10.1177/0095244312462163.

(45) Hu, S.; Luo, X.; Wan, C.; Li, Y. Characterization of Crude Glycerol from Biodiesel Plants. *J. Agric. Food Chem.* **2012**, *60* (23), 5915–5921. https://doi.org/10.1021/jf3008629.

(46) Nitayavardhana, S.; Khanal, S. K. Biodiesel-Derived Crude Glycerol Bioconversion to Animal Feed: A Sustainable Option for a Biodiesel Refinery. *Bioresour. Technol.* **2011**, *102* (10), 5808–5814. https://doi.org/10.1016/j.biortech.2011.02.058.

(47) Luo, X.; Ge, X.; Cui, S.; Li, Y. Value-Added Processing of Crude Glycerol into Chemicals and Polymers. *Bioresour. Technol.* **2016**, *215*, 144–154. https://doi.org/10.1016/j.biortech.2016.03.042.

(48) Devi, B. L. A. P.; Gangadhar, K. N.; Prasad, P. S. S.; Jagannadh, B.; Prasad, R. B. N. A Glycerol-Based Carbon Catalyst for the Preparation of Biodiesel. *ChemSusChem* **2009**, *2* (7), 617–620. https://doi.org/10.1002/cssc.200900097.

(49) Ferrero, G. O.; Almeida, M. F.; Alvim-Ferraz, M. C. M.; Dias, J. M. Glycerol-Enriched Heterogeneous Catalyst for Biodiesel Production from Soybean Oil and Waste Frying Oil. *Energy Convers. Manag.* **2015**, *89*, 665–671. https://doi.org/10.1016/j.enconman.2014.10.032.

(50) Wang, Q.; Huang, X.; Long, Y.; Wang, X.; Zhang, H.; Zhu, R.; Liang, L.; Teng, P.; Zheng, H. Hollow Luminescent Carbon Dots for Drug Delivery. *Carbon N. Y.* **2013**, *59*, 192–199. https://doi.org/10.1016/j.carbon.2013.03.009.

(51) Ding, H.; Du, F.; Liu, P.; Chen, Z.; Shen, J. DNA-Carbon Dots Function as Fluorescent Vehicles for Drug Delivery. *ACS Appl. Mater. Interfaces* **2015**, *7* (12), 6889–6897. https://doi.org/10.1021/acsami.5b00628.

(52) Macairan, J. R.; Jaunky, D. B.; Piekny, A.; Naccache, R. Intracellular Ratiometric Temperature Sensing Using Fluorescent Carbon Dots. *Nanoscale Adv.* **2019**, *1* (1), 105–113. https://doi.org/10.1039/c8na00255j.

(53) Jiang, K.; Sun, S.; Zhang, L.; Lu, Y.; Wu, A.; Cai, C.; Lin, H. Red, Green, and Blue Luminescence by Carbon Dots: Full-Color Emission Tuning and Multicolor Cellular Imaging. *Angew. Chemie* **2015**, *127* (18), 5450–5453. https://doi.org/10.1002/ange.201501193.

(54) Gogoi, N.; Barooah, M.; Majumdar, G.; Chowdhury, D. Carbon Dots Rooted Agarose Hydrogel Hybrid Platform for Optical Detection and Separation of Heavy Metal Ions. *ACS*

Appl. Mater. Interfaces **2015**, *7* (5), 3058–3067. https://doi.org/10.1021/am506558d.

(55)   Cortez Vásquez, A.; Rosales Gerónimo, G.; Naupari Quiroz, R.; Vega Huerta, H. *Smart Materials for Advanced Environmental Applications*; 2016; Vol. 7. https://doi.org/10.1039/9781782622130-FP007.

(56)   Zhang, M.; Yao, Q.; Guan, W.; Lu, C.; Lin, J. M. Layered Double Hydroxide-Supported Carbon Dots as an Efficient Heterogeneous Fenton-like Catalyst for Generation of Hydroxyl Radicals. *J. Phys. Chem. C* **2014**, *118* (19), 10441–10447. https://doi.org/10.1021/jp5012268.

(57)   Kim, K. H.; Lee, O. K.; Lee, E. Y. Nano-Immobilized Biocatalysts for Biodiesel Production from Renewable and Sustainable Resources. *Catalysts* **2018**, *8* (2). https://doi.org/10.3390/catal8020068.

(58)   Xu, X.; Ray, R.; Gu, Y.; Ploehn, H. J.; Gearheart, L.; Raker, K.; Scrivens, W. A. Electrophoretic Analysis and Purification of Fluorescent Single-Walled Carbon Nanotube Fragments. *J. Am. Chem. Soc.* **2004**, *126* (40), 12736–12737. https://doi.org/10.1021/ja040082h.

(59)   Qian, Z.; Shan, X.; Chai, L.; Ma, J.; Chen, J.; Feng, H. Si-Doped Carbon Quantum Dots: A Facile and General Preparation Strategy, Bioimaging Application, and Multifunctional Sensor. *ACS Appl. Mater. Interfaces* **2014**, *6* (9), 6797–6805. https://doi.org/10.1021/am500403n.

(60)   Duan, H.; Wang, D.; Li, Y. Green Chemistry for Nanoparticle Synthesis. *Chem. Soc. Rev.* **2015**, *44* (16), 5778–5792. https://doi.org/10.1039/c4cs00363b.

(61)   Sahu, S.; Behera, B.; Maiti, T. K.; Mohapatra, S. Simple One-Step Synthesis of Highly Luminescent Carbon Dots from Orange Juice: Application as Excellent Bio-Imaging Agents. *Chem. Commun.* **2012**, *48* (70), 8835–8837. https://doi.org/10.1039/c2cc33796g.

(62)   Chen, J.; Li, Y.; Lv, K.; Zhong, W.; Wang, H.; Wu, Z.; Yi, P.; Jiang, J. Cyclam-Functionalized Carbon Dots Sensor for Sensitive and Selective Detection of Copper(II) Ion and Sulfide Anion in Aqueous Media and Its Imaging in Live Cells. *Sensors Actuators, B Chem.* **2016**, *224*, 298–306. https://doi.org/10.1016/j.snb.2015.10.046.

(63)   Kang, Z.; Lee, S. T. Carbon Dots: Advances in Nanocarbon Applications. *Nanoscale* **2019**, *11* (41), 19214–19224. https://doi.org/10.1039/c9nr05647e.

(64)   Wu, X.; Guo, S.; Zhang, J. Selective Oxidation of Veratryl Alcohol with Composites of Au

Nanoparticles and Graphene Quantum Dots as Catalysts. *Chem. Commun.* **2015**, *51* (29), 6318–6321. https://doi.org/10.1039/C5CC00061K.

(65)   Yang, Y.; Zhu, W.; Shi, B.; Lü, C. Construction of a Thermo-Responsive Polymer Brush Decorated Fe3O4@catechol-Formaldehyde Resin Core-Shell Nanosphere Stabilized Carbon Dots/PdNP Nanohybrid and Its Application as an Efficient Catalyst. *J. Mater. Chem. A* **2020**, *8* (7), 4017–4029. https://doi.org/10.1039/c9ta12614g.

(66)   De, B.; Karak, N. Recent Progress in Carbon Dot-Metal Based Nanohybrids for Photochemical and Electrochemical Applications. *J. Mater. Chem. A* **2017**, *5* (5), 1826–1859. https://doi.org/10.1039/C6TA10220D.

(67)   De Medeiros, T. V.; Manioudakis, J.; Noun, F.; Macairan, J. R.; Victoria, F.; Naccache, R. Microwave-Assisted Synthesis of Carbon Dots and Their Applications. *J. Mater. Chem. C* **2019**, *7* (24), 7175–7195. https://doi.org/10.1039/c9tc01640f.

(68)   Kappe, C. O. Controlled Microwave Heating in Modern Organic Synthesis. *Angew. Chemie - Int. Ed.* **2004**, *43* (46), 6250–6284. https://doi.org/10.1002/anie.200400655.

(69)   Ding, H.; Ji, Y.; Wei, J. S.; Gao, Q. Y.; Zhou, Z. Y.; Xiong, H. M. Facile Synthesis of Red-Emitting Carbon Dots from Pulp-Free Lemon Juice for Bioimaging. *J. Mater. Chem. B* **2017**, *5* (26), 5272–5277. https://doi.org/10.1039/c7tb01130j.

(70)   Mandani, S.; Dey, D.; Sharma, B.; Sarma, T. K. Natural Occurrence of Fluorescent Carbon Dots in Honey. *Carbon N. Y.* **2017**, *119*, 569–572. https://doi.org/10.1016/j.carbon.2017.04.075.

(71)   Hu, S.; Wei, Z.; Chang, Q.; Trinchi, A.; Yang, J. A Facile and Green Method towards Coal-Based Fluorescent Carbon Dots with Photocatalytic Activity. *Appl. Surf. Sci.* **2016**, *378*, 402–407. https://doi.org/10.1016/j.apsusc.2016.04.038.

(72)   Rai, S.; Singh, B. K.; Bhartiya, P.; Singh, A.; Kumar, H.; Dutta, P. K.; Mehrotra, G. K. Lignin Derived Reduced Fluorescence Carbon Dots with Theranostic Approaches: Nano-Drug-Carrier and Bioimaging. *J. Lumin.* **2017**, *190* (May), 492–503. https://doi.org/10.1016/j.jlumin.2017.06.008.

(73)   Chen, W.; Hu, C.; Yang, Y.; Cui, J.; Liu, Y. Rapid Synthesis of Carbon Dots by Hydrothermal Treatment of Lignin. *Materials (Basel).* **2016**, *9* (3). https://doi.org/10.3390/ma9030184.

(74)   da Silva Souza, D. R.; Caminhas, L. D.; de Mesquita, J. P.; Pereira, F. V. Luminescent

Carbon Dots Obtained from Cellulose. *Mater. Chem. Phys.* **2018**, *203*, 148–155. https://doi.org/10.1016/j.matchemphys.2017.10.001.

(75)   Yu, J.; Liu, C.; Yuan, K.; Lu, Z.; Cheng, Y.; Li, L.; Zhang, X.; Jin, P.; Meng, F.; Liu, H. Luminescence Mechanism of Carbon Dots by Tailoring Functional Groups for Sensing Fe3+ Ions. *Nanomaterials* **2018**, *8* (4), 1–12. https://doi.org/10.3390/nano8040233.

(76)   Mitra, S.; Chandra, S.; Kundu, T.; Banerjee, R.; Pramanik, P.; Goswami, A. Rapid Microwave Synthesis of Fluorescent Hydrophobic Carbon Dots. *RSC Adv.* **2012**, *2* (32), 12129–12131. https://doi.org/10.1039/c2ra21048g.

(77)   Manioudakis, J.; Victoria, F.; Thompson, C. A.; Brown, L.; Movsum, M.; Lucifero, R.; Naccache, R. Effects of Nitrogen-Doping on the Photophysical Properties of Carbon Dots. *J. Mater. Chem. C* **2019**, *7* (4), 853–862. https://doi.org/10.1039/c8tc04821e.

(78)   Li, H.; Sun, C.; Ali, M.; Zhou, F.; Zhang, X.; MacFarlane, D. R. Sulfated Carbon Quantum Dots as Efficient Visible-Light Switchable Acid Catalysts for Room-Temperature Ring-Opening Reactions. *Angew. Chemie - Int. Ed.* **2015**, *54* (29), 8420–8424. https://doi.org/10.1002/anie.201501698.

(79)   Rosso, C.; Filippini, G.; Prato, M. Carbon Dots as Nano-Organocatalysts for Synthetic Applications. *ACS Catal.* **2020**, acscatal.0c01989. https://doi.org/10.1021/acscatal.0c01989.

(80)   Yang, D.; Yang, G.; Sun, Q.; Gai, S.; He, F.; Dai, Y.; Zhong, C.; Yang, P. Carbon-Dot-Decorated TiO2 Nanotubes toward Photodynamic Therapy Based on Water-Splitting Mechanism. *Adv. Healthc. Mater.* **2018**, *7* (10), 1–11. https://doi.org/10.1002/adhm.201800042.

(81)   Zheng, D. W.; Li, B.; Li, C. X.; Fan, J. X.; Lei, Q.; Li, C.; Xu, Z.; Zhang, X. Z. Carbon-Dot-Decorated Carbon Nitride Nanoparticles for Enhanced Photodynamic Therapy against Hypoxic Tumor via Water Splitting. *ACS Nano* **2016**, *10* (9), 8715–8722. https://doi.org/10.1021/acsnano.6b04156.

(82)   Fernando, K. A. S.; Sahu, S.; Liu, Y.; Lewis, W. K.; Guliants, E. A.; Jafariyan, A.; Wang, P.; Bunker, C. E.; Sun, Y. P. Carbon Quantum Dots and Applications in Photocatalytic Energy Conversion. *ACS Appl. Mater. Interfaces* **2015**, *7* (16), 8363–8376. https://doi.org/10.1021/acsami.5b00448.

(83)   Yan, Y.; Chen, J.; Li, N.; Tian, J.; Li, K.; Jiang, J.; Liu, J.; Tian, Q.; Chen, P. Systematic

Bandgap Engineering of Graphene Quantum Dots and Applications for Photocatalytic Water Splitting and CO2 Reduction. *ACS Nano* **2018**, *12* (4), 3523–3532. https://doi.org/10.1021/acsnano.8b00498.

(84) Wang, H.; Zhuang, J.; Velado, D.; Wei, Z.; Matsui, H.; Zhou, S. Near-Infrared- and Visible-Light-Enhanced Metal-Free Catalytic Degradation of Organic Pollutants over Carbon-Dot-Based Carbocatalysts Synthesized from Biomass. *ACS Appl. Mater. Interfaces* **2015**, *7* (50), 27703–27712. https://doi.org/10.1021/acsami.5b08443.

(85) Bhati, A.; Anand, S. R.; Gunture, G.; Garg, A. K.; Khare, P.; Sonkar, S. K. Sunlight-Induced Photocatalytic Degradation of Pollutant Dye by Highly Fluorescent Red-Emitting Mg-N-Embedded Carbon Dots. *ACS Sustain. Chem. Eng.* **2018**, *6* (7), 9246–9256. https://doi.org/10.1021/acssuschemeng.8b01559.

(86) Majumdar, B.; Mandani, S.; Bhattacharya, T.; Sarma, D.; Sarma, T. K. Probing Carbocatalytic Activity of Carbon Nanodots for the Synthesis of Biologically Active Dihydro/Spiro/Glyco Quinazolinones and Aza-Michael Adducts. *J. Org. Chem.* **2017**, *82* (4), 2097–2106. https://doi.org/10.1021/acs.joc.6b02914.

(87) Mayank; Singh, A.; Kaur, N.; Singh, N.; Jang, D. O. A Carbon Quantum Dot-Encapsulated Micellar Reactor for the Synthesis of Chromene Derivatives in Water. *Mol. Catal.* **2017**, *439*, 100–107. https://doi.org/10.1016/j.mcat.2017.06.032.

(88) Pei, X.; Xiong, D.; Wang, H.; Gao, S.; Zhang, X.; Zhang, S.; Wang, J. Reversible Phase Transfer of Carbon Dots between an Organic Phase and Aqueous Solution Triggered by CO 2 . *Angew. Chemie* **2018**, *130* (14), 3749–3753. https://doi.org/10.1002/ange.201800037.

(89) Sarkar, S.; Das, K.; Das, P. K. Hydrophobically Tailored Carbon Dots toward Modulating Microstructure of Reverse Micelle and Amplification of Lipase Catalytic Response. *Langmuir* **2016**, *32* (16), 3890–3900. https://doi.org/10.1021/acs.langmuir.5b04750.

(90) Wang, Q.; Zhang, S.; Wang, B.; Yang, X.; Zou, B.; Yang, B.; Lu, S. Pressure-Triggered Aggregation-Induced Emission Enhancement in Red Emissive Amorphous Carbon Dots. *Nanoscale Horizons* **2019**, *4* (5), 1227–1231. https://doi.org/10.1039/c9nh00287a.

(91) Siddique, A. B.; Pramanick, A. K.; Chatterjee, S.; Ray, M. Amorphous Carbon Dots and Their Remarkable Ability to Detect 2,4,6-Trinitrophenol. *Sci. Rep.* **2018**, *8* (1), 1–10. https://doi.org/10.1038/s41598-018-28021-9.

(92) Lu, Y.; Lu, Y. C.; Hu, H. Q.; Xie, F. J.; Wei, X. Y.; Fan, X. Structural Characterization of

Lignin and Its Degradation Products with Spectroscopic Methods. *J. Spectrosc.* **2017**, *2017*. https://doi.org/10.1155/2017/8951658.

(93) Guo, F.; Xiu, Z. L.; Liang, Z. X. Synthesis of Biodiesel from Acidified Soybean Soapstock Using a Lignin-Derived Carbonaceous Catalyst. *Appl. Energy* **2012**, *98*, 47–52. https://doi.org/10.1016/j.apenergy.2012.02.071.

(94) He, W.; Gao, W.; Fatehi, P. Oxidation of Kraft Lignin with Hydrogen Peroxide and Its Application as a Dispersant for Kaolin Suspensions. *ACS Sustain. Chem. Eng.* **2017**, *5* (11), 10597–10605. https://doi.org/10.1021/acssuschemeng.7b02582.

(95) Kumar, S.; Ojha, A. K.; Ahmed, B.; Kumar, A.; Das, J.; Materny, A. Tunable (Violet to Green) Emission by High-Yield Graphene Quantum Dots and Exploiting Its Unique Properties towards Sun-Light-Driven Photocatalysis and Supercapacitor Electrode Materials. *Mater. Today Commun.* **2017**, *11*, 76–86. https://doi.org/10.1016/j.mtcomm.2017.02.009.

(96) Balasubramanian, P.; Ramalingam, S.; Javid, M. A.; Rao, J. R. Lignin Based Colorant: Modified Black Liquor for Leather Surface Coating Application. *J. Am. Leather Chem. Assoc.* **2018**, *113* (10), 311–317.

(97) Ma, Z.; Sun, Q.; Ye, J.; Yao, Q.; Zhao, C. Study on the Thermal Degradation Behaviors and Kinetics of Alkali Lignin for Production of Phenolic-Rich Bio-Oil Using TGA-FTIR and Py-GC/MS. *J. Anal. Appl. Pyrolysis* **2016**, *117*, 116–124. https://doi.org/10.1016/j.jaap.2015.12.007.

(98) Ravishankar, K.; Venkatesan, M.; Desingh, R. P.; Mahalingam, A.; Sadhasivam, B.; Subramaniyam, R.; Dhamodharan, R. Biocompatible Hydrogels of Chitosan-Alkali Lignin for Potential Wound Healing Applications. *Mater. Sci. Eng. C* **2019**, *102* (April), 447–457. https://doi.org/10.1016/j.msec.2019.04.038.

(99) Tangy, A.; Kumar, V. B.; Pulidindi, I. N.; Kinel-Tahan, Y.; Yehoshua, Y.; Gedanken, A. In-Situ Transesterification of Chlorella Vulgaris Using Carbon-Dot Functionalized Strontium Oxide as a Heterogeneous Catalyst under Microwave Irradiation. *Energy and Fuels* **2016**, *30* (12), 10602–10610. https://doi.org/10.1021/acs.energyfuels.6b02519.

(100) Satyarthi, J. K.; Srinivas, D.; Ratnasamy, P. Estimation of Free Fatty Acid Content in Oils, Fats, and Biodiesel by 1H NMR Spectroscopy. *Energy and Fuels* **2009**, *23* (4), 2273–2277. https://doi.org/10.1021/ef801011v.

(101) Diehl, B.; Randel, G. Analysis of Biodiesel, Diesel and Gasoline by NMR Spectroscopy – A Quick and Robust Alternative to NIR and GC. *Lipid Technol.* **2007**, *19* (11), 258–260. https://doi.org/10.1002/lite.200700087.

(102) McCurry, J. D.; Wang, C. *Analysis of Fatty Acid Methyl Ester (FAME) Content and Distribution in Biodiesel Blends Using Heart-Cutting 2D Gas Chromatography*; 2008.

(103) Gelbard, G.; Brès, O.; Vargas, R. M.; Vielfaure, F.; Schuchardt, U. F. 1H Nuclear Magnetic Resonance Determination of the Yield of the Transesterification of Rapeseed Oil with Methanol. *J. Am. Oil Chem. Soc.* **1995**, *72* (10), 1239–1241. https://doi.org/10.1007/BF02540998.

(104) Degirmenbasi, N.; Boz, N.; Kalyon, D. M. Biofuel Production via Transesterification Using Sepiolite-Supported Alkaline Catalysts. *Appl. Catal. B Environ.* **2014**, *150–151*, 147–156. https://doi.org/10.1016/j.apcatb.2013.12.013.

(105) Tariq, M.; Ali, S.; Ahmad, F.; Ahmad, M.; Zafar, M.; Khalid, N.; Khan, M. A. Identification, FT-IR, NMR (1H and 13C) and GC/MS Studies of Fatty Acid Methyl Esters in Biodiesel from Rocket Seed Oil. *Fuel Process. Technol.* **2011**, *92* (3), 336–341. https://doi.org/10.1016/j.fuproc.2010.09.025.

(106) Maleki, H.; Kazemeini, M.; Bastan, F. Transesterification of Canola Oil to Biodiesel Using CaO/Talc Nanopowder as a Mixed Oxide Catalyst. *Chem. Eng. Technol.* **2017**, *40* (10), 1923–1930. https://doi.org/10.1002/ceat.201600579.

(107) Chouhan, A. P. S.; Sarma, A. K. Modern Heterogeneous Catalysts for Biodiesel Production: A Comprehensive Review. *Renew. Sustain. Energy Rev.* **2011**, *15* (9), 4378–4399. https://doi.org/10.1016/j.rser.2011.07.112.

(108) Vakros, J. Biochars and Their Use as Transesterification Catalysts for Biodiesel Production: A Short Review. *Catalysts* **2018**, *8* (11). https://doi.org/10.3390/catal8110562.

(109) Wang, J.; Kaskel, S. KOH Activation of Carbon-Based Materials for Energy Storage. *J. Mater. Chem.* **2012**, *22* (45), 23710–23725. https://doi.org/10.1039/c2jm34066f.